#1

VARIABLE-RATE OPTICAL COMMUNICATION THROUGH THE TURBULENT ATMOSPHERE

BARRY K. LEVITT

TECHNICAL REPORT 483

AUGUST 20, 1971

MASSACHUSETTS INSTITUTE OF TECHNOLOGY
RESEARCH LABORATORY OF ELECTRONICS
CAMBRIDGE, MASSACHUSETTS 02139

The Research Laboratory of Electronics is an interdepartmental laboratory in which faculty members and graduate students from numerous academic departments conduct research.

The research reported in this document was made possible in part by support extended the Massachusetts Institute of Technology, Research Laboratory of Electronics, by the JOINT SERVICES ELECTRONICS PROGRAMS (U. S. Army, U. S. Navy, and U.S. Air Force) under Contract No. DA 28-043-AMC-02536(E), and by the National Aeronautics and Space Administration (Grant NGL 22-009-013).

Requestors having DOD contracts or grants should apply for copies of technical reports to the Defense Documentation Center, Cameron Station, Alexandria, Virginia 22314; all others should apply to the Clearinghouse for Federal Scientific and Technical Information, Sills Building, 5285 Port Royal Road, Springfield, Virginia 22151.

MASSACHUSETTS INSTITUTE OF TECHNOLOGY

RESEARCH LABORATORY OF ELECTRONICS

Technical Report 483

August 20, 1971

VARIABLE-RATE OPTICAL COMMUNICATION THROUGH THE TURBULENT ATMOSPHERE

Barry K. Levitt

Submitted to the Department of Electrical Engineering at the Massachusetts Institute of Technology, January 29, 1971, in partial fulfillment of the requirements for the degree of Doctor of Philosophy.

(Manuscript received February 8, 1971)

ABSTRACT

The performance of optical communication links over atmospheric channels is severely limited because of the effects of turbulence. One method of recovering some of the atmospheric fading losses is to match the instantaneous signalling rate to the channel state. We demonstrate that the data transmitter can extract real-time channel-state information by processing the field received when a pilot tone is sent from the data receiver to the data transmitter. Based on these channel measurements, we derive optimal variable-rate techniques, and show that significant improvements in system performance are obtained, particularly at low bit error rates.

TABLE OF CONTENTS

I. INTRODUCTION

A confirmed microwave communication engineer might pose the obvious question, Why would anyone be seriously interested in investigating optical communication systems? We could give him the following answer.

With the continuing development of compact, powerful lasers, and efficient optical processing devices, the potential of optical communication systems for ground-to-ground, ground-to-space, and space-to-ground links is steadily increasing. The advantages of communicating at optical frequencies are quite persuasive: the large available bandwidth affords the luxury of transmitting at high data rates, as well as the possibility of frequency-multiplexing large numbers of parallel channels which is advantageous for communication-satellite applications. Another desirable feature is the characteristically large antenna gains that can be realized for optical transmitters with physically small apertures. From a strictly academic viewpoint, we cannot discount the appealing challenge of studying a relatively new field of communication theory.

Until very recently, there has been a general reluctance to establish optical communication links through the Earth's atmosphere. Optical communication systems that are nearly optimal for the free-space channel can suffer severe performance degradations when used in the atmosphere because of the effects of turbulence. The term "atmospheric turbulence" refers to the interaction of thermal layers in the air which produce microscale temperature variations resulting in random spatial and temporal fluctuations of the optical refractive index. Its effects on optical transmissions through the atmosphere include antenna beamwidth spreading, the appearance of a beam-pointing problem, and a decrease in the spatial and temporal coherence of the received field, because of random amplitude and phase distortion.

We are concerned in this report with digital data transmission through the turbulent atmosphere. The reliability of such optical communication links is often unsatisfactory because the atmospheric channel is characterized by deep fading for a significant fraction of time. We can overcome most of the undesirable effects of atmospheric turbulence on optical communication links by employing certain countermeasures. One technique is the use of a diversity-transmission scheme. Under the assumption that the atmospheric fading over each diversity path is essentially independent, deep fades on a particular diversity path will have a reduced influence on the overall error rate. For example, when the receiving aperture is large relative to a spatial coherence area of the received signal field, a spatial diversity approach can be adopted. This option is not available in a ground-to-space link, however, because the satellite generally intercepts a single spatial mode of the faded signal field. Another approach is to employ a temporal diversity scheme of the following form. We transmit a data stream of K bits, each with baud time T, such that KT exceeds the coherence time T_c of the atmospheric channel. We then repeat the entire K-bit transmission above D-1 more times to establish a D-fold temporal diversity system.

Another method of decreasing the effects of turbulence on the performance of an optical communication link is to use coding techniques. For example, a practical system might transmit binary-coded data and employ two- or three-level receiver quantization corresponding to a binary symmetric channel or a binary erasure channel. Consecutive code words would be interleaved so that adjacent channel symbols in any code word are separated by an interval greater than T_c; then the fading for each channel symbol in a particular code word is independent. Still another option is the use of transmitter feedback: the optical communication system can be designed to permit the receiver to request that a particular data transmission be repeated in the event that the received energy for that bit interval lies below a certain threshold.

One especially promising area of current research involves the development of optical communication systems that measure the atmospheric channel fading. Channel-measurement receivers are being studied as a refinement of diversity communication schemes. These receivers estimate the channel fading over each diversity path, and then incorporate these estimates into their decision strategy.[1]

Channel-measurement transmitters employing adaptive modulation techniques are also being investigated. This approach is feasible because the turbulent atmosphere has two convenient characteristics. The first of these is the point-reciprocal nature of the atmosphere[2]: this permits the atmospheric fading for an optical link to be monitored by the use of a pilot-tone probe sent from the information-signal receiver to the transmitter. Also, the atmospheric fading has a coherence time T_c of a millisecond or more.[3] Consequently, the channel measurements can be time-averaged over sufficiently long periods to minimize the influence of noise, and the transmitter has time to employ adaptive countermeasures based on these channel measurements.

There are two basic approaches to the problem of transmitter adaptation. The transmitter can spatially modulate the information signal wavefront according to its channel-state measurements to compensate for atmospheric distortions.[4] Alternatively, we can consider temporal adaptive modulation. Specifically, the transmitter can use a pilot tone to monitor the atmospheric fading over the channel and adjust the transmitted data rate to match the fading. This report will be concerned exclusively with the last technique.

The concept of variable-rate, channel-measurement transmitters has been successfully applied at microwave frequencies in schemes such as the JANET meteor-burst communication system.[5] At optical frequencies, however, we have an additional burden in that spatial variations in our signals are much more important than in the microwave region. Also, for the case of optical direct-detection receivers, we must contend with Poisson statistics instead of the more familiar Gaussian statistics. Another difficulty is that optical signals transmitted through the atmosphere are subjected to log-normal fading,[6-8] and integral expressions involving the log-normal probability density are often mathematically intractable.

In the rest of this report, we shall focus on the problem of adaptive, variable-rate

optical transmission of binary orthogonal signals over an atmospheric channel. We have chosen to examine this detection problem for two optical communication links: one established from the Earth to a synchronous satellite (a ground-to-space link), and one entirely in the atmosphere (a ground-to-ground link). We shall be primarily concerned with the single-detector case, in which spatial diversity is either unavailable or ignored for simplicity.

In order to establish convenient notation, and to provide a reference frame for the variable-rate results, we shall analyze several nonadaptive, fixed-rate optical communication systems. We shall derive the relevant atmospheric fading statistics for the cases of heterodyne- and direct-detection receiver, and then evaluate the performance of fixed-rate systems for these two cases. To use adaptive-transmission techniques, we must be able to measure the atmospheric channel fading. We shall examine atmospheric reciprocity and the way in which the relatively long fading coherence time can be exploited to provide channel-state information through the use of a pilot-tone probe. Based on these channel measurements, we shall derive some efficient variable-rate transmission strategies, and compare the resulting performance with that of the fixed-rate optical communication systems. Finally, we shall conclude by comparing the performance of our variable-rate schemes with systems employing adaptive spatial modulation or spatial diversity techniques.

II. NONADAPTIVE OPTICAL COMMUNICATION THROUGH THE ATMOSPHERE

2.1 ATMOSPHERIC FADING

Consider an optical communication link between the Earth and a synchronous satellite, which we call a ground-to-space system. As shown in Fig. 1, the ground and space antennas are represented by the parallel planar apertures R_1 and R_3, whose axes are on a common line. The imaginary, infinite plane R_2 is parallel to planes R_1 and R_3 and tangent to the "top" of the atmosphere. Propagation between planes R_1 and R_2 separated by a distance d_a on the order of kilometers, occurs through the clear turbulent atmosphere. Propagation between planes R_2 and R_3, separated by a distance d_f of approximately 40,000 km, is through free space.

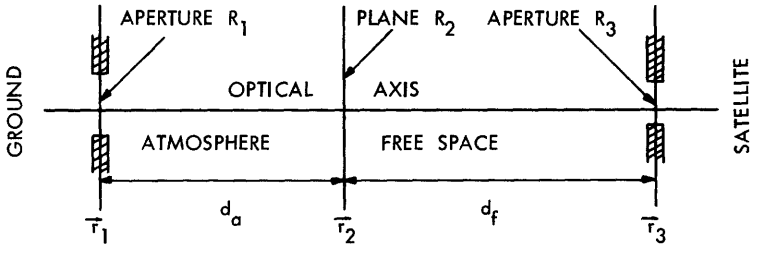

Fig. 1. Channel model for optical ground-to-space link.

Under the assumptions that our information signals are narrow-band relative to the carrier frequency f_c, and the atmosphere-free space channel is nondepolarizing,[9] if we communicate with a single transverse polarization component we can represent the electric field at any point $\vec{r}$ in space and at some time t by

$$\epsilon(\vec{r}, t) = \mathrm{Re}\left[E(\vec{r}, t)\, e^{j2\pi f_c t}\right], \tag{1}$$

where $E(\vec{r}, t)$ is the complex amplitude or envelope of the field. Henceforth, we shall deal mainly with complex field amplitudes, suppressing the carrier. We shall assume that the complex field amplitude of the transmitted information signal can be separated into the product of a spatial and a time-variant waveform. As a reminder that we are now concerned with ground-to-space propagation, and to avoid ambiguity when we later introduce a space-to-ground pilot tone to probe the channel, we shall represent the spatial component of the complex envelope of the field in the R_2-plane by $\underset{\rightarrow}{U}_i(\vec{r}_i)$, $i = 1, 2, 3$, where the arrow indicates the direction of field propagation in the model of Fig. 1.

Thus the complex field amplitude of the information signal transmitted from the ground terminal is given by

$$E_t(\vec{r}_1, t) = \sqrt{\xi}\ \underset{\rightarrow}{U}_1(\vec{r}_1)\ s(t); \qquad \vec{r}_1 \in R_1,\ t \in \mathcal{T}, \tag{2}$$

where $\mathcal{T}$ is the signal baud of duration T seconds. The expression in Eq. 2 is normalized so that the transmitted energy is simply

$$\int_{R_1} d\vec{r}_1 \int_{\mathcal{T}} dt\ |E_t(\vec{r}_1, t)|^2 = \xi \text{ joules.} \tag{3}$$

To this end, we arrange to have

$$\int_{\mathcal{T}} dt\ |s(t)|^2 = 1 \tag{4}$$

and choose the spatial modulation to have the form

$$\underset{\rightarrow}{U}_1(\vec{r}_1) = \frac{1}{\sqrt{A_t}}\, e^{jk\vec{\theta}\cdot\vec{r}_1}; \qquad k = \frac{2\pi}{\lambda},\ \vec{r}_1 \in R_1, \tag{5}$$

where A_t is the area of transmitting aperture R_1. The implication of Eq. 5 is that the signal transmitted by a laser of wavelength λ in the ground station is a collimated section of a plane wave with a tilted phase front. This tilt is characterized by the direction cosine vector $\vec{\theta}$ relative to the optical axis.

Let us now examine the field received at aperture R_3. We have previously assumed that the atmospheric turbulence causes negligible depolarization, and that the transmitted field is linearly polarized. We shall further assume that the coherence bandwidth of the turbulent channel exceeds the bandwidth of s(t),[10] and that channel multipath can be neglected.[11] For convenience we shall ignore the fixed channel propagation time delay from transmitter to receiver. Finally, we shall assume that the signal baud duration T is less than the coherence time T_c of the turbulent atmosphere. Then the complex envelope of the received field can be written in the form

$$E_r(\vec{r}_3, t) = \underbrace{\sqrt{\xi}\ \underset{\rightarrow}{U}_3(\vec{r}_3)\ s(t)}_{E_o(\vec{r}_3, t)} + E_b(\vec{r}_3, t); \qquad \vec{r}_3 \in R_3,\ t \in \mathcal{T} \tag{6}$$

The complex, zero-mean, Gaussian random process $E_b(\vec{r}_3, t)$ represents the relevant polarization component of the additive noise field, which accounts for background light.[12] The real and imaginary parts of $E_b(\vec{r}_3, t)$ are assumed to be statistically independent, identically distributed, and stationary in time and space. Furthermore, $E_b(\vec{r}_3, t)$ can be essentially treated as a spatially and temporally white random process:

$$\overline{E_b(\vec{r}_3, t)\, E_b^*(\vec{r}_3', t')} \cong 2N_b\lambda^2 u_o(\vec{r}_3 - \vec{r}_3')\, u_o(t-t'), \tag{7}$$

where N_b is the radiance of the relevant polarization component of the background light, λ is the wavelength of the optical carrier signal, and $u_o(\cdot)$ is the unit impulse function.

To determine $\underset{\rightarrow}{U}_3(\vec{r}_3)$, we note that the system of Fig. 1 is linear because of the linearity of Maxwell's equations. We can therefore define an impulse response or Green's function $\underset{\rightarrow}{h}_a(\vec{r}_2, \vec{r}_1)$ to characterize the propagation of complex amplitudes of electric fields through the atmosphere from plane R_1 to plane R_2. Similarly, we define $\underset{\rightarrow}{h}_f(\vec{r}_3, \vec{r}_2)$ for propagation through free space from plane R_2 to plane R_3. Then we have

$$\underset{\rightarrow}{U}_3(\vec{r}_3) = \int_{R_2} d\vec{r}_2 \; \underset{\rightarrow}{h}_f(\vec{r}_3, \vec{r}_2) \int_{R_1} d\vec{r}_1 \; \underset{\rightarrow}{h}_a(\vec{r}_2, \vec{r}_1) \; \underset{\rightarrow}{U}_1(\vec{r}_1)$$

$$= \frac{1}{\sqrt{A_t}} \int_{R_1} d\vec{r}_1 \int_{R_2} d\vec{r}_2 \; \underset{\rightarrow}{h}_a(\vec{r}_2, \vec{r}_1) \; \underset{\rightarrow}{h}_f(\vec{r}_3, \vec{r}_2) \, e^{jk\vec{\theta} \cdot \vec{r}_1}; \qquad \vec{r}_3 \in R_3. \tag{8}$$

For a satellite at synchronous altitude, d_f is generally large enough for typical transmitting and receiving apertures that we can accurately approximate the free-space impulse response by

$$\underset{\rightarrow}{h}_f(\vec{r}_3, \vec{r}_2) \cong - \frac{j \, e^{jkd_f}}{\lambda d_f}; \qquad \vec{r}_3 \in R_3. \tag{9}$$

Just as we ignored the fixed channel propagation time delay in Eq. 6, we shall hereafter ignore the constant phase delay $-j \, e^{jkd_f}$ in Eq. 9. Furthermore, the atmosphere is point-reciprocal,[13] which means that for a single atmospheric channel state (that is, within a temporal coherence interval), we have

$$\underset{\rightarrow}{h}_a(\vec{r}_2, \vec{r}_1) = \underset{\leftarrow}{h}_a(\vec{r}_1, \vec{r}_2); \qquad \vec{r}_1 \in R_1, \tag{10}$$

where $\underset{\leftarrow}{h}_a(\vec{r}_1, \vec{r}_2)$ is the impulse response for complex field amplitude propagation through the atmosphere from plane R_2 to plane R_1. We can therefore rewrite Eq. 8 in the form

$$\underset{\rightarrow}{U}_3(\vec{r}_3) = \frac{1}{\lambda d_f \sqrt{A_t}} \int_{R_1} d\vec{r}_1 \, e^{jk\vec{\theta} \cdot \vec{r}_1} \left[\int_{R_2} d\vec{r}_2 \; \underset{\leftarrow}{h}_a(\vec{r}_1, \vec{r}_2) \right]; \qquad \vec{r}_3 \in R_3. \tag{11}$$

The term in brackets in Eq. 11 is the atmospheric perturbation of an infinite plane wave transmitted from plane R_2 to plane R_1. Statistically, it can be represented by a complex log-normal random process of the form[14]

$$\int_{R_2} d\vec{r}_2 \; \underset{\leftarrow}{h}_a(\vec{r}_1, \vec{r}_2) = Z \, e^{\gamma(\vec{r}_1)} = Z \, \exp[\chi(\vec{r}_1) + j\phi(\vec{r}_1)], \tag{12}$$

where $\gamma(\vec{r}_1)$ is a complex Gaussian random process whose real and imaginary parts,

$\chi(\vec{r}_1)$ and $\phi(\vec{r}_1)$, are assumed to be temporally and spatially stationary and often, for simplicity, statistically independent, although this last assumption is not well justified physically.[15] The normalization constant Z can be chosen so that $\overline{\left| e^{\gamma(\vec{r}_1)} \right|^2} = 1$, which implies that $m_\chi = -\sigma_\chi^2$, where m_χ and σ_χ^2 are the mean and variance of the amplitude term $\chi(\vec{r}_1)$. The phase term $\phi(\vec{r}_1)$ has a sufficiently large variance at any point $\vec{r}_1$ so that it appears to be uniformly distributed over $(0, 2\pi)$.[16] The spatial coherence area $A_{c\chi}$ of $\chi(\vec{r}_1)$ is typically larger than the phase coherence area $A_{c\phi}$, so that $A_{c\phi}$ also represents a spatial coherence area of $e^{\gamma(\vec{r}_1)}$.

Therefore, Eq. 11 can be simplified to read

$$\underset{\rightarrow}{U}_3(\vec{r}_3) = \frac{\sqrt{A_t}}{\lambda d_f} u e^{j\psi}; \qquad \vec{r}_3 \in R_3, \tag{13}$$

where we have defined the complex random fading parameter with amplitude u and phase ψ to be

$$u e^{j\psi} \equiv \frac{1}{A_t} \int_{R_1} d\vec{r}_1 \, e^{jk\vec{\theta} \cdot \vec{r}_1} \, Z \, e^{\gamma(\vec{r}_1)}. \tag{14}$$

Equation 13 demonstrates that for typical transmitting and receiving apertures for which the approximation of Eq. 9 is accurate, the synchronous satellite receives a single spatial mode of the faded signal field at the top of the atmosphere; that is, the received signal field is spatially coherent over aperture R_3.

Let us now examine the statistical behavior of the fading parameter $u e^{j\psi}$ for several special cases: (i) If $A_t \leq A_{c\phi}$, then the random process $e^{\gamma(\vec{r}_1)}$ can be represented over the entire aperture R_1 by the random variable $e^{\gamma} = \exp(\chi + j\phi)$. By Eq. 14, the amplitude fading parameter is then given by

$$u = \frac{1}{A_t} \left| \int_{R_1} d\vec{r}_1 \, e^{jk\vec{\theta} \cdot \vec{r}_1} \right| Z \, e^{\chi} \equiv C(\vec{\theta}) \, Z \, e^{\chi}, \tag{15}$$

so that u is a real log-normal random variable. The phase term ψ is uniformly distributed over $(0, 2\pi)$, since ϕ is uniform over $(0, 2\pi)$. (ii) If A_t is slightly larger than $A_{c\phi}$, the random process $e^{\gamma(\vec{r}_1)}$ has an approximately linear phase tilt over aperture R_1:

$$e^{\gamma(\vec{r}_1)} \cong \exp(\chi + j\phi + jk\vec{\phi}_t \cdot \vec{r}_1); \qquad \vec{r}_1 \in R_1, \tag{16}$$

where the tilt is characterized by a random direction cosine vector $\vec{\phi}_t$. Then we have

$$u \cong \frac{1}{A_t} \left| \int_{R_1} d\vec{r}_1 \, e^{jk(\vec{\theta}+\vec{\phi}_t)\cdot\vec{r}_1} \right| Z\, e^{\chi}; \tag{17}$$

the statistical behavior of the amplitude fading parameter u is difficult to evaluate.[17]

(iii) Now suppose aperture R_1 is large enough to contain many spatial coherence areas of $e^{\gamma(\vec{r}_1)}$. Stated another way, suppose $A_t \gg A_{c\chi}$. In this case, it has been demonstrated theoretically that u is essentially a Rayleigh random variable.[18] In fact, a similar theoretical technique is adopted in Appendix A to show that, for sufficiently large apertures R_1, $ue^{j\psi}$ appears to be a zero-mean, complex Gaussian random variable whose real and imaginary parts are identically distributed and statistically independent. This implies that u is Rayleigh, ψ is uniform over $(0, 2\pi)$, and u and ψ are independent. This result is supported by Halme's computer simulation analysis.[19]

From Eqs. 6 and 13, we see that the signal field received at the satellite has complex envelope

$$E_o(\vec{r}_3, t) = \frac{\sqrt{\xi A_t}}{\lambda d_f} ue^{j\psi} s(t); \qquad \vec{r}_3 \in R_3, \; t \in \mathcal{T}. \tag{18}$$

The corresponding signal energy received at the satellite aperture R_3 during a baud interval, averaged over the fading is then

$$E\left[\int_{R_3} d\vec{r}_3 \int_{\mathcal{T}} dt \, |E_o(\vec{r}_3, t)|^2\right] = \overline{u^2} \, \frac{\xi A_t A_r}{\lambda^2 d_f^2} \equiv \overline{u^2} \, E_o, \tag{19}$$

where A_r is the area of receiving aperture R_3. Using Eq. 14 and the covariance function for $e^{\gamma(\vec{r}_1)}$, we can show that $\overline{u^2}$, and hence the average received signal energy, is maximized when the transmitted phase front tilt $\vec{\theta} = \vec{0}$.[20]

Let us now leave the ground-to-space link to consider briefly an optical communication system that is entirely in the atmosphere, such as a ground-to-ground link. We shall use a modified version of the channel model of Fig. 1 (see Fig. 2).

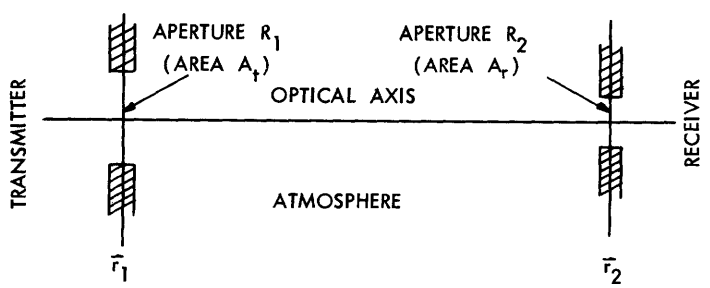

Fig. 2. Channel model for optical ground-to-ground link.

The transmitted information signal is assumed to be similar to that defined by Eqs. 2-5 for the ground-to-space link, except that for simplicity the phase-front tilt $\vec{\theta}$ relative to the optical axis is set to $\vec{0}$:

$$E_t(\vec{r}_1, t) = \sqrt{\xi}\ \underset{\rightarrow}{U}_1(\vec{r}_1)\ s(t); \qquad \vec{r}_1 \in R_1,\ t \in \mathcal{T}, \tag{20}$$

where

$$\int_{\mathcal{T}} dt\ |s(t)|^2 = 1 \tag{21}$$

and

$$\underset{\rightarrow}{U}_1(\vec{r}_1) = \frac{1}{\sqrt{A_t}}; \qquad \vec{r}_1 \in R_1. \tag{22}$$

Making the same assumptions that led to Eq. 6, we can represent the complex amplitude of the received field by

$$E_r(\vec{r}_2, t) = \underbrace{\sqrt{\xi}\ \underset{\rightarrow}{U}_2(\vec{r}_2)\ s(t)}_{E_o(\vec{r}_2, t)} + E_b(\vec{r}_2, t); \qquad \vec{r}_2 \in R_2,\ t \in \mathcal{T}, \tag{23}$$

where

$$\underset{\rightarrow}{U}_2(\vec{r}_2) = \frac{1}{\sqrt{A_t}} \int_{R_1} d\vec{r}_1\ \underset{\rightarrow}{h}_a(\vec{r}_2, \vec{r}_1); \qquad \vec{r}_2 \in R_2, \tag{24}$$

and $\underset{\rightarrow}{h}_a(\vec{r}_2, \vec{r}_1)$ is again the impulse response for complex field amplitude propagation through the atmosphere from plane R_1 to plane R_2. Analogously to Eq. 12, we can write $\underset{\rightarrow}{U}_2(\vec{r}_2)$ in the form

$$\underset{\rightarrow}{U}_2(\vec{r}_2) = \frac{1}{\sqrt{A_t}}\ Z'\ e^{\gamma'(\vec{r}_2)}, \qquad \vec{r}_2 \in R_2 \tag{25}$$

where $\gamma(\vec{r}_2)$ is a complex Gaussian random process with the same general statistical properties as $\gamma(\vec{r}_1)$, and, under the assumption that $\underset{\rightarrow}{U}_2(\vec{r}_2)$ would be a plane wave over aperture R_2 in the absence of atmospheric turbulence, Z' can again be chosen so[21] that $\overline{\left| e^{\gamma'(\vec{r}_2)} \right|^2} = 1$.

In the case of the ground-to-space link, we have seen in Eq. 13 that the received signal field was spatially coherent over the receiving aperture, regardless of the aperture size. For the ground-to-ground link, Eq. 25 tells us that the received signal field is generally incoherent over the receiving aperture, except for sufficiently small apertures R_2.

2.2 HETERODYNE-DETECTION RECEIVERS

We shall now analyze the performances of our fixed-rate optical communication links for the case in which heterodyne-detection receivers are used. Helstrom has argued that if the optical heterodyne receivers have a sufficiently intense local-oscillator field, the detection problem is reduced to the familiar form of an IF signal and additive Gaussian noise;[22] for convenience, his arguments are reviewed in Appendix B.

Applying the results of Appendix B to the ground-to-space link, the angular plane-wave component of $\underset{\rightarrow}{U}_3(\vec{r}_3)$ with direction cosine vector $\vec{\phi}$ is given by

$$\underset{\rightarrow}{U}_r(\vec{\phi}) \equiv \int_{R_3} d\vec{r}_3 \, \underset{\rightarrow}{U}_3(\vec{r}_3) \, e^{-jk\vec{\phi}\cdot\vec{r}_3} = \frac{\sqrt{A_t}}{\lambda d_f} \, u e^{j\psi} \int_{R_3} d\vec{r}_3 \, e^{-jk\vec{\phi}\cdot\vec{r}_3}, \tag{26}$$

using Eq. 13 and Eq. B8. Inserting Eq. 26 into Eq. B14, we find that the output of the heterodyne processor, conditioned on the atmospheric channel state, reduces to the standard form

$$r(t) = \sqrt{2E_s} \, u|s(t)| \cos(2\pi f_h t + \psi_h) + n(t); \qquad t \in \mathcal{T}, \tag{27}$$

where

$$E_s = \frac{\xi A_t}{\lambda^2 d_f^2 A_r} \left| \int_{R_3} d\vec{r}_3 \, e^{-jk\vec{\phi}\cdot\vec{r}_3} \right|^2, \tag{28}$$

and the noise term n(t) is a zero-mean, white Gaussian random process with power density given by Eq. B18. Also, f_h is the frequency offset of the local-oscillator field from the signal carrier frequency f_c, and the phase term ψ_h is uniformly distributed over $(0, 2\pi)$ because ψ is uniform over $(0, 2\pi)$.

The heterodyne receiver extracts the temporal variation of one spatial mode of the received field. It has a very narrow field of view, and if the local-oscillator field is a plane wave in the direction $\vec{\phi}$, it only extracts those plane-wave components of the received field whose angle of propagation differs from $\vec{\phi}$ by λ/D radians, where λ is the wavelength, and D is the diameter of the (circular) receiving aperture R_3.[23] Despite the fading, because of the great distance between the ground and the satellite, essentially all of the received signal energy is contained in the plane-wave component travelling along the optical axis. Consequently, the energy parameter E_s has a sharp maximum at $\vec{\phi} = \vec{0}$, where E_s has the value E_o of Eq. 19, and E_s is approximately zero elsewhere. Thus for $\vec{\phi} = \vec{0}$, the heterodyne receiver recovers all of the signal energy incident on aperture R_3. For the sake of generality, we leave $\vec{\phi}$ explicitly in our calculations, but because of the considerations above we would always use $\vec{\phi} = \vec{0}$ in practice.

Turning next to Eq. 25 and the ground-to-ground link, we can write

$$\underline{U}_r(\vec{\phi}) = \int_{R_2} d\vec{r}_2\, \underline{U}_2(\vec{r}_2)\, e^{-jk\vec{\phi}\cdot\vec{r}_2} = \frac{A_r}{\sqrt{A_t}}\, ue^{j\psi}, \tag{29}$$

where this time we define a complex fading parameter

$$ue^{j\psi} \equiv \frac{1}{A_r}\int_{R_2} d\vec{r}_2\, e^{-jk\vec{\phi}\cdot\vec{r}_2}\, Z'\, e^{\gamma'(\vec{r}_2)}. \tag{30}$$

The statistical properties of $ue^{j\psi}$ defined in Eq. 30 are analogous to those of the fading random variable defined in Eq. 14, except that they now depend on the relative sizes of aperture R_2 and the spatial coherence area $A_{c\phi'}$ of $e^{\gamma'(\vec{r}_2)}$ (which depends on the size of aperture R_1). In particular, if $A_r < A_{c\phi'}$, u is log-normal:

$$u = \frac{1}{A_r}\left|\int_{R_2} d\vec{r}_2\, e^{-jk\vec{\phi}\cdot\vec{r}_2}\right| Z'\, e^{\chi'} \equiv C'(\vec{\phi})\, Z'\, e^{\chi'}. \tag{31}$$

If $A_r \gg A_{c\chi'}$, u is a Rayleigh random variable. The phase term ψ is always essentially uniform over $(0, 2\pi)$.

Thus, an optical heterodyne receiver in the ground-to-ground link can be arranged to produce an output r(t) in the standard form of Eq. 27, with an energy parameter

$$E_s = \xi\, \frac{A_r}{A_t}. \tag{32}$$

As in the case of the ground-to-space link, setting $\vec{\phi}$ equal to $\vec{0}$ maximizes the average signal energy $\overline{u^2}E_s$ in r(t). It appears at first glance from Eq. 32 that we should make the transmitting aperture small to increase the average received signal energy, but this is not the case. For example, if we decrease A_t, there is an accompanying spread in the transmitted beamwidth because of diffraction through aperture R_1. This beamwidth spreading is reflected in a decrease in Z' so that $\overline{u^2}$ decreases to more than offset the increase in E_s.

The single-detector heterodyne-receiver model characterized by Eq. 27 is therefore valid for both the ground-to-space and the ground-to-ground communication links. We should note at this time, however, that a single-detector receiver is not optimal for the ground-to-ground channel when $A_r > A_{c\phi'}$ so that the received signal field $E_o(\vec{r}_2, t)$ is spatially incoherent over aperture R_2. As we have said, the heterodyne receiver is sensitive to only a single spatial mode; consequently, much of the received signal energy would be lost if $E_o(\vec{r}_2, t)$ were incoherent over aperture R_2. A more optimal receiver would use an array of heterodyne detectors to extract signal information from each of the spatial modes of $E_o(\vec{r}_2, t)$ over aperture R_2, thereby taking advantage of the spatial

diversity in the system[24, 25] (see Section V).

We shall now consider the binary detection problem for our optical communication links, using the optimal single-detector model of Eq. 27. We shall treat the case in which we use equiprobable signals of equal energy. Under each of the two hypotheses, H_1 and H_2, r(t) will have the following form, modified from Eq. 27, conditioned on the atmospheric channel state:

$$r(t) = \sqrt{2E_s}\, u\,|s_i(t)|\, \cos(2\pi f_h t + \psi_h) + n(t); \qquad t \in \mathcal{T},\ H_i,\ i = 1, 2, \tag{33}$$

where

$$\int_{\mathcal{T}} dt\ s_i(t)\, s_j^*(t) = \delta_{ij}; \qquad i, j = 1, 2, \tag{34}$$

and δ_{ij} is the Kronecker delta. The binary decision rule has the form[26]

$$\left| \int_{\mathcal{T}} dt\ r(t)\,|s_1(t)|\, e^{j2\pi f_c t} \right|^2 \underset{H_2}{\overset{H_1}{\gtrless}} \left| \int_{\mathcal{T}} dt\ r(t)\,|s_2(t)|\, e^{j2\pi f_c t} \right|^2 \tag{35}$$

independent of the atmospheric channel fading. The probability of a detection error, conditioned on the fading parameter $ue^{j\psi}$, is given by [27]

$$P(\epsilon\,|\,u, \psi) = P(\epsilon\,|\,u) = \frac{1}{2} \exp\left(-\frac{u^2 E_s}{2N_o}\right), \tag{36}$$

which depends only on the amplitude fading parameter u. Averaging $P(\epsilon\,|\,u)$ over the atmospheric fading, the probability of a communication error on a single transmission is

$$P(\epsilon) = \overline{P(\epsilon\,|\,u)}^{\,u} = \frac{1}{2} \int_0^\infty du\ p(u) \exp\left(-\frac{u^2 E_s}{2N_o}\right), \tag{37}$$

where p(u) is the probability density function of u.

Consider first the special case in which u is a Rayleigh random variable, with second moment $\overline{u^2}$ denoted by a

$$p(u) = \frac{2u}{a} e^{-\frac{u^2}{a}} u_{-1}(u), \tag{38}$$

where, using Eq. 14 for the ground-to-space case,

$$a \equiv \overline{u^2} = \frac{Z^2}{A_t^2} \int_{R_1} d\vec{r}_1 \int_{R_1} d\vec{r}_1'\ e^{jk\vec{\theta}\cdot(\vec{r}_1 - \vec{r}_1')}\ \overline{\gamma(\vec{r}_1)\ \gamma^*(\vec{r}_1')}, \tag{39}$$

and $u_{-1}(\cdot)$ is the unit step function. Then we find that[28]

$$P(\epsilon) = \frac{1}{2 + \frac{aE_s}{N_o}}. \tag{40}$$

Now let us consider the case in which u is a log-normal random variable. For the ground-to-space link, using Eq. 15 and the fact that $m_\chi = \sigma_\chi^2$, we have

$$\overline{u^2} = Z^2 C^2(\vec{\theta}), \tag{41}$$

and

$$p(u) = \frac{1}{u\sigma_\chi \sqrt{2\pi}} \exp\left\{-\frac{1}{2\sigma_\chi^2}\left[\ln \frac{1}{ZC(\vec{\theta})} + \sigma_\chi^2\right]^2\right\} u_{-1}(u). \tag{42}$$

Then we find that

$$P(\epsilon) = \frac{1}{2} \mathrm{Fr}\left[\frac{Z^2 C^2(\vec{\theta})\, E_s}{2N_o},\ 0;\ \sigma_\chi\right], \tag{43}$$

where the "frustration" function Fr [. , . ; .] is defined as[29]

$$\mathrm{Fr}\left[\alpha, \beta; \sigma\right] \equiv \int_0^\infty dv\, I_o(2\beta\sqrt{\alpha}\, v)\, e^{-\alpha v^2} \frac{1}{v\sigma\sqrt{2\pi}} \exp\left(-\frac{(\ln v + \sigma^2)^2}{2\sigma^2}\right); \tag{44}$$

$I_o(\cdot)$ is the zero-order modified Bessel function of the first kind, and E_s is given by Eq. 28. Similarly, for the ground-to-ground link, using Eqs. 31 and 32, we can show that $P(\epsilon)$ has the same form as in Eq. 43:

$$P(\epsilon) = \frac{1}{2} \mathrm{Fr}\left[\frac{Z'^2 C'^2(\vec{\phi})\, E_s}{2N_o},\ 0;\ \sigma_{\chi'}\right]. \tag{45}$$

Although the frustration function cannot be evaluated explicitly, reasonably tight upper and lower bounds have been determined for it,[30] and it has been evaluated on the computer by using numerical integration techniques.[31, 32]

2.3 DIRECT-DETECTION RECEIVERS

Now let us turn our attention to the case in which our fixed-rate optical communication systems use direct or energy detection in place of heterodyne detection. As in Eq. B1, the complex envelope of the field reaching the receiver aperture R, for either the ground-to-space case or the ground-to-ground case has the general form

$$E_r(\vec{r}, t) = \underbrace{\sqrt{\xi}\ \underline{U}(\vec{r})\ s(t)}_{E_o(\vec{r}, t)} + E_b(\vec{r}, t); \qquad \vec{r} \in R,\ t \in \mathcal{T}, \tag{46}$$

where $E_o(\vec{r}, t)$ is the complex envelope of the faded received signal field, and the noise term $E_b(\vec{r}, t)$ is a white Gaussian random process over the spatial and temporal modes of $E_o(\vec{r}, t)$ in aperture R.

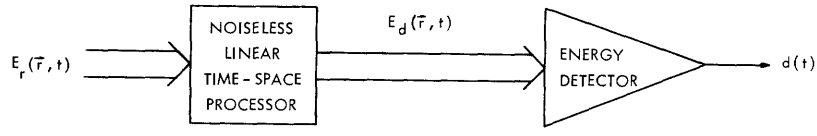

Fig. 3. Block diagram of direct-detection receiver.

The linear field processor shown in the block diagram of Fig. 3 typically contains temporal and spatial filters designed to limit the background noise while passing essentially all of the signal field,[33] so that we can write

$$E_d(\vec{r}, t) \cong E_o(\vec{r}, t) + E_{db}(\vec{r}, t); \qquad \vec{r} \in R,\ t \in \mathcal{T}, \tag{47}$$

where the noise variance $\overline{|E_{db}(\vec{r}, t)|^2}$ is now finite.

The detector output d(t), conditioned on the atmospheric channel state and the background noise, is a filtered Poisson process with rate parameter $\mu(t)$ defined by Eq. B5. Often, after averaging over the Gaussian background noise, d(t) can be treated as a conditional inhomogeneous Poisson process with rate parameter

$$\mu(t) = \frac{\eta}{h\nu} \int_R d\vec{r} \left[|E_o(\vec{r}, t)|^2 + \overline{|E_{db}(\vec{r}, t)|^2} \right], \tag{48}$$

provided that some conditions, which are usually satisfied by practical communication systems and natural background radiation, are met.[34-36]

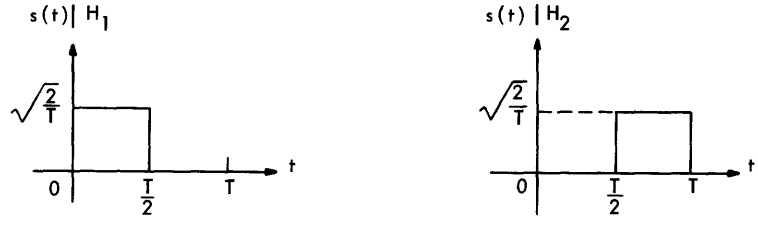

Fig. 4. Binary PPM signals for optical communication links.

We shall now determine error probabilities for our optical links for the case of binary PPM communication. Suppose that under either of two equiprobable hypotheses, s(t) is real and has the form indicated in Fig. 4. Then, under hypothesis H_i, i = 1, 2, Eq. 48 reduces to the form

$$\mu(t)\,|\,H_i = \begin{cases} u^2\mu_s\delta_{i1} + \mu_n; & 0 < t < \frac{T}{2} \\ u^2\mu_s\delta_{i2} + \mu_n; & \frac{T}{2} < t < T \end{cases} \tag{49}$$

where we have used Eqs. 46 and 47 to define

$$u^2\mu_s \equiv \frac{2\eta\xi}{h\nu T}\int_R d\vec{r}\;|\underset{\rightarrow}{U}(\vec{r})|^2 \tag{50}$$

in terms of a real fading random variable u which will be specified below, and

$$\mu_n \equiv \frac{\eta}{h\nu}\int_R d\vec{r}\;\overline{|E_{db}(\vec{r},t)|^2}. \tag{51}$$

For the ground-to-space link, substituting Eq. 13 in Eq. 50, we can identify

$$\mu_s \equiv \frac{2\eta\xi A_t A_r}{h\nu T\lambda^2 d_f^2}, \tag{52}$$

with u defined by Eq. 14:

$$u \equiv \frac{Z}{A_t}\left|\int_{R_1} d\vec{r}_1\, e^{jk\vec{\theta}\cdot\vec{r}_1}\, e^{\gamma(\vec{r}_1)}\right|. \tag{53}$$

As discussed in section 2.1, u is log-normal if $A_t < A_{c\phi}$, and u is essentially Rayleigh when $A_t \gg A_{c\chi}$.

Using Eq. 25 in Eq. 50 for the ground-to-ground link, we can write

$$\mu_s \equiv \frac{2\eta\xi A_r}{h\nu T A_t}, \tag{54}$$

and

$$u^2 = \frac{A_t}{A_r}\int_{R_2} d\vec{r}_2\;|\underset{\rightarrow}{U}_2(\vec{r}_2)|^2 = \frac{Z'^2}{A_r}\int_{R_2} d\vec{r}_2\, e^{2\chi'(\vec{r}_2)}. \tag{55}$$

When $A_r < A_{c\chi'}$, we can deduce from Eq. 55 that u is a log-normal random variable given by

$$u = Z' e^{\chi'}. \tag{56}$$

For the case $A_r \gg A_{c\chi'}$, theoretical studies have shown that u^2, and hence u, is accurately approximated by a log-normal random variable.[37-39]

Let us now determine the probability of a detection error on a single transmission, conditioned on the fading parameter u. Denote the number of counts registered by the direct detector in the first- and second-half signal bauds of duration T/2 by n_1 and n_2; under the Poisson model above, n_1 and n_2 are statistically independent with conditional distributions given by

$$\Pr\left[n_j \mid H_i, u\right] = \frac{1}{n_j!}\left[\left(u^2\mu_s\delta_{ij}+\mu_n\right)\frac{T}{2}\right]^{n_j} \exp\left\{-\left[\left(u^2\mu_s\delta_{ij}+\mu_n\right)\frac{T}{2}\right]\right\}; \quad i,j = 1,2. \tag{57}$$

The optimum decision rule is that of a counting receiver:

$$n_1 \underset{H_2}{\overset{H_1}{\gtrless}} n_2 \tag{58}$$

with the event $n_1 = n_2$ being decided by the flip of a fair coin. For convenience, we shall introduce the following parameter definitions:

$$K \equiv \overline{u^2}\mu_s\frac{T}{2} = \text{average signal counts/baud} \tag{59}$$

$$a \equiv \frac{\mu_s}{\mu_n}$$

$$\Delta \equiv \frac{K}{\mu_n T} = \frac{\overline{u^2}a}{2} = \frac{\text{average signal counts/baud}}{\text{average noise counts/baud}}.$$

Then, using Eqs. 57-59, we can show that the probability of error for a single baud, conditioned on u, is given by[40]

$$P(\epsilon \mid u) = \Pr\left[n_2 \geq n_1 \mid H_1, u\right] - \frac{1}{2}\Pr\left[n_1 = n_2 \mid H_1, u\right]$$

$$= Q_m\left[\sqrt{\frac{K}{\Delta}}, \sqrt{\frac{K}{\Delta}(1+u^2a)}\right] - \frac{1}{2}e^{-\frac{K}{2\Delta}(2+u^2a)} I_o\left(\frac{K}{\Delta}\sqrt{1+u^2a}\right), \tag{60}$$

where $Q_m(\cdot,\cdot)$ is Marcum's Q function of radar theory[41] which is defined by

$$Q_m(a,b) \equiv \int_b^\infty dx\, x\, e^{-\frac{1}{2}(x^2+a^2)} I_o(ax). \tag{61}$$

This function has been evaluated numerically on a computer and tabulated.[42] In Appendix C, a useful approximation is derived for the Marcum Q function.

The problem of averaging the conditional error probability $P(\epsilon|u)$ in Eq. 60 over the atmospheric fading for the case in which u is Rayleigh has been considered elsewhere.[43] It is shown that for Rayleigh fading, the probability of a communication error on a single transmission is given by

$$P(\epsilon) = Q_m\left(\sqrt{\frac{K}{\Delta}}, \sqrt{\frac{K}{\Delta}}\right) - \frac{1}{2}\left(\frac{2K+1}{K+1}\right) e^{\frac{1}{2\Delta(K+1)}} Q_m\left(\sqrt{\frac{K^2}{\Delta(K+1)}}, \sqrt{\frac{K+1}{\Delta}}\right). \quad (62)$$

We can use the approximation derived in Appendix C to calculate an accurate approximation for $P(\epsilon)$ above. Using Eq. C10 in Eq. 62, we have

$$P(\epsilon) \cong \frac{1}{2} - \frac{1}{2}\left(\frac{2K+1}{K+1}\right) e^{\frac{1}{2\Delta(K+1)}} \sqrt{\frac{K+1}{K}}\, Q\left(\frac{1}{\sqrt{\Delta(K+1)}}\right); \qquad \sqrt{\frac{K}{\Delta}} \gg 0.4, \ \frac{K}{\Delta} \gg 1, \quad (63)$$

where $Q(\cdot)$ is the Gaussian Q function defined by[44]

$$Q(Z) \equiv \frac{1}{\sqrt{2\pi}} \int_Z^\infty dx\, e^{-x^2/2}. \quad (64)$$

The two restrictions on Eq. 63 can be replaced by the single sufficient condition $\sqrt{K/\Delta} \gg 1$. The Taylor series expansion for Q(Z) about Z = 0 is given by

$$Q(Z) = \frac{1}{2} - \frac{Z}{\sqrt{2\pi}} + \ldots . \quad (65)$$

Then, since $\sqrt{K/\Delta} \gg 1$ and $\sqrt{K\Delta} \gg 1$ imply that $K \gg 1$ for any Δ, we can use Eq. 65 in Eq. 63 to show that

$$P(\epsilon) \cong \frac{1}{\sqrt{2\pi K\Delta}}; \qquad \sqrt{\frac{K}{\Delta}} \gg 1, \ \sqrt{K\Delta} \gg 1. \quad (66)$$

It is convenient to rewrite Eq. 66, modifying the form of the restrictions as follows:

$$P(\epsilon) \cong \frac{1}{\sqrt{2\pi K\Delta}}; \qquad P(\epsilon) \ll \begin{cases} \dfrac{1}{\sqrt{2\pi}}; & \Delta \leq 1, \\ \dfrac{1}{\Delta\sqrt{2\pi}}; & \Delta \geq 1. \end{cases} \quad (67)$$

Equation 67 is an extremely useful approximation for $P(\epsilon)$ in the very interesting range where the probability of error is reasonably small.

Now let us consider the case in which we have log-normal fading. Unfortunately, our discussion will of necessity be brief: when u is log-normal, the evaluation of $P(\epsilon)$

involves an exceedingly difficult average of $P(\epsilon \mid u)$ over u which has yet to be successfully carried out. Bounds on $P(\epsilon)$ for the more general case of M-ary signalling have been attempted: however, even when $M = 2$ as in our problem, these bounds do not yet have an explicit form for general signal-to-noise ratios.[45, 46]

III. CHANNEL MEASUREMENT

In Section II, we determined the relevant atmospheric fading parameters for the optical ground-to-space and ground-to-ground links employing heterodyne or direct detection receivers. In order to design variable-rate transmitters that can adapt to the atmospheric channel state, we need to show that we can measure these fading parameters at the data-transmitter terminal.

3.1 GROUND-TO-SPACE LINK

We want to track the atmospheric fading over the optical ground-to-space link of Fig. 1 by using a satellite beacon to transmit a pilot tone down to the ground terminal. By exploiting atmospheric reciprocity, we shall show that the received beacon signal can be processed to yield channel-state information, which will allow us to employ adaptive transmission techniques on the uplink. This technique is feasible because all of the fading occurs in a narrow atmospheric layer (having a width d_a of the order of kilometers), which surrounds the Earth. Furthermore, the coherence time T_c of the atmospheric turbulence is of the order of a millisecond or more.[47,48] Consequently, a pilot tone can travel over the downlink and be processed by the ground terminal to determine the atmospheric fading, after which an information signal adapted to the fading can be sent over the uplink, all within the same atmospheric channel state.

Therefore, although the atmospheric fading is a time-variant random process, we shall restrict ourselves to a single atmospheric state in our analysis, and treat the fading as a random variable. The ground terminal transmits the information signal in the direction $\vec{\theta}$ relative to the optical axis, as indicated in Eqs. 2-5. For both the heterodyne and direct detection cases, the relevant complex fading parameter is $ue^{j\psi}$ defined by Eq. 14. The complex envelope $\underset{\rightarrow}{U}_3(\vec{r}_3)$ of the spatial term in the signal field received by the satellite is coherent over aperture R_3 and is written in terms of $ue^{j\psi}$ in Eq. 13. Combining Eqs. 8 and 26, we can represent the angular plane-wave component of $\underset{\rightarrow}{U}_3(\vec{r}_3)$ in an arbitrary direction $\vec{\alpha}$ by

$$\underset{\rightarrow}{U}_r(\vec{\alpha}) = \frac{1}{\sqrt{A_t}} \int_{R_1} d\vec{r}_1 \int_{R_2} d\vec{r}_2 \int_{R_3} d\vec{r}_3 \, \underset{\rightarrow}{h}_a(\vec{r}_2, \vec{r}_1) \, \underset{\rightarrow}{h}_f(\vec{r}_3, \vec{r}_2) \, e^{jk(\vec{\theta}\cdot\vec{r}_1 - \vec{\alpha}\cdot\vec{r}_3)}$$

$$= ue^{j\psi} \frac{\sqrt{A_t}}{\lambda d_f} \int_{R_3} d\vec{r}_3 \, e^{-jk\vec{\alpha}\cdot\vec{r}_3}. \tag{68}$$

We shall show that we can use a pilot tone transmitted from the satellite in the direction $-\vec{\alpha}$ to measure the quantity $\underset{\rightarrow}{U}_r(\vec{\alpha})$ at the ground terminal. Equation 68 shows us that $\underset{\rightarrow}{U}_r(\vec{\alpha})$ is proportional to $ue^{j\psi}$ for any value of $\vec{\alpha}$, and there is no reason to

set $\vec{\alpha}$ equal to the direction $\vec{\phi}$ of the local-oscillator field in the heterodyne-detection case.

Now let us probe the atmospheric channel fading by transmitting a collimated section of a plane wave through aperture R_3 in the direction $-\vec{\alpha}$ at a constant power level P_p. The transmitted pilot tone has a complex field amplitude.

$$E_{pt}(\vec{r}_3, t) = \sqrt{\frac{P_p}{A_r}}\, e^{-jk\vec{\alpha}\cdot\vec{r}_3} \equiv \sqrt{P_p}\ \underset{\rightarrow}{U}_3(\vec{r}_3); \qquad \vec{r}_3 \in R_3. \tag{69}$$

In our analysis, arrows under spatial components of fields will indicate the direction of propagation in reference to Fig. 1.

Under the same assumptions required to justify the form of the received field in Eq. 6, we can represent the pilot-tone signal field incident on aperture R_1 by

$$E_{ps}(\vec{r}_1, t) = \sqrt{P_p}\ \underset{\rightarrow}{U}_1(\vec{r}_1); \qquad \vec{r}_1 \in R_1, \tag{70}$$

where

$$\underset{\rightarrow}{U}_1(\vec{r}_1) = \frac{1}{\sqrt{A_r}} \int_{R_2} d\vec{r}_2 \int_{R_3} d\vec{r}_3\, \underset{\rightarrow}{h}_a(\vec{r}_1, \vec{r}_2)\, \underset{\rightarrow}{h}_f(\vec{r}_2, \vec{r}_3)\, e^{-jk\vec{\alpha}\cdot\vec{r}_3}; \qquad \vec{r}_1 \in R_1. \tag{71}$$

In Eq. 71 we have defined the impulse response $\underset{\rightarrow}{h}_f(\vec{r}_2, \vec{r}_3)$ to characterize complex field amplitude propagation through free space from R_3 to R_2, and $\underset{\rightarrow}{h}_a(\vec{r}_2, \vec{r}_1)$ for propagation through the atmosphere from R_2 to R_1.

Defining $\underset{\rightarrow}{U}_t(\vec{\beta})$ to be the angular plane-wave component of $\underset{\rightarrow}{U}_1(\vec{r}_1)$ over aperture R_1 in the direction $\vec{\beta}$, we can write

$$\underset{\rightarrow}{U}_t(\vec{\beta}) \equiv \int_{R_1} d\vec{r}_1\, \underset{\rightarrow}{U}_1(\vec{r}_1)\, e^{-jk\vec{\beta}\cdot\vec{r}_1}$$

$$= \frac{1}{\sqrt{A_r}} \int_{R_1} d\vec{r}_1 \int_{R_2} d\vec{r}_2 \int_{R_3} d\vec{r}_3\, \underset{\rightarrow}{h}_a(\vec{r}_1, \vec{r}_2)\, \underset{\rightarrow}{h}_f(\vec{r}_2, \vec{r}_3)\, e^{-jk(\vec{\beta}\cdot\vec{r}_1 + \vec{\alpha}\cdot\vec{r}_3)}. \tag{72}$$

Now the free-space channel is point-reciprocal, so that

$$\underset{\rightarrow}{h}_f(\vec{r}_3, \vec{r}_2) = \underset{\rightarrow}{h}_f(\vec{r}_2, \vec{r}_3). \tag{73}$$

Furthermore, since we are concerned with a single atmospheric channel state, the atmospheric reciprocity relation of Eq. 10 is applicable. Therefore, we find that

$$\underset{\rightarrow}{U}_r(\vec{\alpha}) = \sqrt{\frac{A_r}{A_t}}\, \underset{\leftarrow}{U}_t(-\vec{\theta})$$

$$= \sqrt{\frac{A_r}{P_p A_t}} \int_{R_1} d\vec{r}_1\, E_{ps}(\vec{r}_1, t)\, e^{jk\vec{\theta}\cdot\vec{r}_1}, \tag{74}$$

where $\underset{\leftarrow}{U}_t(-\vec{\theta})$ is the angular plane-wave component of $\underset{\leftarrow}{U}_1(\vec{r}_1)$ over aperture R_1 in the direction $-\vec{\theta}$, which is the reverse of the information transmission direction $\vec{\theta}$. Finally, from Eqs. 68 and 74, we can determine the desired relation between the ground-to-space channel fading parameter $ue^{j\psi}$ and the received pilot-tone complex field amplitude $E_{ps}(\vec{r}_1, t)$:

$$ue^{j\psi} = \frac{\lambda d_f \sqrt{A_r} \int_{R_1} d\vec{r}_1\, E_{ps}(\vec{r}_1, t)\, e^{jk\vec{\theta}\cdot\vec{r}_1}}{A_t \sqrt{P_p} \int_{R_3} d\vec{r}_3\, e^{-jk\vec{\alpha}\cdot\vec{r}_3}}. \tag{75}$$

Let us make a few comments about these results. The channel measurement scheme for the ground-to-space link is modelled in Fig. 5. We must emphasize the angular relationships between the information signal and the pilot tone. At the ground terminal we transmit the information signal in the direction $\vec{\theta}$. At the satellite, we can extract the angular plane-wave component $\underset{\rightarrow}{U}_r(\vec{\alpha})$ of the signal field incident on aperture R_3. As shown in Eq. 68, the atmospheric fading over this specific uplink channel, defined by the transmitter/receiver direction pair $(\vec{\theta}, \vec{\alpha})$, is characterized by the random variable $ue^{j\psi}$. To measure this fading parameter, we transmit a pilot tone through the satellite aperture in the direction $-\vec{\alpha}$, and extract the angular plane-wave component $\underset{\leftarrow}{U}_t(-\vec{\theta})$ of the pilot-tone signal field incident on aperture R_1, as indicated in Eq. 74.

Actually, as we saw in Eq. 68, for the ground-to-space link the same fading parameter $ue^{j\psi}$ applies to the channels specified by the direction pairs $(\vec{\theta}, \vec{\alpha})$ for any choice of $\vec{\alpha}$. This is because the signal field received by the satellite is coherent over aperture R_3; that is, the satellite intercepts only a single spatial mode of the faded signal field incident on plane R_2 at the top of the atmosphere. In fact, while it was mathematically convenient in our channel measurement analysis to think in terms of extracting $\underset{\rightarrow}{U}_r(\vec{\alpha})$ for some arbitrary direction $\vec{\alpha}$, this operation is not ordinarily performed by the satellite. The heterodyne detector extracts the particular plane-wave component $\underset{\rightarrow}{U}_r(\vec{\phi})$ as shown in Eq. 26, while the direct detector operates directly on the received field $\underset{\rightarrow}{U}_3(\vec{r}_3)$, which is a superposition of plane waves.

For a general optical communication link that possesses spatial diversity, however, such as the ground-to-ground link for large receiving apertures, the information

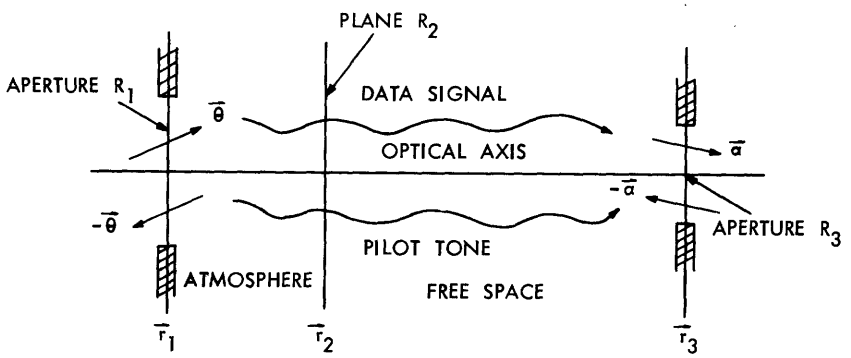

Fig. 5. Channel measurement diagram for optical ground-to-space link.

signal field is incoherent over the receiving aperture. Each independent spatial signal mode is specified by a different value of $\vec{\alpha}$ in the direction pair $(\vec{\theta}, \vec{\alpha})$, and is characterized by a different fading parameter of the form $ue^{j\psi}$. For a system with spatial diversity, an optimal adaptive transmission scheme requires that we transmit a separate pilot tone in an appropriate direction $-\vec{\alpha}$ for each independent spatial signal mode to measure each relevant fading parameter (see Section V).

Returning to the ground-to-space link, we remarked in section 2.1 that we would generally set the transmission direction $\vec{\theta}$ equal to $\vec{0}$ to maximize the average signal energy received by the satellite. (An important exception is the adaptive pointing system discussed below.) Since the direction $\vec{\alpha}$ in our channel measurement scheme above is arbitrary, Eq. 75 tells us that we should set $\vec{\alpha}$ equal to $\vec{0}$ in practice to maximize the average pilot-tone signal power reaching the ground terminal.

The channel measurement result of Eq. 75 affords the option of introducing adaptive pointing at the transmitter terminal to track out some of the atmospherically induced wavefront distortion, thereby increasing the signal energy received by the satellite.[49] This is a limited form of adaptive spatial modulation. In Section V, we shall discuss a more general technique. In the focal plane R_F of the lens in aperture R_1, the field resulting from the received pilot-tone signal $E_{ps}(\vec{r}_1, t)$ is given by

$$E_{pf}(\vec{r}_f, t) = \frac{e^{jk\frac{|\vec{r}_f|^2}{2f_\ell}}}{\lambda f_\ell} \int_{R_1} d\vec{r}_1 \, E_{ps}(\vec{r}_1, t)\, e^{-jk\frac{\vec{r}_f}{f_\ell}\cdot\vec{r}_1}; \quad \vec{r}_f \in R_F, \tag{76}$$

where λ is the wavelength of the pilot-tone signal, f_ℓ is the focal length of the lens in aperture R_1, and we have ignored phase terms that are constant over R_F.[50] Combining Eqs. 19, 75, and 76, we find that the conditional signal energy u^2E_o incident on aperture R_3 for a given atmospheric channel state satisfies the relation

$$u^2E_o = \frac{\xi\lambda^2 f_\ell^2 A_r^2 \left|E_{pf}(-f_\ell\vec{\theta}, t)\right|^2}{P_p A_t \left|\int_{R_3} d\vec{r}_3\, e^{-jk\vec{a}\cdot\vec{r}_3}\right|^2}. \tag{77}$$

Therefore, u^2E_o is proportional to the pilot-tone signal-field intensity $\left|E_{pf}(\vec{r}_f, t)\right|^2$ at the point $\vec{r}_f = -f_\ell\vec{\theta}$ in the focal plane R_F, where $\vec{\theta}$ is the data transmission angle.

We can clearly maximize u^2E_o by observing the point $\vec{r}_{f,max}$ in plane R_F where the pilot-tone signal-field intensity is greatest, and then transmitting the information signal during that atmospheric coherence interval in the direction $\vec{\theta} = -\vec{r}_{f,max}/f_\ell$. In practice, $\vec{r}_{f,max}$ will be near $\vec{0}$ most of the time, so that the problem of scanning R_F to track the temporal variations of $\vec{r}_{f,max}$ and rapidly adjusting $\vec{\theta}$ continuously to match $\vec{r}_{f,max}$ should not present any serious mechanical implementation difficulties.

We can define a new amplitude fading parameter v for the adaptive-pointing scheme, such that the conditional signal energy received by aperture R_3 for a given atmospheric channel state is given by

$$v^2E_o = \frac{\xi\lambda^2 f_\ell^2 A_r^2 \left|E_{pf}(\vec{r}_{f,max}, t)\right|^2}{P_p A_t \left|\int_{R_3} d\vec{r}_3\, e^{-jk\vec{a}\cdot\vec{r}_3}\right|^2}. \tag{78}$$

The fading parameter v has a greater second moment than the fading parameter u characterizing nonadaptive optical systems, so that the adaptive-pointing scheme obviously results in more reliable communication over the ground-to-space link. The degree of improvement depends on the probability density function p(v), which is difficult to evaluate in general. We can approximate p(v) for large apertures R_1 using the following plausibility arguments. Assume that aperture R_1 is large relative to a coherence area of $e^{\gamma(\vec{r}_1)}$, and that it intercepts N independent spatial modes of the received pilot-tone signal field, where N is proportional to the area A_t of aperture R_1. Assume that we can consequently define an array of N points $\{\vec{r}_{f,i} \in R_F:\ 1 \leq i \leq N\}$ in focal plane R_F such that the field intensities $\{\left|E_{pf}(\vec{r}_{f,i}, t)\right|^2\}$ at these points can be essentially treated as a set of identically distributed, statistically independent random variables at any time t. Using Eq. 78, we can correspondingly define a set of N statistically independent, identically distributed amplitude fading parameters v_i, where

$$v_i \equiv \lambda f_\ell A_r \sqrt{\frac{\xi}{E_o P_p A_t}}\, \frac{\left|E_{pf}(\vec{r}_{f,i}, t)\right|}{\left|\int_{R_3} d\vec{r}_3\, e^{-jk\vec{a}\cdot\vec{r}_3}\right|}. \tag{79}$$

Comparing Eqs. 77 and 79, it is clear that the statistical behavior of u is identical to that of v_i, independent of i. As in Section II, we know that when $A_t \gg A_{c\chi}$, corresponding to the constraint $N \gg 1$, v_i is a Rayleigh random variable for each i. The fading parameter v in Eq. 78 can then be approximated by

$$v \cong \max_{1 \leq i \leq N} [v_i]. \tag{80}$$

Using Eqs. 38 and 39 to define the probability density function $p(v_i)$, we can then easily show that the probability density function of v has the approximate form

$$p(v) \cong \frac{2vN}{a} e^{-\frac{v^2}{a}} \left[1 - e^{-\frac{v^2}{a}}\right]^{N-1} ; \qquad N \gg 1. \tag{81}$$

One can presumably determine the improvement in performance of the adaptive-pointing scheme by using Eq. 81; however, we shall not perform the required calculations at this time.

3.2 GROUND-TO-GROUND LINK

3.2.1 Heterodyne-Detection Case

The analysis for the heterodyne-detection/ground-to-ground system is very similar to that of the previous section with some minor modifications, so we shall briefly review the mathematical development of the channel-measurement scheme. Recall from Section II that the data transmission direction $\vec{\theta}$ is set to $\vec{0}$ for the ground-to-ground case. In general, the received signal field $E_o(\vec{r}_2, t)$ defined by Eqs. 23 and 24, is spatially incoherent over receiving aperture R_2. The relevant channel fading parameter $ue^{j\psi}$ is defined in terms of the angular plane-wave component $\underset{\rightarrow}{U}_r(\vec{\phi})$ in Eq. 29, where $\vec{\phi}$ is the direction of the local-oscillator field in the heterodyne receiver. Combining Eqs. 24 and 29, we have

$$\underset{\rightarrow}{U}_r(\vec{\phi}) = \frac{1}{\sqrt{A_t}} \int_{R_1} d\vec{r}_1 \int_{R_2} d\vec{r}_2 \, \underset{\rightarrow}{h}_a(\vec{r}_2, \vec{r}_1) \, e^{-jk\vec{\phi} \cdot \vec{r}_2}$$

$$= ue^{j\psi} \frac{A_r}{\sqrt{A_t}}. \tag{82}$$

To measure the channel fading, we shall transmit a pilot tone through aperture R_2 in the direction $-\vec{\phi}$:

$$E_{pt}(\vec{r}_2, t) = \sqrt{\frac{P_p}{A_r}} e^{-jk\vec{\phi} \cdot \vec{r}_2} \equiv \sqrt{P_p} \, \underset{\rightarrow}{U}_2(\vec{r}_2); \qquad \vec{r}_2 \in R_2. \tag{83}$$

Then the pilot-tone signal field arriving at aperture R_1 has the form

$$E_{ps}(\vec{r}_1, t) = \sqrt{P_p}\, \underset{\sim}{U}_1(\vec{r}_1); \qquad \vec{r}_1 \in R_1, \tag{84}$$

where

$$\underset{\sim}{U}_1(\vec{r}_1) = \frac{1}{\sqrt{A_r}} \int_{R_2} d\vec{r}_2\, \underset{\sim}{h}_a(\vec{r}_1, \vec{r}_2)\, e^{-jk\vec{\phi}\cdot\vec{r}_2}; \qquad \vec{r}_1 \in R_1. \tag{85}$$

Extracting the angular plane-wave component $\underset{\sim}{U}_t(\vec{0})$ of the received field term $\underset{\sim}{U}_1(\vec{r}_1)$ over aperture R_1, we have

$$\underset{\sim}{U}_t(\vec{0}) \equiv \int_{R_1} d\vec{r}_1\, \underset{\sim}{U}_1(\vec{r}_1) = \frac{1}{\sqrt{A_r}} \int_{R_1} d\vec{r}_1 \int_{R_2} d\vec{r}_2\, \underset{\sim}{h}_a(\vec{r}_1, \vec{r}_2)\, e^{-jk\vec{\phi}\cdot\vec{r}_2}. \tag{86}$$

Under the assumption that Eqs. 82-86 refer to a single atmospheric channel state, Eq. 10 applies, and we conclude that

$$ue^{j\psi} = \frac{1}{\sqrt{P_p A_r}} \int_{R_1} d\vec{r}_1\, E_{ps}(\vec{r}_1, t). \tag{87}$$

3.2.2 Direct-Detection Case

For the direct-detection/ground-to-ground system, we want to measure the channel fading parameter u^2 defined by Eq. 55. Combining Eqs. 24 and 55, we can write u^2 in the form

$$u^2 = \frac{1}{A_r} \int_{R_1} d\vec{r}_1 \int_{R_1} d\vec{r}_1' \int_{R_2} d\vec{r}_2\, \underset{\sim}{h}_a(\vec{r}_2, \vec{r}_1)\, \underset{\sim}{h}_a^*(\vec{r}_2, \vec{r}_1'). \tag{88}$$

Let us try to measure u^2, using a single plane-wave pilot-tone field transmitted through aperture R_2 along the optical axis; then Eqs. 83-86 hold with $\vec{\phi} = \vec{0}$. We find that there is no way to process the received pilot-tone signal field $E_{ps}(\vec{r}_1, t)$ to extract u^2. For example, since u^2 is proportional to the total information signal power incident on aperture R_2, we might feel instinctively that, because of the reciprocal nature of the atmosphere, u^2 can be determined by measuring the total pilot-tone signal power received by aperture R_1. Using Eq. 10, however, we find that the last quantity satisfies the relation

$$\int_{R_1} d\vec{r}_1\, |E_{ps}(\vec{r}_1, t)|^2 = \frac{P_p}{A_r} \int_{R_1} d\vec{r}_1 \int_{R_2} d\vec{r}_2 \int_{R_2} d\vec{r}_2'\, \underset{\sim}{h}_a(\vec{r}_2, \vec{r}_1)\, \underset{\sim}{h}_a^*(\vec{r}_2', \vec{r}_1) \tag{89}$$

which resembles the expression for u^2 in Eq. 88. There is, however, no way to reconcile the differences between the integrals in Eqs. 88 and 89, so that the total pilot-tone signal power is not a sufficient observable for determining u^2.

We can argue that, in general, it is impossible to measure u^2 by transmitting a single plane-wave pilot-tone field through aperture R_2. We have already noted that u^2 is proportional to the total information signal power incident on aperture R_2. The received information signal field is, in most cases, spatially incoherent over aperture R_2, so that the total signal power in the receiving aperture is the sum of the power in each of the received spatial signal modes. Since each independent signal mode is characterized by a different fading random variable, to measure u^2 we must use a pilot tone that probes all of these fading parameters. As we remarked in section 3.1, a single plane-wave pilot-tone field transmitted in the direction $-\vec{a}$ only probes the fading parameter relevant to the received spatial signal mode in the direction $\vec{a}$, so it is not sufficient to measure u^2.

We can measure u^2, using a single plane-wave pilot tone for the special case which follows. From Eqs. 31 and 56, we see that for the unimodal situation where $A_r < A_{c\phi'}$, u^2 is the same as the parameter u^2 in the heterodyne-detection/ground-to-ground system for the case where $\vec{\phi} = \vec{0}$. Therefore, from section 3.2.1, we know that if we transmit the pilot-tone field

$$E_{pt}(\vec{r}_2, t) = \sqrt{\frac{P_p}{A_r}}; \qquad \vec{r}_2 \in R_2, \tag{90}$$

then u^2 is related to the received pilot-tone field $E_{ps}(\vec{r}_1, t)$ according to

$$u^2 = \frac{1}{P_p A_r} \left| \int_{R_1} d\vec{r}_1 \, E_{ps}(\vec{r}_1, t) \right|^2. \tag{91}$$

The fact that we do not yet know how to measure u^2 for the general case in which we use a single detector in the direct-detection receiver may not be a serious omission. When $A_r > A_{c\chi'}$, a more optimal direct-detection receiver contains an array of D detectors, where D is of the order of $A_r/A_{c\chi'}$.[51] In this case, there are D separate fading parameters of the form u^2 to measure, and this can be accomplished by the use of D different pilot tones, where each measurement is similar to that defined by Eqs. 90 and 91 (see Section V).

There is a general comment that we should make concerning the channel-measurement/adaptive transmission scheme for the ground-to-ground link. In the analysis in sections 3.1 and 3.2 it was assumed that if we transmitted a pilot-tone over an optical channel in one direction, and then sent an information signal in the reverse direction, both transmissions would be affected by the same atmospheric channel state. Because of the large distance between the Earth and a synchronous satellite, this

restriction prevented us from using a ground-to-space pilot-tone probe to establish an adaptive communication system over the space-to-ground link. In the ground-to-ground case, however, our results could readily be extended to a two-way adaptive communication system in which, for efficiency, the information signal transmitted in each direction becomes the effective pilot tone on which adaptive transmissions in the other direction are based.

3.3 CHANNEL-MEASUREMENT NOISE

We have demonstrated that we could determine the atmospheric fading over our optical communication links (with the exception of the direct detection/ground-to-ground case when $A_r > A_{c\phi'}$) by the use of a pilot-tone probe. Ignoring any accompanying noise, we showed that the received pilot-tone signal field $E_{ps}(\vec{r}_1, t)$ is related to the relevant channel fading process $u(t)\, e^{j\psi(t)}$ by an expression of the general form

$$z(t) \equiv u(t)\, e^{j\psi(t)} = B \int_{R_1} d\vec{r}_1\, E_{ps}(\vec{r}_1, t)\, e^{jk\vec{\theta}\cdot\vec{r}_1}, \tag{92}$$

where we have extended our earlier results beyond a single temporal coherence interval allowing the atmospheric fading parameter to vary with time. From Eq. 75, the complex parameter B for the ground-to-space link is given by

$$B = \frac{\lambda d_f \sqrt{A_r}}{A_t \sqrt{P_p} \int_{R_3} d\vec{r}_3\, e^{-jk\vec{\alpha}\cdot\vec{r}_3}}. \tag{93}$$

From Eqs. 87 and 91, we see that for the ground-to-ground link, with the exception of the direct-detection system when $A_r > A_{c\chi'}$, the direction $\vec{\theta}$ is equal to $\vec{0}$, and

$$B = \frac{1}{\sqrt{P_p A_r}}. \tag{94}$$

Actually, as in Eq. 6, the received pilot-tone field can be written in the form

$$E_{pr}(\vec{r}_1, t) = E_{ps}(\vec{r}_1, t) + E_{pb}(\vec{r}_1, t); \qquad \vec{r}_1 \in R_1, \tag{95}$$

where the complex, zero-mean Gaussian random process $E_{pb}(\vec{r}_1, t)$ represents the relevant polarization component of the additive background noise field. The real and imaginary parts of $E_{pb}(\vec{r}_1, t)$ are assumed to be independent, stationary, and identically distributed; also, $E_{pb}(\vec{r}_1, t)$ can be treated as a white random process in time and space. Then we can write

$$E_1(\vec{r}_1, t) \equiv \mathrm{Re}\,[E_{pb}(\vec{r}_1, t)]$$

$$E_2(\vec{r}_1, t) \equiv \mathrm{Im}\,[E_{pb}(\vec{r}_1, t)] \tag{95}$$

$$\overline{E_1(\vec{r}_1, t)} = \overline{E_2(\vec{r}_1, t)} = 0$$

$$\overline{E_1(\vec{r}_1, t)\, E_2(\vec{r}_1', t')} = 0$$

$$\overline{E_1(\vec{r}_1, t)\, E_1(\vec{r}_1', t')} = \overline{E_2(\vec{r}_1, t)\, E_2(\vec{r}_1', t')} = N_b' \lambda^2 u_o(\vec{r}_1 - \vec{r}_1')\, u_o(t-t'), \tag{96}$$

where N_b' is the radiance of the relevant polarization component of the background light, and λ is the wavelength of the pilot tone.

Let us now eliminate the spatial dependence of the observable $E_{pr}(\vec{r}_1, t)$ which we want to use to monitor the fading process $z(t)$. Using Eq. 92, we can define a new observable $x(t)$ by extracting the angular plane-wave component of $E_{pr}(\vec{r}_1, t)$ in the direction $-\vec{\theta}$:

$$x(t) \equiv \int_{R_1} d\vec{r}_1\, E_{pr}(\vec{r}_1, t)\, e^{jk\vec{\theta}\cdot\vec{r}_1} = \frac{1}{B} z(t) + n_b(t), \tag{97}$$

where $n_b(t)$ is a complex, white Gaussian random process specified by

$$n_b(t) \equiv \int_{R_1} d\vec{r}_1\, E_{pb}(\vec{r}_1, t)\, e^{jk\vec{\theta}\cdot\vec{r}_1}. \tag{98}$$

Using Eq. 96, we can show that the real and imaginary parts of $n_b(t)$, denoted by $n_1(t)$, satisfy the following conditions:

$$\overline{n_1(t)} = \overline{n_2(t)} = 0$$

$$\overline{n_1(t)\, n_2(t')} = 0$$

$$\overline{n_1(t)\, n_1(t')} = \overline{n_2(t)\, n_2(t')} = A_t N_b' \lambda^2 u_o(t-t'). \tag{99}$$

Suppose we want to transmit an information signal during the interval (t_o, t_o+T). We shall assume that the baud time T is less than the atmospheric channel coherence time T_c so that the relevant fading parameter $z(t) \cong z(t_o)$. We could try to

design a realizable filter that makes an optimal estimate of $z(t_o)$, or $u(t_o)$ for that matter, based on the observation of x(t) over the interval $(-\infty, t_o)$ and the temporal covariance function of z(t) or u(t). While this technique appears to be interesting, the associated mathematics may be rather difficult.

We shall therefore consider an alternative, and much simpler, approach. Define a new observable r(t), which is a continually updated T_o-second time average of x(t) over the interval $(t-T_o, t)$, normalized so that the mean of r(t) is z(t):

$$r(t) \equiv \frac{B}{T_o} \int_{t-T_o}^{t} dt' \, x(t'). \tag{100}$$

Suppose we want to transmit an information signal during the T-second interval $\mathcal{T} \equiv (t_o, t_o+T)$, where

$$T + T_o \leq T_c \tag{101}$$

so that $z(t) \cong z(t_o)$ over the interval (t_o-T_o, t_o+T). The adaptive transmitter will use some variable-rate strategy, still undetermined (see Section IV), to adjust the baud time T according to the observable $r(t_o)$. Denoting the random variables $r(t_o)$ and $z(t_o)$ by r and z, and the averaging interval (t_o-T_o, t_o) by $\mathcal{T}_o$, for convenience, we have

$$r = \frac{B}{T_o} \int_{\mathcal{T}_o} dt \int_{r_1} d\vec{r}_1 \, E_{pr}(\vec{r}_1, t) \, e^{jk\vec{\theta} \cdot \vec{r}_1} = z + n, \tag{102}$$

where the noise term n is a complex Gaussian random variable which is independent of z and is defined by

$$n \equiv \frac{B}{T_o} \int_{\mathcal{T}_o} dt \, n_b(t). \tag{103}$$

Using Eq. 99, we can show that the real and imaginary parts of n, represented by n_1 and n_2, satisfy the relations

$$\overline{n_1} = \overline{n_2} = 0 \qquad \overline{n_1 n_2} = 0$$

$$n_1^2 = n_2^2 = \frac{|B|^2 A_t N_b' \lambda^2}{T_o} \equiv \frac{N_m}{2}. \tag{104}$$

3.4 CHANNEL-MEASUREMENT STATISTICS FOR RAYLEIGH FADING

For convenience, we shall represent the complex random variables in Eq. 102 in polar form and also in terms of their real and imaginary components:

$$r \equiv \rho e^{j\alpha} = r_1 + jr_2, \qquad n \equiv \eta e^{j\beta} = n_1 + jn_2, \qquad z = ue^{j\psi} = z_1 + jz_2. \tag{105}$$

In Eqs. 36 and 60, we showed that the probability of a communication error on a single transmission, conditioned on the atmospheric channel state, depends only on the amplitude fading parameter u for both the heterodyne- and direct-detection cases. Accordingly, our adaptive-transmission strategy for a given signal baud will depend on our determination of u based on the observable r.

At this point, it is mathematically convenient to restrict ourselves to the case in which u is Rayleigh and ψ is uniform over $(0, 2\pi)$. (We shall say more about this restriction later.) For the Rayleigh fading situation, we shall demonstrate that, given observable r, ρ is a sufficient observable for measuring u: that is,

$$p(u|\rho, \alpha) = p(u|\rho). \tag{106}$$

If $\overline{u^2} \equiv a$ as in Eq. 39, z_1 and z_2 are zero-mean, independent, jointly Gaussian random variables, each with variance a/2. By Eq. 104, n_1 and n_2 are zero-mean, independent, jointly Gaussian random variables, each with variance $N_m/2$. Therefore, r_1 and r_2 are zero-mean, independent, jointly Gaussian random variables, each with variance $(a+N_m)/2$. This implies that ρ is Rayleigh with probability density function

$$p(\rho) = \frac{2\rho}{a + N_m} e^{-\frac{\rho^2}{a+N_m}} u_{-1}(\rho), \tag{107}$$

α is uniform over $(0, 2\pi)$, and ρ and α are independent. Also, using a simple transformation of random variables, we can write

$$\begin{aligned} p(\rho, \alpha|u, \psi) &= \rho\, p_{r_1, r_2|u, \psi}(\rho\cos\alpha, \rho\sin\alpha|u, \psi) \\ &= \rho\, p_{n_1}(\rho\cos\alpha - u\cos\psi)\, p_{n_2}(\rho\sin\alpha - u\sin\psi) \\ &= \frac{\rho}{\pi N_m} e^{-\frac{\rho^2+u^2}{N_m}} e^{\frac{2\rho u}{N_m}\cos(\alpha-\psi)} \qquad ; \qquad \rho \geq 0,\ 0 < \alpha < 2\pi. \end{aligned} \tag{108}$$

Integrating $p(\rho, \alpha|u, \psi)$ over the phase term α, we find that $p(\rho|u, \psi)$ is independent of ψ:

$$\begin{aligned} p(\rho|u, \psi) &= \int_0^{2\pi} d\alpha\, p(\rho, \alpha|u, \psi) \\ &= \frac{2\rho}{N_m} e^{-\frac{\rho^2+u^2}{N_m}} I_o\left(\frac{2\rho u}{N_m}\right) u_{-1}(\rho) = p(\rho|u). \end{aligned} \tag{109}$$

Also, averaging $p(\rho, \alpha | u, \psi)$ over ψ, we can show that

$$p(\rho, \alpha | u) = \overline{p(\rho, \alpha | u, \psi)}^{\psi}$$

$$= \frac{\rho}{\pi N_m} e^{-\frac{\rho^2+u^2}{N_m}} I_o\left(\frac{2\rho u}{N_m}\right); \qquad \rho \geq 0, \ 0 < \alpha < 2\pi. \tag{110}$$

Therefore, by Bayes' rule, we have

$$p(u | \rho, \alpha) = \left[\frac{p(\rho, \alpha | u)}{p(\alpha)}\right] \frac{p(u)}{p(\rho)}$$

$$= \frac{2\rho}{N_m} e^{-\frac{\rho^2+u^2}{N_m}} I_o\left(\frac{2\rho u}{N_m}\right) u_{-1}(\rho) \frac{p(u)}{p(\rho)}$$

$$= \frac{p(\rho|u)\, p(u)}{p(\rho)} = p(u | \rho), \tag{111}$$

so that, given r, ρ is a sufficient observable for measuring u, when u is Rayleigh. Therefore, during a given signal baud, our adaptive transmitter will adjust the baud time T according to the observable ρ defined by Eqs. 102 and 105:

$$\rho = \frac{|B|}{T_o} \left| \int_{\mathcal{T}_o} dt \int_{R_1} d\vec{r}_1 \, E_{pr}(\vec{r}_1, t) \, e^{jk\vec{\theta} \cdot \vec{r}_1} \right|. \tag{112}$$

The variable-rate strategy based on ρ will be determined in Section IV.

Intuitively, we feel that the result of Eq. 106 should hold for log-normal fading as well. Since ψ and β are again uniform over $(0, 2\pi)$, and are independent of u, η, and each other, we could probably show that α is uniform over $(0, 2\pi)$ and independent of u, and that, given ρ, α adds no information about u. We shall not demonstrate this here, since $p(\rho | u)$ appears to be too complicated for us to be able to develop any mathematically tractable variable-rate strategy when u is log-normal.

We now prove two mathematical identities that follow trivially from our results above, and which we shall need later. From Eqs. 38, 107, and 109, we can write

$$\frac{2\rho}{\alpha + N_m} e^{-\frac{\rho^2}{\alpha + N_m}} u_{-1}(\rho) = p(\rho) = \int_0^\infty du \, p(\rho | u) \, p(u)$$

$$= \frac{4\rho}{\alpha N_m} e^{-\frac{\rho^2}{N_m}} \int_0^\infty du \, u \, e^{-u^2\left(\frac{\alpha + N_m}{\alpha N_m}\right)} I_o\left(\frac{2\rho}{N_m}\right).$$

Rearranging terms and defining

$$b \equiv \frac{a + N_m}{aN_m} > 0, \qquad c \equiv \frac{2\rho}{N_m} > 0,$$

we find that

$$\int_0^\infty du\ u\ e^{-bu^2} I_o(cu) = \frac{1}{2b} e^{\frac{c^2}{4b}}; \qquad b, c > 0. \tag{113}$$

Also, differentiating both sides of Eq. 113 with respect to b, we have

$$\int_0^\infty du\ u^3\ e^{-bu^2} I_o(cu) = \frac{1 + \frac{c^2}{4b}}{2b^2} e^{\frac{c^2}{4b}}; \qquad b, c > 0. \tag{114}$$

3.5 POINT-AHEAD PROBLEM AND ISOPLANATIC ANGLE

For the ground-to-space link, because of the large transmission distance, we must take into account the point-ahead problem.[52] This is indicated geometrically in Fig. 6. At time t_1, the synchronous satellite (assumed for convenience to be in an equatorial orbit)

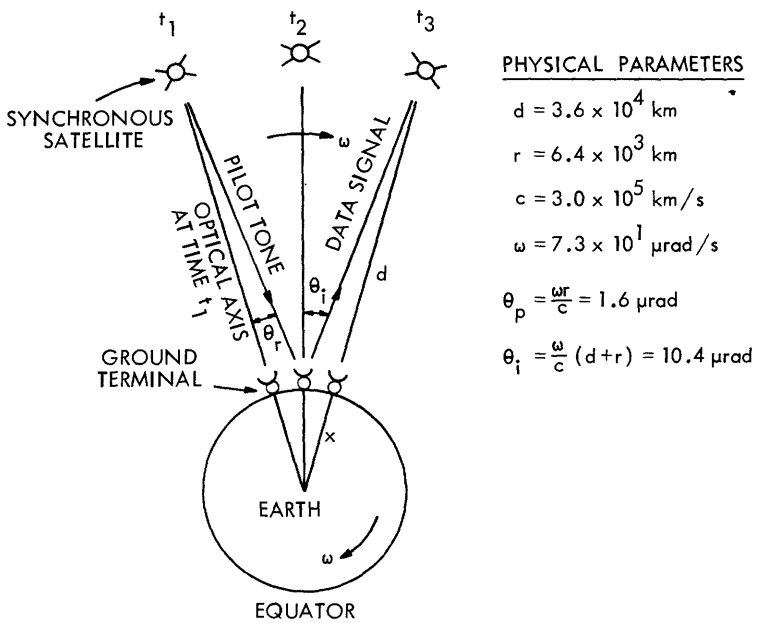

Fig. 6. Point-ahead configuration for ground-to-space link. Physical parameters above include: distance d between synchronous satellite and ground terminal, velocity c of light in a vacuum, radius r of Earth, angular velocity ω of Earth at equator, pilot-tone point-ahead angle θ_p, information-signal point-ahead angle θ_i.

transmits a pilot tone down to Earth. Because the Earth and satellite are rotating in space with approximately the same angular velocity ω, the satellite must transmit its pilot tone in a direction θ_p ahead of the optical axis at time t_1 to ensure that the pilot tone arrives at the ground terminal at time t_2. At time t_2, the ground terminal transmits an information signal at a point-ahead angle θ_i relative to the optical axis at time t_2 so that the information signal reaches the satellite at time t_3. For simplicity, we have ignored the time the adaptive transmitter requires to adjust the information-signal baud time according to the received pilot tone.

Therefore, although the total atmospheric propagation time for the pilot-tone/information signal combination is of the order of 10 μs, which is much smaller than the atmospheric coherence time T_c, the point-ahead requirement affects our previous contention that the pilot tone and the succeeding information signal reflect the same atmospheric channel state. This condition, which is critical in the operation of our variable-rate optical ground-to-space link, will still be satisfied, provided the isoplanatic angle is greater than $2\theta_i \sim 21$ μrad. (The isoplanatic angle can be interpreted as the maximum angular separation between two infinite plane waves incident on plane R_2 which are characterized by the same atmospheric fading parameter in propagating to aperture R_1.) Fortunately, recent experimental evidence suggests that the isoplanatic angle is great enough for our channel measurement results so that the ground-to-space link is still valid despite the point-ahead issue.[53] We might add that there is no comparable point-ahead problem for the ground-to-ground link.

IV. VARIABLE-RATE ADAPTIVE TRANSMISSION

4.1 Problem Specification

In Section II, we showed that the probability of a communication error occurring on a given transmission over the optical links under consideration, conditioned on the atmospheric channel state, depends on a channel-fading parameter u. We saw that for many cases of interest, u is either a log-normal or a Rayleigh random variable. In Section III, we demonstrated that the information-signal transmitter can measure u by processing a received pilot-tone field to produce an observable ρ, which is equal to u in the absence of measurement noise. For the case in which u is Rayleigh, we also determined the statistical behavior of ρ conditioned on u.

We would now like to develop some adaptive-transmission strategies based on the observation of ρ in order to improve the communication performance of our optical links relative to conventional fixed-rate systems. As in the fixed-rate analysis in Section II, we shall confine our attention to the continuous transmission of binary, equiprobable, orthogonal signals of equal energy. The transmitter will now adjust the signal baud time T for each transmission according to some preselected mapping $T(\rho)$ of the value of ρ observed immediately prior to the transmission. In order for the results of Sections II and III to be valid, according to Eq. 101 we should only consider mappings $T(\rho)$ with the restricted range

$$T(\rho) \leq T_c - T_o; \qquad \forall\ \rho, \tag{115}$$

where T_c is the atmospheric coherence time, and T_o is the channel-measurement averaging time defined in Eq. 100. To simplify our variable-rate analysis below, for the time being we shall disregard the restriction of Eq. 115 and assume that any mappings $T(\rho)$ that we eventually select will satisfy this restriction most, if not all, of the time.

For convenience we define an instantaneous information bit rate conditioned on the observable ρ:

$$R(\rho) \equiv \frac{1}{T(\rho)} \text{ bits/second.} \tag{116}$$

Under the assumption that the channel-fading process is ergodic, the average signalling rate is then given by

$$R_{avg} \equiv \overline{R(\rho)}^{\rho} = \int_0^\infty d\rho\, R(\rho) \int_0^\infty du\, p(\rho|u)\, p(u) \text{ bits/second.} \tag{117}$$

In order to completely define the variable-rate problem, we must introduce a power constraint. In practice, a laser transmitter is limited by its average and peak short-term average power output capabilities, denoted by P_{avg} and P_{peak}, respectively: that is, a given information signal can be transmitted at a maximum average power level P_{peak} in general, although the transmitted power averaged over many signals must not exceed

P_{avg}. In the fixed-rate case it is desirable to transmit each information signal at the fixed average power level P_{avg}. To be sufficiently general in our variable-rate problem specification, we should assume that each information signal is transmitted at an average power level $P_t(\rho)$, which depends on the observable ρ, subject to the restrictions

$$\overline{P_t(\rho)}^{\rho} \leq P_{avg}, \qquad P_t(\rho) \leq P_{peak}; \quad \forall \rho. \tag{118}$$

Maintaining this degree of generality, however, would greatly complicate our variable-rate analysis. To simplify matters, we shall place a more severe restriction on $P_t(\rho)$:

$$P_t(\rho) = \begin{cases} P_{avg}; & \forall \rho \ni R(\rho) \neq 0, \\ 0; & \forall \rho \ni R(\rho) = 0. \end{cases} \tag{119}$$

That is, the information signals in both the fixed-rate and variable-rate cases are transmitted at the same fixed average power level P_{avg}. We shall show that variable-rate systems based on the power constraint of Eq. 119 represent a marked improvement over corresponding fixed-rate optical systems. Variable-rate systems based on the more general power constraint of Eq. 118 should perform even better still

Using Eq. 119, the transmitted energy ξ defined in Eq. 3 now depends on ρ according to the prescription

$$\xi = P_{avg} T(\rho) = \frac{P_{avg}}{R(\rho)}; \qquad \forall \rho \ni R(\rho) \neq 0. \tag{120}$$

This implies that the energy parameters E_s in Eqs. 28 and 32 for the heterodyne-detection case have the form

$$E_s = \frac{P_s}{R(\rho)}, \tag{121}$$

where the power parameter P_s is independent of ρ, and $u^2 P_s$ is the received signal power averaged over a signal baud and conditioned on u. For the ground-to-space link, P_s is specified by

$$P_s = \frac{P_{avg} A_t}{\lambda^2 d_f^2 A_r} \left| \int_{R_3} d\vec{r}_3 \, e^{-jk\vec{\phi} \cdot \vec{r}_3} \right|^2, \tag{122}$$

while in the ground-to-ground case, we have

$$P_s = P_{avg} \frac{A_r}{A_t}. \tag{123}$$

The conditional probability of error in Eq. 36 for the heterodyne receiver must

now be modified to read

$$P(\epsilon|u,\rho) = \frac{1}{2} e^{-\frac{u^2 P_s}{2N_o R(\rho)}}. \tag{124}$$

Similarly, as a consequence of the power constraint of Eq. 119, the signal-rate parameter μ_s defined in Eqs. 52 and 54 for the direct-detection case has the form

$$\mu_s = \frac{2\eta P_{avg} A_t A_r}{h\nu\lambda^2 d_f^2} \tag{125}$$

for the ground-to-space link, and

$$\mu_s = \frac{2\eta P_{avg} A_r}{h\nu A_t} \tag{126}$$

for the ground-to-ground system. Then the conditional probability of error in Eq. 60 for the direct-detection case can be rewritten as

$$P(\epsilon|u,\rho) = Q_m\left[\sqrt{\frac{\mu_n}{R(\rho)}}, \sqrt{\frac{\mu_n(1+u^2\alpha)}{R(\rho)}}\right] - \frac{1}{2} e^{-\frac{\mu_n(2+\mu^2\alpha)}{2R(\rho)}} I_o\left[\frac{\mu_n\sqrt{1+u^2\alpha}}{R(\rho)}\right]. \tag{127}$$

Since we are signalling continuously at the variable information bit rate $R(\rho)$, the bit error rate may be expressed as

$$\epsilon' \equiv \overline{R(\rho)\, P(\epsilon|u,\rho)}^{u,\rho} = \int_0^\infty d\rho\, R(\rho) \int_0^\infty du\, p(\rho|u)\, p(u)\, P(\epsilon|u,\rho)\, \frac{\text{bit errors}}{\text{second}}, \tag{128}$$

which means that the fraction ϵ of bit errors to received bits is given by

$$\epsilon \equiv \frac{\epsilon'}{R_{avg}} \frac{\text{bit errors}}{\text{received bit}}. \tag{129}$$

Our design objective is to select mappings $R(\rho)$ that are optimal, in the sense that they maximize R_{avg} for a given ϵ or ϵ' subject to any limitations we may find it necessary to place on the form of $R(\rho)$. For the sake of comparison, we reinterpret the fixed-rate performance results of Section II in terms of the generalized notation that we have developed in this section. We define

$$R_{avg} = R(\rho) \equiv R_F \tag{130}$$

for the fixed-rate case, and note that the error rate ϵ in Eq. 129 is equal to the probability of error $P(\epsilon)$ in Section II. From Eq. 40, for the heterodyne receiver when u is Rayleigh, we have

$$R_F = \frac{\frac{aP_S}{2N_o}}{\frac{1}{2\epsilon} - 1}; \qquad \overline{u^2} = a. \tag{131}$$

For the heterodyne-detection/ground-to-space link when u is log-normal, Eq. 43 defines R_F implicitly as a function of ϵ:

$$\epsilon = \frac{1}{2} \mathrm{Fr}\left[\frac{Z^2 C^2(\vec{\theta})\, P_S}{2N_o R_F},\ 0;\ \sigma_\chi\right]; \qquad \overline{u^2} = Z^2 C^2(\vec{\theta}). \tag{132}$$

Similarly, from Eq. 45, for the heterodyne-detection/ground-to-ground link when u is log-normal, we have the implicit relation

$$\epsilon = \frac{1}{2} \mathrm{Fr}\left[\frac{Z'^2 C'^2(\vec{\phi})\, P_S}{2N_o R_F},\ 0;\ \sigma_{\chi'}\right]; \qquad \overline{u^2} = Z'^2 C'^2(\vec{\phi}). \tag{133}$$

Finally, for the direct-detection/ground-to-space link when u is Rayleigh, the approximation of Eq. 67 implies that

$$R_F \cong 2\pi\mu_n \Delta^2 \epsilon^2; \qquad \epsilon \ll \begin{cases} \frac{1}{\sqrt{2\pi}}; & \Delta \leq 1, \\ \frac{1}{\Delta\sqrt{2\pi}}; & \Delta \geq 1, \end{cases} \tag{134}$$

where Δ is defined in Eq. 59.

4.2 HETERODYNE-DETECTION SYSTEMS

4.2.1 Noiseless Channel-Measurement Case

We shall initially develop optimal variable-rate strategy for the special case in which the channel-measurement noise is sufficiently small that we can effectively set the power spectral density N_m, defined in Eq. 104, equal to zero. The mathematical analysis is greatly simplified for this noiseless channel-measurement case, particularly when the fading parameter u is log-normal. The variable-rate concepts developed in this section will be representative of those later derived for the more general noisy channel-measurement case.

When N_m is zero, the conditional probability density $p(\rho|u) = u_o(\rho-u)$, so that Eqs. 117 and 128 have the modified form

$$R_{avg} = \int_0^\infty du\, p(u)\, R(u)$$

$$\epsilon' = \int_0^\infty du\, p(u)\, R(u)\, P(\epsilon|u), \tag{135}$$

where, in general, $P(\epsilon|u)$ is simply $P(\epsilon|u, \rho)$ in Eq. 128 evaluated at $\rho = u$.

We would like to determine the mapping R(u) which maximizes R_{avg} for a given ϵ' under the assumption that P_s and N_o are fixed. Using the Lagrange multiplier approach with parameter λ, we want to find the non-negative function R(u) which maximizes the expression

$$R_{avg} - \lambda\epsilon' = \int_0^\infty du\, p(u)\, R(u)[1-\lambda P(\epsilon|u)]. \tag{136}$$

Since p(u) is non-negative, we can equivalently determine the value R(u) which maximizes the portion of the integrand in Eq. 136 defined by

$$f[R(u), \lambda] \equiv R(u)[1-\lambda P(\epsilon|u)] \tag{137}$$

at each value of u in the range $(0, \infty)$. Since $P(\epsilon|u) \leq \frac{1}{2}$, for $\lambda < 2$, $f[R(u), \lambda]$ is trivially maximized when R(u) is infinite for all values of u. This is a singular solution which is only valid for infinite ϵ'. When $\lambda > 2$, we can show that there is a unique, nontrivial maximum that satisfies the constraint

$$P(\epsilon|u) + R(u) \frac{\partial}{\partial R(u)} P(\epsilon|u) = \frac{1}{\lambda} \tag{138}$$

at each value of u.

Note that the constraint above on the optimal R(u) is independent of the statistical behavior of the channel-fading parameter u, characterized by the probability density p(u): It is also independent of the actual form of $P(\epsilon|u)$. In particular, suppose the conditional probability of error can be expressed in the form

$$P(\epsilon|u) = A\, e^{-\frac{B(u)}{R(u)}}, \tag{139}$$

where A is independent of u, and B(u) is a function of u but is not explicitly dependent on R(u). From Eqs. 138 and 139, we find that the optimal mapping R(u) must then satisfy the condition

$$e^{-\frac{B(u)}{R(u)}\left[1+\frac{B(u)}{R(u)}\right]} = \frac{1}{\lambda A}. \tag{140}$$

Since the Lagrange multiplier λ has the same value for all u, depending only on the given error rate ϵ', this implies that the optimal R(u) must have the form

$$R(u) = CB(u); \qquad 0 < u < \infty, \tag{141}$$

where C is a constant that depends on the desired bit error rate.

Now for the heterodyne-detection case, we see in Eq. 124 that $P(\epsilon|u)$ has the form of Eq. 139; therefore the optimal R(u) is proportional to u^2:

$$R(u) = \frac{CP_s}{2N_o} u^2; \qquad 0 < u < \infty. \tag{142}$$

We must stress that this result is independent of p(u), and was a primary motivation for considering the special case where $N_m = 0$. Combining Eqs. 129, 135, and 142, and denoting the average information rate R_{avg} in this case by R_V, we find that

$$R_V \equiv R_{avg} = \frac{CP_s}{2N_o} \overline{u^2}, \tag{143}$$

and

$$\epsilon' = \frac{CP_s}{4N_o} \overline{u^2}\, e^{-\frac{1}{C}}, \tag{144}$$

which implies that

$$\epsilon = \frac{1}{2} e^{-\frac{1}{C}}. \tag{145}$$

We can rearrange Eqs. 143 and 145 to show that

$$R_V = \frac{\frac{\overline{u^2}P_s}{2N_o}}{\ln\left(\frac{1}{2\epsilon}\right)} \tag{146}$$

independent of p(u).

Now let us compare the performance of the optimal variable-rate transmission scheme in the absence of channel-measurement noise with that of the fixed-rate system.

The improvement in average bit transmission rate may be specified by the quantity R_V/R_F for a given bit error rate ϵ. From Eqs. 131 and 146, when u is Rayleigh, we find that

$$\frac{R_V}{R_F} = \frac{\frac{1}{2\epsilon} - 1}{\ln\left(\frac{1}{2\epsilon}\right)}, \tag{147}$$

which is independent of the value of $\overline{u^2}$. When u is log-normal, we can use Eqs. 132, 133, and 146 to represent R_V/R_F as a parametric function of ϵ, with parameter a:

$$\frac{R_V}{R_F} = \frac{a}{-\ln\left[\mathrm{Fr}\,(a, 0; \sigma)\right]} \tag{148}$$

$$\epsilon = \frac{1}{2}\,\mathrm{Fr}\,(a, 0; \sigma),$$

where σ equals σ_χ for the ground-to-space link and $\sigma_{\chi'}$ for the ground-to-ground link. This last result is independent of the channel-fading normalization constants Z and Z' and the transmitting and receiving directions $\vec{\theta}$ and $\vec{\phi}$ defined earlier.

The average rate gain parameter R_V/R_F, specified by Eqs. 147 and 148, is plotted against ϵ in the graph of Fig. 7. It is evident from this graph that the variable-rate transmission scheme is a significant improvement over the fixed-rate system. Also, for the log-normal case, we see that R_V/R_F increases as σ increases, when ϵ is fixed: variable-rate transmission is clearly more advantageous when the variation of the channel fading is larger.

Up to this point, we have ignored the channel coherence restriction of Eq. 115 in the interest of simplicity. The mapping R(u) in Eq. 142 clearly violates this restriction: a reasonable modification of this result which satisfies the coherence restriction is the mapping

$$R(u) = \begin{cases} \dfrac{C'P_s}{2N_o}\,u^2; & u \geq u_o \\ \dfrac{C'P_s}{2N_o}\,u_o^2; & 0 < u \leq u_o \end{cases} \tag{149}$$

where

$$u_o \equiv \sqrt{\frac{2N_o}{C'P_s(T_c - T_o)}} \tag{150}$$

and the constant C' depends on the given bit error rate. We could insert the modified

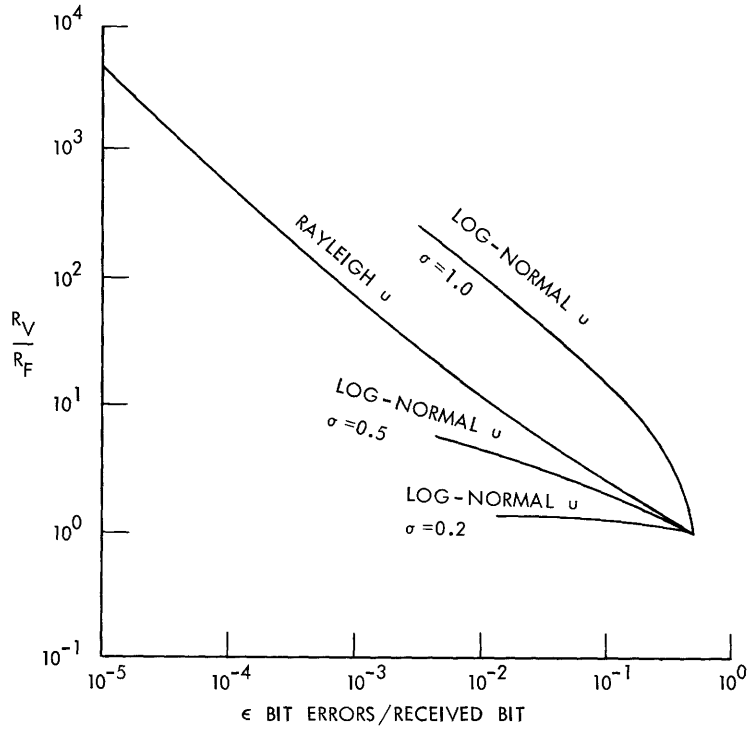

Fig. 7. Performance comparison of optimal variable-rate transmission scheme and fixed-rate optical system for heterodyne-detection case, ignoring channel-measurement noise. R_V and R_F are the average information rates in bits/second for the variable- and fixed-rate schemes, ϵ is the error rate in bit errors/received bit, u is the channel-fading parameter, and σ is the standard deviation of ln u when u is log-normal.

mapping R(u) above into Eqs. 129 and 135 to recalculate R_{avg} and ϵ, and then use Eq. 131 to evaluate the corresponding variable-rate improvement; however, this will be left as an exercise for the reader. (When u is log-normal, we find that ϵ must be expressed in terms of an integral which resembles the frustration function defined in Eq. 44 and cannot be evaluated explicitly.) Typically, because T_c is quite large, u_o is often small enough that the variable-rate results of Eqs. 143-148 are still approximately valid.

4.2.2 Noisy Channel-Measurement Case

We now consider the more general variable-rate optimization problem in which the channel-measurement noise parameter N_m is nonzero. Using the Lagrange multiplier approach as in section 4.2.1, we now want to determine the mapping $R(\rho)$ which maximizes R_{avg} for a given ϵ', with P_s, N_o, and N_m fixed. Using Eqs. 117, 124, and 128, with Lagrange multiplier λ, we want to find the non-negative function $R(\rho)$ which maximizes the expression

$$R_{avg} - \lambda\epsilon' = \int_0^\infty dp\, R(\rho) \int_0^\infty du\, p(\rho|u)\, p(u) \left[1 - \frac{\lambda}{2} e^{-\frac{u^2 P_s}{2N_o R(\rho)}}\right]. \tag{151}$$

But this is clearly equivalent to maximizing the integrand

$$g[R(\rho), \lambda] \equiv R(\rho) \int_0^\infty du\, p(\rho|u)\, p(u) \left[1 - \frac{\lambda}{2} e^{-\frac{u^2 P_s}{2N_o R(\rho)}}\right] \tag{152}$$

at each value of $\rho > 0$. If there is a unique, nontrivial value of $R(\rho)$ which maximizes $g[R(\rho), \lambda]$ at a given value of ρ, it must satisfy the condition

$$\frac{\partial}{\partial R(\rho)} g[R(\rho), \lambda] = \underbrace{\int_0^\infty du\, p(\rho|u)\, p(u)}_{\text{I}} \underbrace{- \frac{\lambda}{2} \int_0^\infty du\, p(\rho|u)\, p(u)\, e^{-\frac{u^2 P_s}{2N_o R(\rho)}}}_{\text{II}}$$

$$\underbrace{- \frac{\lambda P_s}{4N_o R(\rho)} \int_0^\infty du\, p(\rho|u)\, p(u)\, u^2\, e^{-\frac{u^2 P_s}{2N_o R(\rho)}}}_{\text{III}}. \tag{153}$$

We noted in section 3.4 that when u is log-normal, the expression for $p(\rho|u)$ appears to be too complicated for us to develop any mathematically explicit variable-rate results. We therefore confine our attention to the case in which u is Rayleigh. From Eq. 107, we have

$$\text{I} = p(\rho) = \frac{2\rho}{a + N_m} e^{-\frac{\rho^2}{a + N_m}} u_{-1}(\rho). \tag{154}$$

Using Eqs. 38, 109, and 113, we can show that

$$\text{II} = \frac{2\lambda\rho}{aN_m} e^{-\frac{\rho^2}{N_m}} u_{-1}(\rho) \int_0^\infty du\, u\, e^{-u^2\left[\frac{a + (\beta+1)N_m}{aN_m}\right]} I_o\left(\frac{2\rho u}{N_m}\right)$$

$$= \frac{\lambda\rho}{a + (\beta+1)N_m} e^{-\frac{(\beta+1)\rho^2}{a + (\beta+1)N_m}} u_{-1}(\rho), \tag{155}$$

where, for convenience, we have introduced the parameter

$$\beta(\rho) \equiv \frac{aP_s}{2N_o R(\rho)}. \tag{156}$$

From Eqs. 38, 109, and 114, we find that

$$\text{III} = \frac{2\lambda\beta\rho}{a^2 N_m} e^{-\frac{\rho^2}{N_m}} u_{-1}(\rho) \int_0^\infty du\, u^3 e^{-u^2\left[\frac{a+(\beta+1)N_m}{aN_m}\right]} I_o\left(\frac{2\rho u}{N_m}\right)$$

$$= \frac{\lambda\beta\rho\left[a\rho^2+aN_m+(\beta+1)N_m^2\right]}{[a+(\beta+1)N_m]^3} e^{-\frac{(\beta+1)\rho^2}{a+(\beta+1)N_m}} u_{-1}(\rho). \tag{157}$$

Inserting the results of Eqs. 154-157 into Eq. 153, we can show that the optimal value of $\beta(\rho)$, which is inversely proportional to the optimal mapping $R(\rho)$ that we are seeking, must satisfy the condition

$$\frac{a(a+\beta\rho^2)+(3\beta+2)aN_m+(\beta+1)(2\beta+1)N_m^2}{[a+(\beta+1)N_m]^3} e^{-\frac{a\beta\rho^2}{(a+N_m)[a+(\beta+1)N_m]}} = \frac{2}{\lambda(a+N_m)} \tag{158}$$

at each value of $\rho > 0$. As a check, we can readily verify that when we set N_m equal to zero, which implies that $\rho = u$, Eqs. 156 and 158 yield the result of Eq. 142. Unfortunately, for nonzero values of N_m we are unable to determine a closed-form solution for the optimal mapping $R(\rho)$, defined implicitly by Eqs. 156 and 158.

Note that in all of our variable-rate analysis thus far, we have implicitly assumed that the information-signal receiver can maintain perfect bit synchronization despite the continually varying signal baud times of the data transmissions. There may be a way to resolve the synchronization problem, provided the baud times are small relative to the channel coherence time T_c: in this case, the baud times vary slowly, over many data bits, so that phase-locked loop techniques should be able to maintain adequate bit synchronization.

Because we were unable to explicitly determine the optimal mapping $R(\rho)$ and evaluate the performance of the corresponding variable-rate scheme above for the general case where N_m is nonzero, we shall now examine a suboptimal class of variable-rate transmission referred to as burst communication, defined as follows. The information-signal transmitter divides its time scale into consecutive, nonoverlapping, time slots

of duration T. A single data bit is transmitted in a given time slot if and only if the observable ρ sampled at the beginning of that interval exceeds a threshold η. Otherwise, no data are sent in that particular time slot, and the information is stored until the next acceptable transmission interval occurs. We must hope, of course, that the associated transmitter buffering problem is not too severe. In Appendix D, we examine the buffering problem further and estimate the required storage capacity of the buffer.

One distinct advantage of a burst communication system, relative to the more general variable-rate schemes, is that the bit-synchronization problem is less difficult to resolve. Because the time slots have a fixed T-second periodicity, the data receiver should be able rapidly to acquire bit synchronization and maintain it within satisfactory operating limits.

The data receiver is now faced with a word-synchronization problem. It must decide whether an information signal was actually transmitted in a particular time slot. If it reaches an incorrect decision, a transmitted bit will be lost or an extraneous bit will be inserted in the decoded data bit stream. When this occurs, a word-synchronization error is made. To prevent such an error from propagating to subsequent words, commas should be periodically inserted in the transmitted word stream.

We have not yet mentioned how the receiver can decide whether a data signal was sent in a given time slot. One method of resolving this problem is to transmit a pilot tone at a fixed power level from the data transmitter to the data receiver. In Section III we saw how a pilot tone transmitted in the reverse direction could be used to track the channel-fading parameter u. In like manner, the data receiver can process its received pilot tone to monitor u. On the basis of this measurement, the data receiver can form a maximum-likelihood estimate $\hat{\rho}_{ML}$ of the observable ρ associated with each time slot. Depending on whether $\hat{\rho}_{ML}$ is greater or less than the threshold η, the data receiver would decide that an information signal was or was not sent in a given time slot. An alternative and more efficient approach is to extract channel-fading information directly from the received data-signal carrier instead of using a separate pilot-tone probe. In either case, if the channel-fading measurements made by the data receiver are averaged over a sufficiently long time interval, of the order of T_c in length, the probability of a word-synchronization error occurring will be quite small. For simplicity, the analysis below disregards word-synchronization errors.

In the context of our variable-rate notation defined earlier, the burst communication system is characterized by the prescription

$$R(\rho) = Ru_{-1}(\rho-\eta), \tag{159}$$

where $R = 1/T$ bits/second, and we assume that the temporal coherence restriction of Eq. 115 is satisfied:

$$T + T_o < T_c. \tag{160}$$

We would like to determine the mapping $R(\rho)$, within the class defined by Eq. 159, which maximizes R_{avg} for a given value of ϵ', when P_s, N_o, and N_m are fixed. Our analysis is again restricted to the case where u is Rayleigh. From Eqs. 107, 117, and 159, we can show that

$$R_{avg} = \frac{2R}{a + N_m} \int_{\eta}^{\infty} d\rho\, \rho\, e^{-\frac{\rho^2}{a+N_m}} = R\, e^{-\frac{\eta^2}{a+N_m}}. \tag{161}$$

Also, using Eqs. 38, 109, 113, 124, and 128, we find that

$$\epsilon' = \frac{2R}{aN_m} \int_{\eta}^{\infty} d\rho\, \rho\, e^{-\frac{\rho^2}{N_m}} \int_{0}^{\infty} du\, u\, e^{-u^2\left[\frac{a+(\zeta+1)N_m}{aN_m}\right]} I_o\left(\frac{2\rho u}{N_m}\right)$$

$$= \frac{R}{a + (\zeta+1)N_m} \int_{\eta}^{\infty} d\rho\, \rho\, e^{-\frac{(\zeta+1)\rho^2}{a+(\zeta+1)N_m}} = \frac{R}{2(\zeta+1)}\, e^{-\frac{(\zeta+1)\eta^2}{a+(\zeta+1)N_m}}, \tag{162}$$

where, for convenience, we have defined the parameter

$$\zeta \equiv \frac{aP_s}{2N_o R}. \tag{163}$$

Combining Eqs. 129, 161, and 162, we have

$$\epsilon \equiv \frac{\epsilon'}{R_{avg}} = \frac{1}{2(\zeta+1)}\, e^{-\frac{a\zeta\eta^2}{(a+N_m)[a+(\zeta+1)N_m]}}; \tag{164}$$

substituting Eq. 163 in Eq. 161, we can write

$$\zeta = \frac{aP_s}{2N_o R_{avg}}\, e^{-\frac{\eta^2}{a+N_m}}. \tag{165}$$

If R_{avg}, P_s, N_o, a, and N_m are fixed, Eqs. 164 and 165 implicitly define ϵ as a function of η.

Now, instead of trying to determine the values of R and η which maximize R_{avg} for a given ϵ', when P_s, N_o, and N_m are fixed, it is mathematically simpler to

equivalently minimize ϵ over η^2 for a given R_{avg}. In the nontrivial case, the optimal value of η^2 must satisfy the condition

$$\frac{d\epsilon}{d\eta^2} = \frac{\partial\epsilon}{\partial\eta^2} + \frac{\partial\epsilon}{\partial\zeta}\frac{d\zeta}{d\eta^2} = 0. \tag{166}$$

We can readily evaluate the derivatives required by Eq. 166:

$$\frac{\partial\epsilon}{\partial\eta^2} = -\left\{\frac{a\zeta}{(a+N_m)[a+(\zeta+1)N_m]}\right\}\epsilon,$$

$$\frac{\partial\epsilon}{\partial\zeta} = -\left\{\frac{[a+(\zeta+1)N_m]^2 + (\zeta+1)a\eta^2}{(\zeta+1)[a+(\zeta+1)N_m]^2}\right\}\epsilon,$$

and

$$\frac{d\zeta}{d\eta^2} = -\frac{\zeta}{a+N_m}.$$

Therefore, the optimal value of η^2 is specified by

$$\eta^2 = \begin{cases} \dfrac{[a+(\zeta+1)N_m][a\zeta-(\zeta+1)N_m]}{a(\zeta+1)}; & N_m \leq \dfrac{a\zeta}{\zeta+1}, \\ 0; & N_m \geq \dfrac{a\zeta}{\zeta+1}. \end{cases} \tag{167}$$

Note that Eq. 167 tells us that when $N_m \geq a$, the optimal threshold η is zero for all values of ζ, which corresponds to the entire range of ϵ. On the other hand, even if $N_m \leq a$, the optimal threshold η is zero over the range $0 \leq \zeta \leq N_m/(a-N_m)$, or equivalently $(a-N_m)/2a \leq \epsilon \leq \frac{1}{2}$. Of course, when the optimal threshold η is zero, the best burst communication system is simply the fixed-rate scheme with average information rate R_F defined by Eq. 131. In other words, the burst communication scheme does not buy us anything unless the channel-measurement noise is small enough, and even then only when we desire a sufficiently small error rate.

Denoting R_{avg} by R_B, and for convenience defining the parameter

$$\delta \equiv \frac{N_m}{a}, \tag{168}$$

the optimal burst communication system is characterized by the following parameters:

$$\frac{1-\delta}{2} \leq \epsilon \leq \frac{1}{2}$$

$$T = \frac{1}{R_F}, \quad R = R_F, \quad \eta^2 = 0, \quad R_B = R_F = \frac{\frac{aP_s}{2N_o}}{\frac{1}{2\epsilon} - 1};$$

$$0 \leq \epsilon \leq \frac{1-\delta}{2}, \quad \frac{\delta}{1-\delta} \leq \zeta < \infty, \quad \delta \leq 1$$

$$T = \frac{2N_o\zeta}{aP_s}, \qquad R = \frac{aP_s}{2N_o\zeta},$$

$$\eta^2 = \frac{a[1+(\zeta+1)\delta][\zeta-(\zeta+1)\delta]}{\zeta+1},$$

$$R_B = \frac{aP_s}{2N_o\zeta} e^{-\frac{[1+(\zeta+1)\delta][\zeta-(\zeta+1)\delta]}{(\zeta+1)(1+\delta)}},$$

$$\epsilon = \frac{1}{2(\zeta+1)} e^{-\frac{\zeta[\zeta-(\zeta+1)\delta]}{(\zeta+1)(1+\delta)}}. \tag{169}$$

In order to design a burst communication system according to the prescription of Eq. 169 for the nontrivial case where $\epsilon \leq \frac{1}{2}(1-\delta)$, one first determines the value of the parameter ζ which yields the desired bit error rate ϵ. The optimal threshold η and baud time T then result in an average signalling rate R_B, all specified by Eq. 169 in terms of the previously calculated value of ζ. The designer must still verify that the temporal coherence restriction of Eq. 160 is satisfied. Notice that there is a trade-off between T and T_o. By Eq. 104, a larger value of T_o makes N_m smaller, which decreases δ according to Eq. 168. This increased noise immunity for the channel-measurement operation results in a lower value of ζ being required to produce the desired error rate ϵ, which yields a smaller value of T. One can verify that in this case R_B is increased, so in general we should try to make T_o as large as possible. A good starting point in designing a burst communication system is to set T_o approximately equal to T_c, and then check whether the value of T specified in Eq. 169 is much smaller than T_c. If this is not the case, one can try to satisfy Eqs. 160 and 169 with smaller values of T_o. There will be situations for which we cannot satisfy these restrictions for any value of T_o: this will happen if the desired value of ϵ is too

small for the available signal-to-noise ratios P_s/N_o and P_p/N_b' (see Eqs. 93, 94, and 104) for the information signal and pilot tone, respectively.

Using Eqs. 131 and 169, we can characterize the improvement in average bit transmission rate, for a given bit error rate ϵ, of the optimal burst communication system relative to the corresponding fixed-rate scheme by

$$\frac{R_B}{R_F} = \begin{cases} 1; & \frac{1-\delta}{2} \leq \epsilon \leq \frac{1}{2} \\ \frac{\frac{1}{2\epsilon} - 1}{\zeta} e^{-\frac{[1+(\zeta+1)\delta][\zeta-(\zeta+1)\delta]}{(\zeta+1)(1+\delta)}}; & 0 \leq \epsilon \leq \frac{1-\delta}{2}, \end{cases} \tag{170}$$

for the case in which u is Rayleigh. When $\epsilon \leq \frac{1-\delta}{2}$, Eqs. 169 and 170 define R_B/R_F as a parametric function of ϵ, with parameter ζ. The average rate gains R_B/R_F, plotted as functions of ϵ for several values of δ in the graph of Fig. 8, are significantly large for small values of δ and ϵ. Comparing R_B/R_F for the special case where $\delta = 0$ with

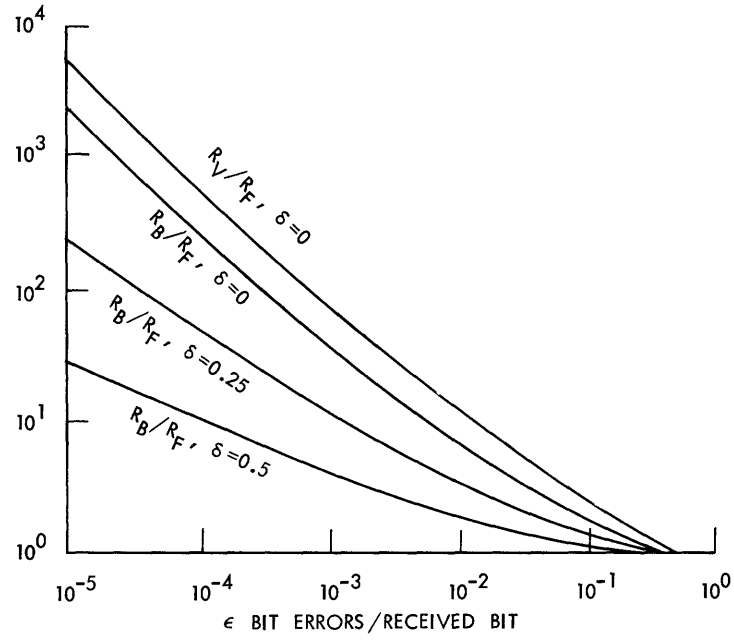

Fig. 8. Performance comparison of optimal burst communication scheme and fixed-rate system for heterodyne-detection case and Rayleigh fading. R_B and R_F are the average information rates in bits/second for the burst and fixed-rate schemes, ϵ is the error rate in bit errors/received bit, and δ is a channel-measurement noise parameter (see Eq. 168). Also, R_V is the average information rate for the optimal general variable-rate system.

the noiseless channel-measurement result R_V/R_F for Rayleigh fading, reproduced from Fig. 7, it is evident that the optimal burst communication system performs almost as well as the general optimal variable-rate scheme in this case.

Remember that the burst communication strategy developed above is optimal with respect to the power constraint of Eq. 119, which can be rewritten in the form

$$P_t(\rho) = \begin{cases} P_{avg}; & \rho > \eta \\ 0; & \rho < \eta. \end{cases} \tag{171}$$

For the nontrivial case wherein the threshold η specified in Eq. 169 is nonzero, we can combine Eqs. 107, 168, 169, and 171 to show that the average transmitted power is given in terms of ζ (which depends on ϵ) and δ by

$$\overline{P_t(\rho)}^{\rho} = P_{avg}\, e^{-\frac{[1+(\zeta+1)\delta][\zeta-(\zeta+1)\delta]}{(\zeta+1)(1+\delta)}} < P_{avg}. \tag{172}$$

Therefore, in this case we are not using all of the available transmitter power. Even though the burst communication scheme above represents a dramatic improvement over the fixed-rate system, indicated by the large average rate gains R_B/R_F shown in Fig. 8, we could do even better by modifying the power restriction of Eq. 171 for the burst communication scheme so that $P_t(\rho)$ is given by

$$P_t(\rho) = \begin{cases} \min\left(P_{peak},\ P_{avg}\, e^{\frac{[1+(\zeta+1)\delta][\zeta-(\zeta+1)\delta]}{(\zeta+1)(1+\delta)}}\right); & \rho > \eta, \\ 0; & \rho < \eta, \end{cases} \tag{173}$$

which satisfies the more general power constraint of Eq. 118. If we make the assumption that

$$P_{peak} > P_{avg}\, e^{\frac{[1+(\zeta+1)\delta][\zeta-(\zeta+1)\delta]}{(\zeta+1)(1+\delta)}} \tag{174}$$

the average transmitted power for the modified burst communication system is simply P_{avg}, as in the fixed-rate case. When Eq. 174 is valid, the modified burst communication system is specified by Eq. 169 with P_s replaced everywhere by

$$P_s\, e^{\frac{[1+(\zeta+1)\delta][\zeta-(\zeta+1)\delta]}{(\zeta+1)(1+\delta)}}$$

Denoting the average information rate for this modified burst communication scheme by R_B', we can use Eqs. 131 and 169 to write

$$\frac{R_B'}{R_F} = \frac{\frac{1}{2\epsilon} - 1}{\zeta}; \qquad 0 \leq \epsilon \leq \frac{1-\delta}{2}, \tag{175}$$

where ϵ is still given by Eq. 169. For the special case where $\delta = 0$, we find that the modified burst communication scheme, subject to the assumption of Eq. 174, performs better than the general variable-rate scheme which is optimal for the power constraint of Eq. 119. Yet both systems have an everage transmitted power of P_{avg}. For example, when $\delta = 0$, we can use Eqs. 147, 169, and 175 to show that at $\epsilon = 10^{-5}$ bit errors/received bit, $R_B'/R_F = 5.33 \times 10^3$ while $R_V/R_F = 4.62 \times 10^3$.

4.3 DIRECT-DETECTION SYSTEMS

The conditional probability of error defined in Eq. 127 for the direct-detection case is more complex than the equivalent expression in Eq. 124 for the heterodyne-detection case. Consequently, the development of optimal variable-rate direct-detection systems presents a more difficult mathematical problem. To illustrate these difficulties, we shall try to determine the optimal variable-rate system for the relatively simple case where the channel-measurement noise is insignificant so that N_m is essentially zero.

The optimization analysis proceeds initially as in the heterodyne-detection case of section 4.2.1 using the Lagrange multiplier approach with parameter λ. As before, the optimal mapping R(u) must satisfy the constraint of Eq. 138 at each value of u, where $\lambda > 2$. In the discussion that followed Eq. 138, we showed that if $P(\epsilon|u)$ could be expressed in the form of Eq. 139, the optimal R(u) would be given by Eq. 141.

Consider for a moment the Chernoff upper bound on $P(\epsilon|u)$ for the direct-detection case, which is given by[54]

$$P(\epsilon|u) \leq e^{-\frac{\mu_n\left(\sqrt{1+u^2\alpha}-1\right)^2}{2R(u)}}, \tag{176}$$

where the parameters μ_n and α are defined in Eqs. 51, 52, 54, and 59. When this bound becomes sufficiently tight that it accurately reflects the functional dependence of $P(\epsilon|u)$ on u, Eqs. 139 and 141 suggest that the optimal R(u) has the approximate form

$$R(u) \cong \frac{C\mu_n}{2}\left(\sqrt{1+u^2\alpha}-1\right)^2, \tag{177}$$

where the constant C depends on the given bit error rate. Furthermore, over the range $u \gg 1/\sqrt{a}$, Eq. 177 yields the familiar result that the optimal R(u) is proportional to u^2 as in the heterodyne-detection case (see Eq. 142).

Let us now try to solve Eq. 138 for the optimal R(u) using the exact conditional probability of error for the direct-detection system. Modifying Eq. 127 for the special case where $\rho = u$, we have

$$P(\epsilon|u) = Q_m\left[\sqrt{\frac{\mu_n}{R(u)}}, \sqrt{\frac{\mu_n(1+u^2a)}{R(u)}}\right] - \frac{1}{2} e^{-\frac{\mu_n(2+u^2a)}{2R(u)}} I_o\left[\frac{\mu_n\sqrt{1+u^2a}}{R(u)}\right]. \quad (178)$$

Inserting Eq. 178 into the constraint of Eq. 138, we find that the optimal R(u) satisfies the condition

$$\left[1 + \frac{\mu_n}{2R(u)}\right] Q_m\left[\sqrt{\frac{\mu_n}{R(u)}}, \sqrt{\frac{\mu_n(1+u^2a)}{R(u)}}\right]$$

$$- \frac{1}{2}\left[1 - \frac{\mu_n a u^2}{2R(u)} e^{-\frac{\mu_n(2+u^2a)}{2R(u)}}\right] I_o\left[\frac{\mu_n\sqrt{1+u^2a}}{R(u)}\right]$$

$$+ \frac{\mu_n\sqrt{1+u^2a}}{2R(u)} e^{-\frac{\mu_n(2+u^2a)}{2R(u)}} I_1\left[\frac{\mu_n\sqrt{1+u^2a}}{R(u)}\right]$$

$$- \frac{1}{2}\sqrt{\frac{\mu_n}{R(u)}} \int_{\sqrt{\frac{\mu_n(1+u^2a)}{R(u)}}}^{\infty} dx\, x^2 e^{-\frac{\mu_n}{2R(u)}} e^{-\frac{x^2}{2}} I_1\left[x\sqrt{\frac{\mu_n}{R(u)}}\right] = \frac{1}{\lambda}. \quad (179)$$

The Lagrange multiplier λ is specified by the constraint of Eq. 135 on bit error rate ϵ'. Then Eqs. 135, 178, and 179 implicitly determine the optimal mapping R(u) for a given value of ϵ'.

Although we have considered the relatively simple case where $N_m = 0$, we cannot explicitly determine the optimal variable-rate direct-detection system. It may be possible to evaluate approximately the optimal R(u) over some range of u, μ_n, and a by approximating the terms in Eqs. 135, 178, and 179. Rather than considering a complicated approximation problem, we shall now turn our attention to determining the optimal burst communication system in the hope that the associated mathematical analysis will be less difficult and provide more insight. As in the heterodyne-detection

case, the analysis below ignores the word-synchronization problem; a practical direct-detection, burst communication system will therefore not perform quite as well as the idealized system considered below. We note, however, that the data receiver can achieve a significant measure of word synchronization by estimating ρ as in the heterodyne-detection case.

For the general case of noisy channel measurement ($N_m \neq 0$) we would like to determine the mapping $R(\rho)$, restricted to the form of Eq. 159, which maximizes R_{avg} for a given value of ϵ', when μ_n, a, and N_m are fixed. For mathematical simplicity, we again confine our attention to the case in which u is Rayleigh. As in the heterodyne-detection case, R_{avg} is given by Eq. 161. Using Eqs. 38, 109, 128, and 159, we have

$$\epsilon' = \frac{4R}{aN_m} \int_\eta^\infty d\rho\, \rho\, e^{-\frac{\rho^2}{N_m}} \int_0^\infty du\, u\, e^{-\frac{u^2}{a}} e^{-\frac{u^2}{N_m}} I_o\left[\frac{2\rho u}{N_m}\right] P(\epsilon|u, \rho). \tag{180}$$

From Eqs. 127 and 159, we note that $P(\epsilon|u, \rho)$ is independent of ρ when $\rho > \eta$:

$$P(\epsilon|u, \rho) = Q_m\left[\sqrt{\frac{\mu_n}{R}}, \sqrt{\frac{\mu_n(1+u^2a)}{R}}\right] - \frac{1}{2} e^{-\frac{\mu_n(2+u^2a)}{2R}} I_o\left[\frac{\mu_n\sqrt{1+u^2a}}{R}\right]$$

$$\equiv P'(\epsilon|u); \qquad \rho > \eta. \tag{181}$$

Inserting Eq. 181 in Eq. 180 and interchanging the order of integration, we have

$$\epsilon' = \frac{2R}{a} \int_0^\infty du\, u\, e^{-\frac{u^2}{a}} P'(\epsilon|u) \int_\eta^\infty d\rho\, \frac{2\rho}{N_m} e^{-\frac{\rho^2+u^2}{N_m}} I_o\left(\frac{2\rho u}{N_m}\right). \tag{182}$$

Letting $x = \rho\sqrt{2/N_m}$ in Eq. 182, and using the definition of the Marcum Q function of Eq. 61, we find that

$$\epsilon' = \frac{2R}{a} \int_0^\infty du\, u\, e^{-\frac{u^2}{a}} P'(\epsilon|u)\, Q_m\left(\frac{u}{\gamma}, \frac{\eta}{\gamma}\right), \tag{183}$$

where for convenience we have defined a new channel-measurement noise parameter

$$\gamma \equiv \sqrt{\frac{N_m}{2}}. \tag{184}$$

Unfortunately, we cannot explicitly solve Eq. 183 for ϵ' in general; however, for the case wherein the channel-measurement noise is sufficiently small, we can determine

a perturbation solution for ϵ'. In the remaining analysis, we assume that γ is nonzero but small. Using Eq. C3, we have the approximation

$$Q_m\left(\frac{u}{\gamma}, \frac{\eta}{\gamma}\right) \cong \sqrt{\frac{\gamma}{2\pi u}} \int_{\eta/\gamma}^{\infty} dx\, \sqrt{x}\; e^{-\frac{1}{2}\left(x-\frac{u}{\gamma}\right)^2}.$$

Then, letting $y = x\gamma$, we have

$$Q_m\left(\frac{u}{\gamma}, \frac{\eta}{\gamma}\right) \cong \frac{1}{\sqrt{u}} \int_{\eta}^{\infty} dy\, \sqrt{y}\; N_y(u, \gamma^2), \tag{185}$$

where $N_y(u, \gamma^2)$ is the probability density function of a Gaussian random variable y with mean u and variance γ^2:

$$N_y(u, \gamma^2) \equiv \frac{1}{\sqrt{2\pi\gamma^2}}\, e^{-\frac{(y-u)^2}{2\gamma^2}}. \tag{186}$$

For small values of γ, $N_y(u, \gamma^2)$ is a very narrow pulse centered at $y = u$. In fact, in the limiting case,

$$N_y(u, \gamma^2) \xrightarrow[\gamma \to 0]{} u_o(y-u),$$

so that

$$Q_m\left(\frac{u}{\gamma}, \frac{\eta}{\gamma}\right) \xrightarrow[a \to 0]{} u_{-1}(u-\eta). \tag{187}$$

Inserting Eq. 187 into Eq. 183, we find that

$$\epsilon' \xrightarrow[\gamma \to 0]{} \frac{2R}{a} \int_{\eta}^{\infty} du\, u\, e^{-\frac{u^2}{a}}\, P'(\epsilon|u) \equiv \epsilon'_o, \tag{188}$$

where ϵ'_o is the zero-order perturbation solution for ϵ' about $\gamma = 0$, which is the value of ϵ' in the absence of channel-measurement noise. Using Eqs. 181 in Eq. 188, we have

$$\epsilon_o' = \underbrace{\frac{2R}{a}\int_\eta^\infty du\, u\, e^{-\frac{u^2}{a}}\, Q_m\left[\sqrt{\frac{\mu_n}{R}}, \sqrt{\frac{\mu_n(1+u^2a)}{R}}\right]}_{I}$$

$$\underbrace{-\frac{R}{a}\int_\eta^\infty du\, u\, e^{-\frac{u^2}{a}}\, e^{-\frac{\mu_n(2+u^2a)}{2R}}\, I_o\left(\frac{\mu_n\sqrt{1+u^2a}}{R}\right)}_{II}. \tag{189}$$

Using Eq. 61, we can rewrite the first integral in the form

$$I = \frac{R}{a\alpha}\, e^{\frac{1}{a\alpha}}\int_\eta^\infty du\, 2u\alpha\, e^{-\frac{1+u^2a}{a\alpha}}\int_{\sqrt{\frac{\mu_n(1+u^2a)}{R}}}^\infty dx\, x\, e^{-\frac{x^2}{2}}\, e^{-\frac{\mu_n}{2R}}\, I_o\left(x\sqrt{\frac{\mu_n}{R}}\right). \tag{190}$$

Letting $y = 1 + u^2\alpha$ in Eq. 190, we can write

$$I = \frac{R}{2\Delta}\, e^{\frac{1}{2\Delta}}\int_{\nu^2}^\infty dy\, e^{-\frac{y}{2\Delta}}\int_{\sqrt{\frac{Jy}{\Delta}}}^\infty dx\, x\, e^{-\frac{x^2}{2}}\, e^{-\frac{J}{2\Delta}}\, I_o\left(x\sqrt{\frac{J}{\Delta}}\right), \tag{191}$$

where Δ is defined in Eq. 59, and for mathematical convenience we have introduced two new parameters:

$$J \equiv \frac{\mu_n\Delta}{R} = u^2\,\frac{\mu_s T}{2}; \qquad \nu \equiv \sqrt{1+\eta^2\alpha}. \tag{192}$$

The parameter J is the average number of signal counts per baud when η is equal to zero. We note, however, that for the general burst communication system, J does not represent either the average number of signal counts per baud, or that quantity conditioned on the event $\rho > \eta$ (that is, on an information signal having been sent in the baud interval).

Interchanging the order of integration in Eq. 191, we find that

$$I = R\, e^{\frac{1}{2\Delta}}\int_{\nu\sqrt{J/\Delta}}^\infty dx\, x\, e^{-\frac{x^2}{2}}\, e^{-\frac{J}{2\Delta}}\, I_o\left(x\sqrt{\frac{J}{\Delta}}\right)\underbrace{\int_{\nu^2}^{\frac{\Delta x^2}{J}} dy\, \frac{1}{2\Delta}\, e^{-\frac{y}{2\Delta}}}_{e^{-\frac{\nu^2}{2\Delta}} - e^{-\frac{x^2}{2J}}}$$

$$= R\, e^{-\left(\frac{\nu^2-1}{2\Delta}\right)}Q_m\left(\sqrt{\frac{J}{\Delta}}, \nu\sqrt{\frac{J}{\Delta}}\right) - R\, e^{\frac{1}{2\Delta}}\int_{\nu\sqrt{J/\Delta}}^\infty dx\, x\, e^{-\frac{x^2(J+1)}{2J}}\, e^{-\frac{J}{2\Delta}}\, I_o\left(x\sqrt{\frac{J}{\Delta}}\right). \tag{193}$$

Let $y = x\sqrt{(J+1)/J}$, then Eq. 193 reduces to

$$I = R\, e^{-\left(\frac{\nu^2-1}{2\Delta}\right)} Q_m\left(\sqrt{\frac{J}{\Delta}},\ \nu\sqrt{\frac{J}{\Delta}}\right) - \left(\frac{JR}{J+1}\right) e^{\frac{1}{2\Delta(J+1)}} Q_m\left(\sqrt{\frac{J^2}{\Delta(J+1)}},\ \nu\sqrt{\frac{J+1}{\Delta}}\right). \tag{194}$$

To solve the second integral in Eq. 189, we can let $x = \sqrt{(J+1)(1+u^2\alpha)/\Delta}$; then we show that

$$II = \frac{R}{2(J+1)}\, e^{\frac{1}{2\Delta(J+1)}} Q_m\left(\sqrt{\frac{J^2}{\Delta(J+1)}},\ \nu\sqrt{\frac{J+1}{\Delta}}\right). \tag{195}$$

Therefore, the zero-order perturbation solution for ϵ' about $\gamma = 0$ is given by

$$\epsilon'_o = R\left[e^{-\left(\frac{\nu^2-1}{2\Delta}\right)} Q_m\left(\sqrt{\frac{J}{\Delta}},\ \nu\sqrt{\frac{J}{\Delta}}\right) - \frac{1}{2}\left(\frac{2J+1}{J+1}\right) e^{\frac{1}{2\Delta(J+1)}} Q_m\left(\sqrt{\frac{J^2}{\Delta(J+1)}},\ \nu\sqrt{\frac{J+1}{\Delta}}\right)\right]. \tag{196}$$

Continuing now with the general perturbation problem, we can combine Eqs. 183, 185, and 186 to give

$$\epsilon' \cong \frac{2R}{a}\int_\eta^\infty dy\,\sqrt{y}\int_0^\infty du\, f(u)\, N_u(y, \gamma^2), \tag{197}$$

where

$$f(u) \equiv \sqrt{u}\; e^{-\frac{u^2}{a}}\; P'(\epsilon|u) \tag{198}$$

and $N_u(y, \gamma^2)$ is the probability density function of a Gaussian random variable u with mean y and variance γ^2. Functionally, $N_u(y, \gamma^2)$ is the same mathematical expression as $N_y(u, \gamma^2)$ in Eq. 186. Since $N_u(y, \gamma^2)$ is a narrow pulse centered at u = y, we will approximate f(u) in Eq. 197 by the first three terms of its Taylor series expansion about u = y:

$$\epsilon' \cong \frac{2R}{a}\int_\eta^\infty dy\,\sqrt{y}\left[f(y)\int_0^\infty du\,\frac{e^{-\frac{(u-y)^2}{2\gamma^2}}}{\sqrt{2\pi\gamma^2}} + f'(y)\int_0^\infty du\,(u-y)\,\frac{e^{-\frac{(u-y)^2}{2\gamma^2}}}{\sqrt{2\pi\gamma^2}}\right.$$
$$\left. + \frac{1}{2}f''(y)\int_0^\infty du\,(u-y)^2\,\frac{e^{-\frac{(u-y)^2}{2\gamma^2}}}{\sqrt{2\pi\gamma^2}}\right]. \tag{199}$$

It is a simple exercise, which will be left to the reader's initiative, to demonstrate that to order γ^2, if $\gamma^2 \ll \eta^2$, Eq. 186 reduces to

$$\epsilon' \cong \underbrace{\frac{2R}{a}\int_\eta^\infty dy\ \sqrt{y}\ f(y)}_{\epsilon'_o} + \underbrace{\frac{\gamma^2 R}{a}\int_\eta^\infty dy\ \sqrt{y}\ f''(y)}_{\Delta\epsilon'_1} \equiv \epsilon'_1, \tag{200}$$

where ϵ'_1 is the desired first-order perturbation solution for ϵ' about $\gamma = 0$, and $\Delta\epsilon'_1$ is the corresponding first-order correction term.

We shall now try to evaluate $\Delta\epsilon'_1$ near $\gamma = 0$. Note that f(y) and f'(y) vanish rapidly as y gets large; therefore, integrating by parts twice, we have

$$\Delta\epsilon'_1 = \frac{\gamma^2 R}{a}\left[-\sqrt{\eta}\ f'(\eta) + \frac{1}{2\sqrt{\eta}}\ f(\eta) - \underbrace{\frac{1}{4}\int_\eta^\infty dy\ y^{-\frac{3}{2}} f(y)}_{\text{III}}\right]. \tag{201}$$

From Eq. 198, we can write

$$-\sqrt{\eta}\ f'(\eta) = -\frac{1}{2\sqrt{\eta}}\ f(\eta) + \frac{2\eta^{3/2}}{a}\ f(\eta) - \eta\, e^{-\frac{\eta^2}{a}}\ \frac{d}{du}\ P'(\epsilon|u)\Big|_{u=\eta}. \tag{202}$$

Furthermore, using Eqs. 181 and 192, we find that

$$\frac{d}{du}\ P'(\epsilon|u) = -\frac{Ju\alpha}{2\Delta\nu}\, e^{-\frac{J(\nu^2+1)}{2\Delta}}\left[\nu I_o\left(\frac{J\nu}{\Delta}\right) + I_1\left(\frac{J\nu}{\Delta}\right)\right]. \tag{203}$$

Then, combining Eqs. 181, 192, 198, and 201-203, we have

$$\Delta\epsilon'_1 = \frac{\gamma^2 R}{a}\left[\left(\frac{\nu^2-1}{\Delta}\right)e^{-\left(\frac{\nu^2-1}{2\Delta}\right)}Q_m\left(\sqrt{\frac{J}{\Delta}},\ \nu\sqrt{\frac{J}{\Delta}}\right) + \frac{(J-1)(\nu^2-1)}{2\Delta}\ e^{-\left(\frac{\nu^2-1}{2\Delta}\right)}e^{-\frac{J(\nu^2+1)}{2\Delta}}\ I_o\left(\frac{J\nu}{\Delta}\right)\right.$$

$$\left. + \frac{J(\nu^2-1)}{2\Delta\nu}\ e^{-\left(\frac{\nu^2-1}{2\Delta}\right)}e^{-\frac{J(\nu^2+1)}{2\Delta}}\ I_1\left(\frac{J\nu}{\Delta}\right) - \text{III}\right]. \tag{204}$$

We cannot evaluate the integral labelled III in Eqs. 201 and 204 exactly, but we shall now derive a condition under which III can be neglected, and later show that this condition can be met in practice. Using Eqs. 200 and 201, we can bound III as follows:

$$0 < \text{III} = \frac{1}{4}\int_{\eta}^{\infty} dy\, \frac{1}{y^2}\sqrt{y}\ f(y) < \frac{1}{4\eta^2}\underbrace{\int_{\eta}^{\infty} dy\,\sqrt{y}\ f(y)}_{\frac{a\epsilon_o'}{2R}} \equiv \frac{a\epsilon_o'}{8R\eta^2}. \tag{205}$$

Introducing the parameters Δ and ν defined in Eqs. 59 and 192, and using Eq. 196 to upperbound ϵ_o', the bound in Eq. 205 implies that

$$0 < \text{III} < \frac{\Delta}{4R(\nu^2-1)}\ \epsilon_o' < \frac{\Delta}{4(\nu^2-1)}\ e^{-\left(\frac{\nu^2-1}{2\Delta}\right)} Q_m\left(\sqrt{\frac{J}{\Delta}},\ \nu\sqrt{\frac{J}{\Delta}}\right). \tag{206}$$

Comparing the upper bound for III in Eq. 206 with the first term inside the square brackets in Eq. 204, it is clear that a sufficient condition under which we can neglect III in the expression for $\Delta\epsilon_1'$ is given by

$$\Delta^2 \ll 4(\nu^2-1)^2. \tag{207}$$

After we select a suitable value of ν, we show that the constraint of Eq. 207 is satisfied for any value of Δ. For the time being, we simply assume that III can be neglected in the expression for $\Delta\nu_1'$.

Combining Eqs. 168, 184, 196, 200, and 204, and neglecting III, we can express the first-order perturbation solution for ϵ' about $\gamma = 0$ by

$$\begin{aligned}\epsilon' \cong \epsilon_1' \cong R\Bigg\{ & e^{-\left(\frac{\nu^2-1}{2\Delta}\right)} Q_m\left(\sqrt{\frac{J}{\Delta}},\ \nu\sqrt{\frac{J}{\Delta}}\right)\left[1 + \frac{\delta(\nu^2-1)}{2\Delta}\right] \\ & - \frac{1}{2}\left(\frac{2J+1}{J+1}\right) e^{\frac{1}{2\Delta(J+1)}}\, Q_m\left(\sqrt{\frac{J^2}{\Delta(J+1)}},\ \nu\sqrt{\frac{J+1}{\Delta}}\right) \\ & + \frac{\delta(\nu^2-1)}{4\Delta\nu}\, e^{-\left(\frac{\nu^2-1}{2\Delta}\right)} e^{-\frac{J(\nu^2+1)}{2\Delta}}\left[(J-1)\,\nu I_o\left(\frac{J\nu}{\Delta}\right) + J I_1\left(\frac{J\nu}{\Delta}\right)\right]\Bigg\}. \end{aligned} \tag{208}$$

From Eqs. 59, 161, 168, and 192, we find that

$$R_{avg} = R\, e^{-\frac{(\nu^2-1)}{2\Delta(1+\delta)}} = \frac{\mu_n\Delta}{J}\, e^{-\frac{\nu^2-1}{2\Delta(1+\delta)}}. \tag{209}$$

Finally, using Eqs. 129, 208, and 209, we deduce that our burst communication

system has a bit error rate given by

$$\epsilon \cong e^{-\frac{\delta(\nu^2-1)}{2\Delta(1+\delta)}} Q_m\left(\sqrt{\frac{J}{\Delta}},\ \nu\sqrt{\frac{J}{\Delta}}\right)\left[1+\frac{\delta(\nu^2-1)}{2\Delta}\right]$$

$$-\frac{1}{2}\left(\frac{2J+1}{J+1}\right) e^{\frac{(\nu^2-1)}{2\Delta(1+\delta)}} e^{\frac{1}{2\Delta(J+1)}} Q_m\left(\sqrt{\frac{J^2}{\Delta(J+1)}},\ \nu\sqrt{\frac{J+1}{\Delta}}\right)$$

$$+\frac{\delta(\nu^2-1)}{4\Delta\nu} e^{-\frac{\delta(\nu^2-1)}{2\Delta(1+\delta)}} e^{-\frac{J(\nu^2+1)}{2\Delta}}\left[(J-1)\,\nu I_o\left(\frac{J\nu}{\Delta}\right)+JI_1\left(\frac{J\nu}{\Delta}\right)\right]. \tag{210}$$

Thus R_{avg} is parametrically expressed as a function of ϵ in Eqs. 209 and 210. Now, instead of optimizing our burst communication system over the initial parameters R and η we equivalently optimize over J and ν. Rearranging Eq. 209, we can write

$$J = \frac{\mu_n \Delta}{R_{avg}} e^{-\frac{\nu^2-1}{2\Delta(1+\delta)}}. \tag{211}$$

We assume that μ_n, Δ, and δ are fixed system parameters that we must work with. Then Eqs. 210 and 211 implicitly define ϵ as a function of R_{avg} and ν. Our optimization problem is to determine that value of ν which minimizes ϵ for a given R_{avg}. One soon discovers that even for the special case where $\delta = 0$ (corresponding to noiseless channel measurement), we cannot explicitly evaluate this optimal value of ν.

We assume that we are interested in reliable communication systems characterized by a small bit error rate ϵ. Now when J gets very large, ϵ becomes very small, and Eq. 210 can be approximated by a relatively simple expression. We can then use this expression together with Eq. 211 to determine the value of ν which is optimal in the limit as ϵ approaches zero. Inserting this value of ν into Eqs. 209 and 210 will then completely define a burst communication system. While it will not be the optimal burst communication system over the entire range of ϵ, it should be nearly optimal in the interesting case where ϵ is small.

We will need several approximations to simplify Eq. 210. Note from Eq. C10 that

$$Q_m(a, b) \cong \sqrt{\frac{b}{a}}\, Q(b-a); \qquad ab \gg 1,\ b \gg 0.4,\ b \geq a. \tag{212}$$

Furthermore, when (b-a) is large, we can approximate the Gaussian Q function

in Eq. 212,[55] so that

$$Q_m(a,b) \cong \sqrt{\frac{b}{2\pi a}}\,\frac{e^{-\frac{(b-a)^2}{2}}}{(b-a)}; \qquad ab \gg 1,\ b \gg 0.4,\ b-a \gg 1. \tag{213}$$

Finally, as a generalization of Eq. C2, we have

$$I_o(z) \cong I_1(z) \cong \frac{e^z}{\sqrt{2\pi z}}; \qquad z \gg 1. \tag{214}$$

Using the approximations of Eqs. 213 and 214, we find that for sufficiently large values of J, Eq. 210 reduces to

$$\epsilon \cong \frac{(\nu+1)}{2\sqrt{2\pi}} e^{-\frac{\delta(\nu^2-1)}{2\Delta(1+\delta)}} e^{-\frac{J(\nu-1)^2}{2\Delta}} \left\{ \frac{\sqrt{\nu\Delta}}{(\nu-1)\sqrt{J}\,[(J+1)\nu-J]} + \delta\left[\sqrt{\frac{\nu}{J\Delta}} + \frac{(J-1)(\nu-1)}{2\sqrt{J\nu\Delta}} + \frac{(\nu-1)\sqrt{J}}{2\nu^{3/2}\sqrt{\Delta}}\right]\right\}; \quad J \text{ large.} \tag{215}$$

If $J \gg 1$, Eq. 215 further simplifies to

$$\epsilon \cong \frac{(\nu+1)}{2\sqrt{2\pi}} e^{-\frac{\delta(\nu^2-1)}{2\Delta(1+\delta)}} e^{-\frac{J(\nu-1)^2}{2\Delta}} \left\{ \frac{\sqrt{\nu\Delta}}{J^{3/2}(\nu-1)^2} + \delta\left[\frac{(\nu+1)}{2\sqrt{J\nu\Delta}} + \frac{(\nu^2-1)\sqrt{J}}{2\nu^{3/2}\sqrt{\Delta}}\right]\right\}; \quad J \gg 1. \tag{216}$$

In Eq. 216, the terms in the square brackets constitute the first-order correction portion of the approximation for ϵ, valid for small values of δ and large values of J (corresponding to small values of ϵ). Clearly, for large J, the second of these terms dominates the first. Retaining only the dominant terms in the first-order perturbation approximation for ϵ for small δ and large J, Eq. 216 becomes

$$\epsilon \cong \underbrace{\frac{(\nu+1)\sqrt{\nu\Delta}\; e^{-\frac{J(\nu-1)^2}{2\Delta}}\; e^{-\frac{\delta(\nu^2-1)}{2\Delta(1+\delta)}}}{2\sqrt{2\pi}\,J^{3/2}(\nu-1)^2}}_{\epsilon_o} \left[1 + \delta\,\frac{J^2(\nu-1)^3\,(\nu+1)}{2\Delta\nu^2}\right], \tag{217}$$

where ϵ_o is the zero-order perturbation approximation of ϵ about $\delta = 0$ for large

values of J.

We now want to determine the value of ν which minimizes ϵ for a given value of R_{avg} in Eqs. 211 and 217. The desired value of ν must satisfy the constraint

$$\frac{\partial \epsilon}{\partial \nu} + \frac{\partial \epsilon}{\partial J} \frac{dJ}{d\nu} = 0. \tag{218}$$

We find that

$$\frac{\partial \epsilon}{\partial \nu} \cong \frac{\partial \epsilon_o}{\partial \nu} \left[1 + \delta \frac{J^2 (\nu-1)^3 (\nu+1)}{2\Delta \nu^2} \right]$$

$$+ \delta \frac{J^2}{2\Delta} \left[\frac{3(\nu-1)^2 (\nu+1)}{\nu^2} + \frac{(\nu-1)^3}{\nu^2} - \frac{2(\nu-1)^3 (\nu+1)}{\nu^3} \right] \epsilon_o,$$

where

$$\frac{\partial \epsilon_o}{\partial \nu} = \left[\left(\frac{1}{\nu+1} \right) + \frac{1}{2\nu} - \left(\frac{2}{\nu-1} \right) - \frac{J(\nu-1)}{\Delta} - \delta \frac{\nu}{\Delta(1+\delta)} \right] \epsilon_o.$$

To order δ and to dominant order in J, we then have

$$\frac{\partial \epsilon}{\partial \nu} \cong - \frac{J(\nu-1)}{\Delta} \epsilon. \tag{219}$$

Also,

$$\frac{\partial \epsilon}{\partial J} \cong \frac{\partial \epsilon_o}{\partial J} \left[1 + \delta \frac{J^2 (\nu-1)^3 (\nu+1)}{2\Delta \nu^2} \right] + \delta \frac{J(\nu-1)^3 (\nu+1)}{\Delta \nu^2} \epsilon_o,$$

where

$$\frac{\partial \epsilon_o}{\partial J} = - \left[\frac{(\nu-1)^2}{2\Delta} + \frac{3}{2J} \right] \epsilon_o.$$

Therefore, retaining only the dominant terms as in Eq. 219, we have

$$\frac{\partial \epsilon}{\partial J} \cong - \frac{(\nu-1)^2}{2\Delta} \epsilon. \tag{220}$$

Finally, from Eq. 211 we can show that

$$\frac{\partial J}{\partial \nu} = - \frac{J\nu}{\Delta(1+\delta)}. \tag{221}$$

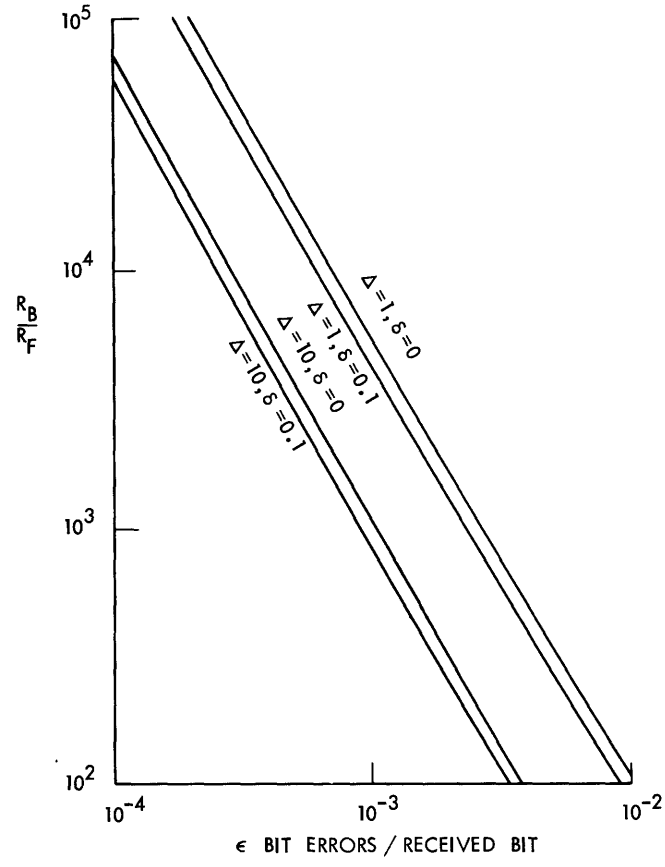

Fig. 9. Performance improvement of burst communication system over fixed-rate scheme for direct-detection case with Rayleigh fading. The following parameters appear above: R_B and R_F are the average information rates in bits/second for the burst and fixed-rate schemes, ϵ is the error rate in bit errors/received bit, δ is a measure of the channel-estimation noise, and Δ is a measure of the ratio of average signal counts to average noise counts in the detector.

Combining Eqs. 218-221, we find that to dominant order in J and to order δ, the desired value of ν is specified by

$$\nu \cong \frac{1}{2}\left[1+\sqrt{1+8\Delta(1+\delta)}\right]. \tag{222}$$

Eqs. 209, 210, and 222 now completely define our direct-detection burst communication system for small δ.

Let us show that the restriction of Eq. 207 is satisfied for ν given by Eq. 222. Since δ and Δ are non-negative, we can lowerbound ν^2 as follows:

$$\nu^2 \geq \frac{1}{4}\left(1+\sqrt{1+8\Delta}\right)^2 \geq 1 + 2\Delta. \tag{223}$$

This implies that the value of ν specified in Eq. 222 satisfies the condition in Eq. 207 over the entire range of Δ.

Denoting R_{avg} by R_B for our burst communication system specified by Eqs. 209, 210, and 222, and using Eq. 134, we can characterize the improvement in average bit transmission rate, for Rayleigh fading, by

$$\frac{R_B}{R_F} \cong \frac{e^{-\frac{(\nu^2-1)}{2\Delta(1+\delta)}}}{2\pi J \Delta \epsilon^2}; \qquad \epsilon \ll \begin{cases} \frac{1}{\sqrt{2\pi}}; & \Delta \leq 1, \\ \frac{1}{\Delta\sqrt{2\pi}}; & \Delta \geq 1. \end{cases} \tag{224}$$

Eqs. 210, 222, and 224 define R_B/R_F as a parametric function of ϵ, with parameter J. The average rate gain R_B/R_F is plotted against ϵ in Fig. 9, and we see that the improvement is again impressive for small ϵ despite the fact that the value of ν in Eq. 222 is not in general optimal.

V. ALTERNATIVE TECHNIQUES FOR COMBATTING ATMOSPHERIC TURBULENCE

Thus far we have confined our attention to deriving variable-rate strategies for optical communication systems through the turbulent atmosphere for the special case of single-diversity transmission with no spatial modulation. We shall now compare the performance of our variable-rate schemes with alternative systems employing adaptive spatial modulation or spatial diversity techniques. We shall also try to combine our variable-rate concepts with systems incorporating these techniques.

5.1 ADAPTIVE SPATIAL MODULATION

We have noted that channel-measurement transmitters generally fall into one of two categories, namely, those employing adaptive temporal modulation and those using adaptive spatial modulation. This report has been concerned primarily with the development of variable-rate strategies for optical communication systems used in the turbulent atmosphere which fit into the first classification above. Optical communication systems employing adaptive spatial modulation techniques have been investigated by Shapiro.[56] Since these two approaches represent alternative methods of combatting the effects of atmospheric fading, it is informative to compare them and consider their respective merits. We shall define an adaptive spatial modulation system for an optical ground-to-space/hererodyne-detection link based on Shapiro's work in this area, using the notation of our previous sections. Then we shall consider a hybrid variable-rate/adaptive spatial modulation system to determine the additional improvement provided by incorporating variable-rate techniques in an optical link of the adaptive spatial modulation variety.

In our mathematical analysis, we restrict ourselves to a single atmospheric channel state, suppressing the temporal variations of the atmospheric fading. Referring again to the model of the optical ground-to-space link in Fig. 1, we measure the channel fading by transmitting a pilot tone at a constant power level P_p along the downlink, as in Eq. 69, with direction $\vec{a} = \vec{0}$ for simplicity:

$$E_{pt}(\vec{r}_3, t) = \sqrt{\frac{P_p}{A_r}}; \qquad \vec{r}_3 \in R_3. \tag{225}$$

Then, according to Eqs. 70 and 71, the pilot-tone signal field incident on aperture R_1 is given by

$$E_{ps}(\vec{r}_1, t) = \sqrt{\frac{P_p}{A_r}} \int_{R_2} d\vec{r}_2 \int_{R_3} d\vec{r}_3 \, \underleftarrow{h}_a(\vec{r}_1, \vec{r}_2) \, \underleftarrow{h}_f(\vec{r}_2, \vec{r}_a); \qquad \vec{r}_1 \in R_1. \tag{226}$$

Finally, using Eqs. 9 and 12, and ignoring constant phase delay terms, Eq. 226 becomes

$$E_{ps}(\vec{r}_1, t) = \frac{\sqrt{P_p A_r}}{\lambda d_f} Z\, e^{\gamma(\vec{r}_1)}; \qquad \vec{r}_1 \in R_1, \tag{227}$$

where $e^{\gamma(\vec{r}_1)}$ is the log-normal random process characterizing the atmospheric fading and Z is the associated normalization constant.

As in our previous work, we transmit an information signal $E_t(\vec{r}_1, t)$ with energy ξ, defined by Eqs. 2-4:

$$E_t(\vec{r}_1, t) = \sqrt{\xi}\, \underset{\rightarrow}{U}_1(\vec{r}_1)\, s(t); \qquad \vec{r}_1 \in R_1,\ t \in \mathcal{T}$$

$$\int_{R_1} d\vec{r}_1 \int_{\mathcal{T}} dt\ |E_t(\vec{r}_1, t)|^2 = \xi \tag{228}$$

$$\int_{\mathcal{T}} dt\ |s(t)|^2 = 1,$$

where $\mathcal{T}$ is the signal baud of duration T seconds. Whereas before the spatial term $\underset{\rightarrow}{U}_1(\vec{r}_1)$ was uniform and invariant over aperture R_1 as in Eq. 5, we shall now try to match $\underset{\rightarrow}{U}_1(\vec{r}_1)$ to the measured channel state. Ignoring channel-measurement noise, Shapiro has shown that we can maximize the signal energy incident on the satellite aperture by arranging to have

$$\underset{\rightarrow}{U}_1(\vec{r}_1) = \frac{\lambda d_f E^*_{ps}(\vec{r}_1, t)}{Z\sqrt{P_p A_r \int_{R_1} d\vec{r}_1 \left| e^{\gamma(\vec{r}_1)} \right|^2}}; \qquad \vec{r}_1 \in R_1,$$

$$= \frac{e^{\gamma^*(\vec{r}_1)}}{\sqrt{\int_{R_1} d\vec{r}_1 \left| e^{\gamma(\vec{r}_1)} \right|^2}}; \qquad \vec{r}_1 \in R_1. \tag{229}$$

In Eq. 229, $\underset{\rightarrow}{U}_1(\vec{r}_1)$ has been normalized to be consistent with Eq. 228. There are two assumptions implicit in the prescription of Eq. 229:

(i) The ground terminal can measure the received pilot-tone signal field $E_{ps}(\vec{r}_1, t)$ at each point $\vec{r}_1$ within aperture R_1.

(ii) The ground terminal can transmit the complex conjugate field $E^*_{ps}(\vec{r}_1, t)$ within an atmospheric coherence time of measuring $E_{ps}(\vec{r}_1, t)$.

Both of these assumptions represent gross idealizations which can only be approximated by any practical transmitter in general.

The field received at the satellite has the form of Eq. 6 with signal component

$$E_o(\vec{r}_3, t) = \sqrt{\xi}\ \underset{\rightarrow}{U}_3(\vec{r}_3)\ s(t); \qquad \vec{r}_3 \in R_3,\ t \in \mathcal{T}. \tag{230}$$

Using Eqs. 8, 9, 10, and 12, we have

$$\underset{\rightarrow}{U}_3(\vec{r}_3) = \frac{Z}{\lambda d_f} \sqrt{\int_{R_1} d\vec{r}_1 \left| e^{\gamma(\vec{r}_1)} \right|^2}; \qquad \vec{r}_3 \in R_3. \tag{231}$$

Then the average received signal energy over a baud interval is given by

$$E\left[\int_{R_3} d\vec{r}_3 \int_y dt\ |E_o(\vec{r}_3, t)|^2\right] = \frac{Z^2 \xi A_t A_r}{\lambda^2 d_f^2}, \tag{232}$$

where we have used the fact that $\overline{\left| e^{\gamma(\vec{r}_1)} \right|^2} = 1$. This is equal to the maximum average received signal energy for our optical ground-to-space link in the absence of turbulence, that is, it is a diffraction-limited result.

It is interesting to compare the result in Eq. 232 with the same quantity defined in Eq. 19 for the nonadaptive transmission case. The gain G in average received signal energy of the adaptive spatial modulation system over the nonadaptive system is given by

$$G = Z^2/\overline{u^2}, \tag{233}$$

where u is the random fading parameter for the nonadaptive case, defined in Eq. 14. We have noted in section 2.1 that $\overline{u^2}$ is maximized when the transmission direction $\vec{\theta}$ is set to $\vec{0}$. Then

$$u = \frac{Z}{A_t} \left| \int_{R_1} d\vec{r}_1\ e^{\gamma(\vec{r}_1)} \right|. \tag{234}$$

We now examine G for very small and very large transmitting apertures, A_t. Recall that $A_{c\chi}$ and $A_{c\phi}$ denote the spatial coherence areas of the amplitude and phase terms in $e^{\gamma(\vec{r}_1)}$, and $A_{c\phi}$ is the smaller of the two.

(i) If $A_t \leq A_{c\phi}$, we see from Eq. 234, or Eq. 15 with $\vec{\theta} = \vec{0}$, that u is log-normal:

$$u = Z\, e^{\chi}. \tag{235}$$

This implies that $\overline{u^2} = Z^2$, so that G = 1. Thus, when the transmission aperture is of the order of a coherence area of $e^{\gamma(\vec{r}_1)}$ or smaller, adaptive spatial modulation does not increase the average energy transfer behavior of an optical ground-to-space link.

(ii) If $A_t \gg A_{c\chi}$, we have noted in section 2.1 that u is essentially a Rayleigh random variable. From Eq. 234, we have

$$\overline{u^2} = \frac{Z^2}{A_t^2} \int_{R_1} d\vec{r}_1 \int_{R_1} d\vec{r}_1' \; \overline{e^{\gamma(\vec{r}_1)} \; e^{\gamma^*(\vec{r}_1')}}. \tag{236}$$

We can determine an approximate expression for $\overline{u^2}$ by assuming that the covariance of $e^{\gamma(\vec{r}_1)}$ has the approximate form

$$\overline{e^{\gamma(\vec{r}_1)} \; e^{\gamma^*(\vec{r}_1')}} \cong \begin{cases} 1; & |\vec{r}_1 - \vec{r}_1'| < \frac{r_o}{2} \\ 0; & |\vec{r}_1 - r_1'| > \frac{r_o}{2}, \end{cases} \tag{237}$$

where r_o is the coherence length of the atmospheric turbulence from the structure function of the phase.[57, 58] The parameter r_o is roughly equal to the diameter of a circular phase coherence area, so that

$$A_{c\phi} \cong \frac{\pi r_o^2}{4}. \tag{238}$$

Since $A_t \gg A_{c\chi} > A_{c\phi}$, we can use Eqs. 237 and 238 to write

$$\int_{R_1} d\vec{r}_1' \; \overline{e^{\gamma(\vec{r}_1)} \; e^{\gamma^*(\vec{r}_1')}} \cong A_{c\phi}; \qquad \forall \; \vec{r}_1 \in R_1. \tag{239}$$

Inserting Eq. 239 in Eq. 236, we have

$$\overline{u^2} \cong Z^2 \frac{A_{c\phi}}{A_t} \equiv \frac{Z^2}{N_\phi}, \tag{240}$$

where we have defined N_ϕ to be the number of phase coherence areas of $e^{\gamma(\vec{r}_1)}$ contained in aperture R_1. From Eqs. 233 and 240, we see that

$$G \cong N_\phi, \tag{241}$$

so that the average received energy is greatly increased when adaptive spatial modulation is used in the case wherein the data transmitting aperture R_1 is very large relative to a coherence area of $e^{\gamma(\vec{r}_1)}$.

Now, for a heterodyne-detection receiver, the parameter of interest is the

angular plane-wave component of $\underset{\rightarrow}{U}_3(\vec{r}_3)$ in some direction $\vec{\phi}$ as in Eq. 26. Using Eq. 231, we have

$$\underset{\rightarrow}{U}_r(\vec{\phi}) = \int_{R_3} d\vec{r}_3 \; e^{-jk\vec{\phi}\cdot\vec{r}_3} \; \underset{\rightarrow}{U}_3(\vec{r}_3)$$

$$= \frac{Z}{\lambda d_f} \sqrt{\int_{R_1} d\vec{r}_1 \left| e^{\gamma(\vec{r}_1)} \right|^2} \int_{R_3} d\vec{r}_3 \; e^{-jk\vec{\phi}\cdot\vec{r}_3}. \tag{242}$$

Then, combining Eqs. B14 and 242, the output of a heterodyne receiver in an optical ground-to-space link employing adaptive spatial modulation has the form of Eq. 27:

$$r(t) = \sqrt{2E_s}\; u\left|s(t)\right| \cos\left(2\pi f_h t + \psi_h\right) + n(t); \qquad t \in \mathcal{T}, \tag{243}$$

where the energy parameter E_s is given by

$$E_s = \frac{\xi A_t}{\lambda^2 d_f^2 A_r} \left| \int_{R_3} d\vec{r}_3 \; e^{-jk\phi\cdot\vec{r}_3} \right|^2 \tag{244}$$

as in Eq. 28. Unlike the nonadaptive case, however, the random fading parameter u is now specified by

$$u = \frac{Z}{\sqrt{A_t}} \sqrt{\int_{R_1} d\vec{r}_1 \left| e^{\gamma(\vec{r}_1)} \right|^2}. \tag{245}$$

(i) If $A_t \leq A_{c\chi}$, it is clear that u is log-normal:

$$u = Z\, e^{\chi}; \qquad \overline{u^2} = Z^2. \tag{246}$$

(ii) If $A_t \gg A_{c\chi}$, we can show theoretically that u is essentially a log-normal random variable of the form[59-61]

$$u = Z\, e^{\mu}, \tag{247}$$

where μ is a real Gaussian random variable with mean m_μ and variance σ_μ^2. From Eq. 245, we have

$$\overline{u^2} = Z^2, \tag{248}$$

which implies that

$$m_\mu = -\sigma_\mu^2. \tag{249}$$

To determine σ_μ^2, we examine the variance of u^2 defined in Eq. 245:

$$\mathrm{Var}\,(u^2) = \overline{u^4} - \left(\overline{u^2}\right)^2$$

$$= \frac{Z^4}{A_t^2}\int_{R_1} d\vec{r}_1 \int_{R_1} d\vec{r}_1'\ \mathrm{Cov}\left[\left|e^{\gamma(\vec{r}_1)}\right|^2, \left|e^{\gamma(\vec{r}_1')}\right|^2\right]. \tag{250}$$

As in Eq. 237, for simplicity we can approximate the covariance of the intensity $\left|e^{\gamma(\vec{r}_1)}\right|^2$ by

$$\mathrm{Cov}\left[\left|e^{\gamma(\vec{r}_1)}\right|^2, \left|e^{\gamma(\vec{r}_1')}\right|^2\right] \cong \begin{cases} \mathrm{Var}\,(e^{2\chi}); & |\vec{r}_1 - \vec{r}_1'| < \frac{D_o}{2} \\ 0; & |\vec{r}_1 - \vec{r}_1'| > \frac{D_o}{2}, \end{cases} \tag{251}$$

where D_o is the intensity coherence length of the turbulence.[62] The intensity coherence area A_{cI} can be written

$$A_{cI} = \frac{\pi D_o^2}{4}. \tag{252}$$

For $A_t \gg A_{cI}$, Eqs. 251 and 252 yield the approximate result

$$\int_{R_1} d\vec{r}_1'\ \mathrm{Cov}\left[\left|e^{\gamma(\vec{r}_1)}\right|^2, \left|e^{\gamma(\vec{r}_1')}\right|^2\right] \cong A_{cI}\ \mathrm{Var}\,(e^{2\chi}); \qquad \forall\ \vec{r}_1 \in R_1. \tag{253}$$

From Eqs. 250 and 253, we find that

$$\mathrm{Var}\,(u^2) = Z^4\,\frac{A_{cI}}{A_t}\,\mathrm{Var}\,(e^{2\chi}) = \frac{Z^4}{N_I}\,\mathrm{Var}\,(e^{2\chi}), \tag{254}$$

where we have defined N_I to be the number of intensity coherence areas of $e^{\gamma(\vec{r}_1)}$ contained in aperture R_1. Using Eqs. 247, 249, and 254, and recalling that $m_\chi = -\sigma_\chi^2$, we can show that

$$e^{4\sigma_\mu^2} - 1 = \frac{1}{N_I}\left(e^{4\sigma_\chi^2} - 1\right). \tag{255}$$

For $N_I \gg 1$, σ_μ is therefore significantly smaller than σ_χ.

Let us now evaluate the performance of the fixed-rate optical ground-to-space/heterodyne-detection system employing adaptive spatial modulation, restricting ourselves to the interesting case of large N_I. Denoting R_{avg} by R_{SF}, and using Eq. 132 with $C(\vec{\theta}) = 1$ since $\vec{\theta} = \vec{0}$, and replacing σ_χ by σ_μ, we have

$$\epsilon = \frac{1}{2} \mathrm{Fr}\left[\frac{Z^2 P_s}{2N_o R_{SF}},\ 0;\ \sigma_\mu\right]. \tag{256}$$

Note that as A_t, and therefore N_I, gets very large, Eq. 255 tells us that σ_μ approaches zero; then Eq. 256 becomes

$$\epsilon \xrightarrow[A_t \to \infty]{} \frac{1}{2} e^{-\frac{Z^2 P_s}{2N_o R_{SF}}}. \tag{257}$$

Let us compare these results with those of our optimal variable-rate scheme for the noiseless channel-measurement case. For large A_t, the channel-fading parameter u is Rayleigh, and we can combine Eqs. 143, 145, and 240 to show that

$$\epsilon = \frac{1}{2} e^{-\frac{Z^2 P_s}{2N_o R_V N_\phi}}. \tag{258}$$

Clearly, as A_t, and hence N_ϕ, gets large, we see from Eqs. 257 and 258 that for any given ϵ, R_{SF} will eventually become larger than R_V. This implies that the adaptive spatial modulation system is inherently better than the variable-rate system for large transmitting apertures. We must note that the adaptive spatial modulation system is generally much more complex than the variable rate system. Shapiro shows that to yield the performance levels above, a practical adaptive spatial modulation system must use an array of roughly N_ϕ heterodyne detectors, each with a different local-oscillator field, to measure fully all of the spatial modes in the pilot-tone signal field received by the ground terminal. Furthermore, to modulate the information signals accurately, as in Eq. 229, the ground terminal must use a Taylor series array of approximately N_ϕ transmission elements. If system complexity is an important consideration, the variable-rate system may be more attractive than the adaptive spatial modulation system.

Let us compare the variable-rate system characterized by Eq. 258 with the adaptive spatial modulation system of Eq. 256. We can use Eqs. 238, 240, 252, and 254 to show that N_ϕ and N_I are related according to the expression

$$N_\phi = \left(\frac{D_o}{r_o}\right)^2 N_I. \tag{259}$$

Combining Eqs. 256, 258, and 259, we can represent the rate gain R_{SF}/R_V as a parametric function of ϵ, with parameter β in terms of D_o, r_o, and N_I:

$$\frac{R_{SF}}{R_V} = \frac{N_I\left(\frac{D_o}{r_o}\right)^2 \ln\left(\frac{1}{2\epsilon}\right)}{\beta}$$

$$\epsilon = \frac{1}{2}\,\mathrm{Fr}\,(\beta, 0; \sigma_\mu). \tag{260}$$

Fried has found that $D_o = 2.86$ cm,[62] and r_o is typically of the order of a centimeter. Suppose we consider the case $\sigma_\mu = 0.5$, and to maintain a reasonably low level of complexity for the adaptive spatial modulation system let us set $N_I = 5$. Equations 255 and 259 then imply that $N_\phi \cong 41$ and $\sigma_\chi \cong 7.5$. Substituting these values of D_o, r_o, and N_I in Eq. 260, we can show that at $\epsilon = 4.5 \times 10^{-3}$, $R_{SF}/R_V = 7.3$. Therefore, at the cost of a higher level of complexity, the adaptive spatial modulation system will perform moderately better than the variable-rate scheme.

As a final exercise, let us see what can be gained by using variable-rate strategy on the adaptive spatial modulation system when A_t is large. We saw that the adaptive spatial modulation system is characterized in this case by a log-normal channel fading parameter u defined by Eq. 247. For the noiseless channel-measurement situation, we can simply apply the log-normal variable-rate results of section 4.2.1. Denoting R_{avg} for the hybrid variable-rate/adaptive spatial modulation system by R_{SV}, Eq. 148 is valid with $\sigma = \sigma_\mu$: that is, the rate gain R_{SV}/R_{SF} is specified parametrically in terms of ϵ, with parameter a by

$$\frac{R_{SV}}{R_{SF}} = \frac{a}{-\ln\left[\mathrm{Fr}\,(a, 0; \sigma_\mu)\right]}$$

$$\epsilon = \frac{1}{2}\,\mathrm{Fr}\,(a, 0; \sigma_\mu). \tag{261}$$

Suppose we consider the case $N_I = 5$ and $\sigma_\mu = 0.5$; then by Eq. 255, $\sigma_\chi \cong 7.5$ as before. Then R_{SV}/R_{SF} is represented graphically by the $\sigma = 0.5$ curve for log-normal u in Fig. 7. Therefore variable-rate techniques provide nominal improvements in performance when applied to the adaptive spatial modulation system. Note that we can use Eqs. 252 and 254 to express the diameter D_t of aperture R_1 in terms of N_I and D_o:

$$D_t = D_o\sqrt{N_I}. \tag{262}$$

For the example above, it is interesting to discover that the transmitting aperture diameter D_t must be 6.4 cm.

5.2 SPATIAL DIVERSITY TRANSMISSION

Still another method of combatting the effects of atmospheric turbulence on optical communication systems is the use of spatial diversity techniques, provided this option is available. To illustrate the relevant principles, we consider a D-fold spatial diversity system for the ground-to-ground/direct-detection case. We show that within an atmospheric coherence interval, the channel fading for such a system is characterized by a D-dimensional random vector $\vec{u}$. For variable-rate purposes, we demonstrate that u can be measured by transmitting D separate pilot tones simultaneously from the data receiver to the data transmitter. We then set up the variable-rate problem for this operation, but because of mathematical difficulties we shall not complete the analysis at this time.

Referring to the channel model of Fig. 2, we again transmit a collimated section of a plane wave through aperture R_1 in some direction $\vec{\theta}$, so that Eqs. 2-5 are applicable. The field incident on receiver aperture R_2 is then specified by Eq. 46:

$$E_r(\vec{r}_2, t) = \sqrt{\xi}\ \underset{\rightarrow}{U}_2(\vec{r}_2)\ s(t) + E_b(\vec{r}_2, t); \qquad \vec{r}_2 \in R_2,\ t \in \mathcal{T}. \tag{263}$$

For convenience, we do our data processing in the focal plane R_F of the data receiver, which is separated from the aperture plane R_2 by the focal length f_ℓ. As in Eq. 76, the received field in the focal plane has the form

$$E_f(\vec{r}_f, t) = \sqrt{\xi}\ \underset{\rightarrow}{U}_f(\vec{r}_f)\ s(t) + E_b'(\vec{r}_f, t); \qquad \vec{r}_f \in R_F,\ t \in \mathcal{T}, \tag{264}$$

where

$$\underset{\rightarrow}{U}_f(\vec{r}_f) \equiv \frac{e^{jk\frac{|\vec{r}_f|^2}{2f_\ell}}}{\lambda f_\ell} \int_{R_2} d\vec{r}_2\ \underset{\rightarrow}{U}_2(\vec{r}_2)\ e^{-jk\frac{\vec{r}_f}{f_\ell}\cdot\vec{r}_2}; \qquad \vec{r}_f \in R_F, \tag{265}$$

and

$$E_b'(\vec{r}_f, t) \equiv \frac{e^{jk\frac{|\vec{r}_f|^2}{2f_\ell}}}{\lambda f_\ell} \int_{R_2} d\vec{r}_2\ E_b(\vec{r}_2, t)\ e^{-jk\frac{\vec{r}_f}{f_\ell}\cdot\vec{r}_2}; \qquad \vec{r}_f \in R_F. \tag{266}$$

The noise term $E_b'(\vec{r}_f, t)$ is a white Gaussian random process over the spatial modes of $U_f(\vec{r}_f)$ in the focal plane R_F and the temporal modes of s(t) in the baud interval $\mathcal{T}$. Using Eqs. 25 and 265, we can write

$$\underset{\rightarrow}{U}_f(\vec{r}_f) = \frac{e^{jk\frac{|\vec{r}_f|^2}{2f_\ell}}}{\lambda f_\ell \sqrt{A_t}} \int_{R_2} d\vec{r}_2\, Z' e^{\gamma'(\vec{r}_2)} e^{-jk\frac{\vec{r}_f}{f_\ell}\cdot\vec{r}_2}; \qquad \vec{r}_f \in R_F. \tag{267}$$

where $e^{\gamma'(\vec{r}_2)}$ is the log-normal random process characterizing the atmospheric fading and Z' is the associated normalization constant.

The signal field in the focal plane contains D independent spatial modes, where D is of the order of the number of spatial amplitude coherence areas of $e^{\gamma'(\vec{r}_2)}$ contained in the receiver aperture R_2, provided the focal plane R_F is large enough. We can define a complex random fading process

$$u(\vec{r}_f)\, e^{j\psi(\vec{r}_f)} \equiv \int_{R_2} d\vec{r}_2\, Z' e^{\gamma'(\vec{r}_2)} e^{-jk\frac{\vec{r}_f}{f_\ell}\cdot\vec{r}_2}; \qquad \vec{r}_f \in R_F, \tag{268}$$

with amplitude $u(\vec{r}_f)$ and phase $\psi(\vec{r}_f)$. To simplify our mathematical analysis, we use the following model for our direct-detection operation. We assume that we can partition the focal plane R_F approximately into D focal coherence regions R_k, k = 1, 2, ..., D, of equal area A_d. Over each region R_k, we assume that the amplitude fading parameter $u(\vec{r}_f)$ is essentially constant and denoted by the random variable u_k; that is,

$$\left| \int_{R_2} d\vec{r}_2\, Z' e^{\gamma'(\vec{r}_2)} e^{-jk\frac{\vec{r}_f}{f_\ell}\cdot\vec{r}_2} \right| \cong u_k; \qquad \vec{r}_f \in R_k. \tag{269}$$

We furthermore assume that the u_k's are statistically independent.

Suppose that we assemble an array of D photodetectors in the focal plane R_F, with appropriate time-space processing to limit the background noise. Each detector is used to intercept all of the received energy in one of the focal coherence regions R_k. As in section 2.3, the output of the k^{th} detector, averaged over the Gaussian background noise, can often be treated as a conditional inhomogeneous Poisson process with rate parameter $\mu_k(t)$. For the binary PPM case, with equiprobable hypotheses H_1 and H_2, we can modify Eq. 49 to write

$$\mu_k(t)\,|H_i = \begin{cases} u_k^2 \mu_s \delta_{i1} + \mu_n; & 0 < t < \frac{T}{2} \\ u_k^2 \mu_s \delta_{i2} + \mu_n; & \frac{T}{2} < t < T \end{cases} \tag{270}$$

as in Eqs. 50 and 51, we can define

$$u_k^2 \mu_s \equiv \frac{2\eta\xi}{h\nu T} \int_{R_k} d\vec{r}_f \; |\underset{\rightarrow}{U}_f(\vec{r}_f)|^2, \tag{271}$$

and

$$\mu_n \equiv \frac{\eta}{h\nu} \int_{R_k} d\vec{r}_f \; |E'_{db}(\vec{r}_f, t)|^2, \tag{272}$$

where $E'_{db}(\vec{r}_f, t)$ is the result of passing the noise field $E'_b(\vec{r}_f, t)$ through the linear time-space processor associated with the k^{th} detector. Combining Eqs. 267, 269, and 271, we can identify

$$\mu_s \equiv \frac{2\eta\xi A_d}{h\nu T \lambda^2 f_\ell^2 A_t}. \tag{273}$$

Note that the parameters μ_s and μ_n are constant over the index k by our earlier assumptions.

Denote the number of counts registered by the k^{th} detector in the first- and second-half signal bauds of duration T/2 by $n_{1,k}$ and $n_{2,k}$. Then the $n_{1,k}$'s and $n_{2,k}$'s form a set of 2D statistically independent random variables with conditional distributions given by

$$\Pr[n_{j,k}|H_i, u_k] = \frac{1}{n_{j,k}!} \left[\left(u_j^2 \mu_s \delta_{ij} + \mu_n\right) \frac{T}{2}\right]^{n_{j,k}} \exp -\left[\left(u_k^2 \mu_s \delta_{ij} + \mu_n\right) \frac{T}{2}\right];$$

$$i, j = 1, 2; \; k = 1, 2, \ldots, D. \tag{274}$$

as in Eq. 57. Let us assume that the u_k's are identically distributed over the index k; then we can use the decision rule

$$n_1 \equiv \sum_{k=1}^{D} n_{1,k} \underset{H_2}{\overset{H_1}{\gtrless}} \sum_{k=1}^{D} n_{2,k} \equiv n_2 \tag{275}$$

with the event $n_1 = n_2$ being decided by the flip of a fair coin.

We can define a random fading vector $\vec{u} = (u_1, u_2, \ldots, u_D)$ which completely characterizes the channel fading for our spatial diversity system. Conditioned on $\vec{u}$ and hypothesis H_i, n_1 and n_2 are independent Poisson random variables, with distributions.

$$\Pr[n_j|H_i, v] = \frac{1}{n_j!} \left[\left(v\mu_s \delta_{ij} + D\mu_n\right) \frac{T}{2}\right]^{n_j} \exp -\left[\left(v\mu_s \delta_{ij} + D\mu_n\right) \frac{T}{2}\right]; \quad i, j = 1, 2. \tag{276}$$

where we have defined a sufficient fading statistic

$$v \equiv \sum_{k=1}^{D} u_k^2. \tag{277}$$

By our earlier work and previous assumptions, the u_k's are identically distributed, statistically independent Rayleigh random variables, each with $\overline{u_k^2}$ equal to some parameter a. This implies that v is a central Chi-square random variable with 2D degrees of freedom, and probability density function[63]

$$p(v) = \frac{v^{D-1} e^{-v/2}}{(D-1)!\, a^D}. \tag{278}$$

As in Eq. 60, we can show that the probability of error for a single baud, conditioned on the atmospheric fading, is given by

$$P(\epsilon|v) = Q_m\left[\sqrt{\frac{K}{\Delta}}, \sqrt{\frac{K}{\Delta}(1+v\alpha)}\right] - \frac{1}{2}\exp\left[-\frac{K}{2\Delta}(2+v\alpha)\right] I_o\left(\frac{K}{\Delta}\sqrt{1+v\alpha}\right), \tag{279}$$

where the parameters K, α, and Δ are defined in Eq. 59. The problem of averaging $P(\epsilon|v)$ over v is mathematically difficult and will not be attempted here.

In order to use variable-rate techniques with the spatial diversity system above, we must be able to measure $\vec{u}$, whose components u_k correspond to the D independent spatial signal modes. In the notation of section 3.1, each u_k is associated with a direction pair $(\vec{\theta}, \vec{a}_k)$ where $\vec{a}_k = \vec{r}_f/f_\ell$ for some central point $\vec{r}_f$ in the focal coherence region R_k. As we pointed out, we can measure each u_k by transmitting a pilot tone in the direction $-\vec{a}_k$ from the data receiver to the data transmitter, and extracting the angular plane-wave component of the pilot-tone field incident on aperture R_1 in the direction $-\vec{\theta}$. We can separate the simultaneous channel measurements by using different carrier frequencies for each pilot tone and by using frequency-selective filters at the data transmitter. Having measured u, we can then determine the relevant fading parameter v.

Notice that although the spatial diversity system is characterized by a random fading vector $\vec{u}$, the probability of a communication error conditioned on the fading depends only on a single parameter v as shown in Eq. 279. And since we know how to measure v, we can derive variable-rate strategies in a manner analogous to section 4.3. For example, a burst communication scheme would have the usual prescription

$$R(v) = Ru_{-1}(v-\eta) \tag{280}$$

as in Eq. 159, where $R \equiv 1/T$ and η is a threshold to be determined later. Just as it was mathematically difficult to average $P(\epsilon|v)$ over the fading parameter v, it is even more difficult to analyze the performance of a burst communication system, so that task will not be performed in this report.

VI. CONCLUSION

Let us briefly summarize the major accomplishments of the research reported herein, and suggest some areas wherein further work is warranted.

The principal reason for undertaking this research was to demonstrate that variable-rate transmission techniques could be applied to optical communication links over atmospheric channels to significantly reduce the effects of turbulence on system performance. To simplify our analysis, we restricted our attention to the binary communication problem. We considered ground-to-ground and ground-to-space communication systems employing either heterodyne- or direct-detection receivers.

To provide a basis for comparing our variable-rate results, in Section II we analyzed the performance of fixed-rate optical systems in the turbulent atmosphere. For the ground-to-space link, we showed that the atmospheric fading is log-normal when the area A_t of the transmitting aperture is smaller than $A_{c\phi}$, and Rayleigh when A_t is very much greater than $A_{c\chi}$; $A_{c\chi}$ and $A_{c\phi}$ are the amplitude and phase coherence areas of the signal field that would be received by the ground terminal if an infinite plane-wave field were transmitted from the top of the atmosphere. These results are valid whether heterodyne or direct detection is used. For the ground-to-ground/heterodyne-detection case, we demonstrated that the atmospheric fading is log-normal when the area A_r of the data-receiving aperture is smaller than the phase coherence area $A_{c\phi'}$ of the received data signal field; however, we showed that the fading is Rayleigh when A_r is very much greater than the amplitude coherence area $A_{c\chi'}$. The Rayleigh results are of considerable importance, since they disputed a widespread initial belief that the atmospheric fading statistics were always log-normal. Finally, for the ground-to-ground/direct-detection case, we found that the atmospheric fading is log-normal whether $A_r \leq A_{c\phi'}$, or $A_r \gg A_{c\chi'}$. These results are summarized in Table 1.

Table 1. Atmospheric fading statistics.

	Ground-to-Space Link		Ground-to-Ground Link	
	$A_t < A_{c\phi}$	$A_t \gg A_{c\chi}$	$A_r \leq A_{c\phi'}$	$A_r \gg A_{c\chi'}$
Heterodyne Detection	Log-normal Fading	Rayleigh Fading	Log-normal Fading	Rayleigh Fading
Direct Detection	Log-normal Fading	Rayleigh Fading	Log-normal Fading	Log-normal Fading

We made use of previously established results in Section II in presenting the performance of fixed-rate optical systems employing heterodyne-detection receivers when the atmospheric fading is log-normal or Rayleigh; however, the performance analysis

for the direct-detection/Rayleigh fading case was an original piece of work. Mathematical difficulties deterred us from determining the system performance for the direct-detection/log-normal fading case: for completeness, this situation should eventually be rectified by approximating any integrals which cannot be explicitly evaluated.

In order to establish a variable-rate transmission system, it was necessary to first demonstrate that a pilot tone transmitted from the data receiver to the data transmitter could be used to provide the data transmitter with real-time channel-state information. In Section III, we initially ignored any background noise accompanying the received pilot-tone field and showed that the data transmitter could measure the relevant atmospheric fading parameter for systems employing single-detector receivers in every situation except the ground-to-ground/direct-detection case when $A_r > A_{c\phi}$. For the Rayleigh fading cases in Table 1, we then extended these results to include the effects of channel-measurement noise. Additional work is required to derive noisy channel measurement results for the log-normal fading case. We also briefly discussed an adaptive-pointing scheme for an optical ground-to-space link in Section III, and we considered the point-ahead problem and the concept of an isoplanatic angle to verify that channel measurement is in fact possible for the ground-to-space link.

Section IV represents the heart of this report and contains all of the variable-rate analysis for the case where no adaptive spatial modulation is used on the transmitted information signal and a single-detector receiver is employed. The problem we considered was how to vary the transmitted data rate based on channel-state measurements to maximize the average signalling rate for a given bit error rate subject to a power constraint. We can briefly encapsulate our results as follows:

(i) For the heterodyne-detection case, ignoring channel-measurement noise, we determined the optimal variable-rate scheme subject to the criterion above, for both log-normal and Rayleigh fading.

(ii) For the heterodyne-detection/Rayleigh fading case, for which noisy-channel measurement statistics had been derived in Section III, we determined the optimal burst communication system.

(iii) For the direct-detection/Rayleigh fading case, we derived an efficient burst communication system for the case where the channel-measurement noise is small; this scheme becomes the optimal burst communication system in the limit as the bit error rate becomes very small.

In each of the cases above, a comparison of variable- and fixed-rate performance indicated that adaptive, variable-rate techniques could significantly improve the performance of optical communication systems over atmospheric channels, particularly when the desired bit error rate is low. Additional variable-rate analysis is desirable for the log-normal fading case. The buffering and word-synchronization problems for burst communication systems should also be examined in greater detail.

Finally, in Section V we briefly considered adaptive spatial modulation and spatial diversity systems as alternative approaches to the problem of reducing the effects of

atmospheric turbulence on optical communication links. It would be beneficial to derive variable-rate strategies for the spatial-diversity case, and at the end of Section V we suggested one possible burst-communication approach to this problem.

APPENDIX A

Atmospheric Fading Statistics for Optical Ground-to-Space Links with Large Transmitting Apertures

We shall examine the statistical behavior of the complex fading parameter $ue^{j\psi}$ defined in Eq. 14 for the case where aperture R_1 is large enough to contain many spatial coherence areas of $e^{\gamma(\vec{r}_1)}$. To do this we use a mathematical technique which demonstrates whether a probability density function $p_y(a)$ converges to an arbitrary probability density function $p_x(a)$, provided only that lower order moments for both x and y can be determined.[64]

Formally, we can expand $p_y(a)$ in terms of any $p_x(a)$ as follows:

$$p_y(a) = p_x(a)\left[1 + \sum_{i=1}^{\infty} r_i(a)\right] \tag{A1}$$

where

$$r_i(a) = \frac{D_i(a)}{D_i D_{i-1}} \sum_{k=0}^{i} C_{i,k}(\ell_k - m_k); \qquad i \geq 1$$

$$D_i(a) \equiv \begin{vmatrix} m_o & m_1 & \cdots & m_i \\ m_1 & m_2 & \cdots & m_{i+1} \\ \cdot & \cdot & & \cdot \\ \cdot & \cdot & & \cdot \\ \cdot & \cdot & & \cdot \\ m_{i-1} & m_i & \cdots & m_{2i-1} \\ a^o & a^1 & \cdots & a^i \end{vmatrix}$$

$$D_i \equiv \begin{vmatrix} m_o & m_1 & \cdots & m_i \\ m_1 & m_2 & \cdots & m_{i+1} \\ \cdot & \cdot & & \cdot \\ \cdot & \cdot & & \cdot \\ \cdot & \cdot & & \cdot \\ m_{i-1} & m_i & \cdots & m_{2i-1} \\ m_i & m_{i+1} & \cdots & m_{2i} \end{vmatrix}$$

$$\ell_k \equiv \overline{y^k} \qquad m_k \equiv \overline{x^k}$$

and $C_{i,k}$ is the cofactor of a^k in $D_i(a)$.

If $p_x(a)$ is specified by two independent parameters of our choosing, we can arrange to have $m_1 = \ell_1$ and $m_2 = \ell_2$, so that $r_3(a)$ is then the first nonvanishing correction term in the expansion of Eq. A1:

$$p_y(a) = p_x(a)\left\{1 + \underbrace{(\ell_3 - m_3)\frac{D_3(a)}{D_3}}_{r_3(a)} + \underbrace{\left[C_{4,3}(\ell_3 - m_3)\frac{D_4(a)}{D_3 D_4} + (\ell_4 - m_4)\frac{D_4(a)}{D_4}\right]}_{r_4(a)} + \ldots\right\}. \tag{A2}$$

Let us use Eqs. 12 and 14 to rewrite $ue^{j\psi}$ in terms of its real and imaginary parts:

$$ue^{j\psi} \equiv a + jb,$$

where

$$a = \frac{Z}{A_t}\int_{R_1} d\vec{r}_1\, e^{\chi(\vec{r}_1)} \cos\mu(\vec{r}_1)$$

$$b = \frac{Z}{A_t}\int_{R_1} d\vec{r}_1\, e^{\chi(\vec{r}_1)} \sin\mu(\vec{r}_1) \tag{A3}$$

and

$$\mu(\vec{r}_1) \equiv \phi(\vec{r}_1) + k\vec{\theta}\cdot\vec{r}_1.$$

We note that at any point $\vec{r}_1$, the random variable $\mu(\vec{r}_1)$ is uniformly distributed over $(0, 2\pi)$, since $\vec{\theta}$ is deterministic and $\phi(\vec{r}_1)$ is assumed to be uniform over $(0, 2\pi)$.

By demonstrating that an arbitrary linear combination

$$I \equiv Aa + Bb; \qquad A^2 + B^2 \neq 0 \tag{A4}$$

converges to a Gaussian random variable for large A_t, we shall show that a and b converge to jointly Gaussian random variables as A_t gets large. We cannot determine a sufficient number of lower order moments of I using the integral expressions of Eq. A3 required to use the probability density expansion technique above. Therefore we will assume that these integrals can be approximated by finite sums of n identically distributed independent random terms:

$$I \cong I_n \equiv Aa_n + Bb_n, \tag{A5}$$

where

$$a_n = \frac{Z}{n} \sum_{\ell=1}^{n} e^{\chi_\ell} \cos \mu_\ell,$$

$$b_n = \frac{Z}{n} \sum_{\ell=1}^{n} e^{\chi_\ell} \sin \mu_\ell.$$

In Eq. A5, the Gaussian random variables χ_ℓ are each $N(m_\chi, \sigma_\chi^2)$, the μ_ℓ's are uniformly distributed over $(0, 2\pi)$, and the χ_ℓ's and μ_ℓ's are statistically independent. The number of terms n is a measure of the size of A_t: n is the number of degrees of freedom of $e^{\gamma(\vec{r}_1)}$ over aperture R_1, and can be interpreted as the number of spatial coherence areas of $e^{\gamma(\vec{r}_1)}$ contained in aperture R_1 (assume $A_{c\chi} \approx A_{c\phi}$ here).

Finally, for convenience, we shall normalize I_n so that our test variable y has zero mean and unit variance:

$$y = \frac{1}{Z} \sqrt{\frac{2n}{A^2 + B^2}}\, e^{-\left(m_\chi + \sigma_\chi^2\right)} I_n; \qquad A^2 + B^2 \neq 0. \tag{A6}$$

The first four moments of y are then given by

$$\ell_1 = 0 \qquad \ell_2 = 1$$

$$\ell_3 = 0 \qquad \ell_4 = 3 + \frac{3\left(e^{4\sigma_\chi^2} - 2\right)}{2n}. \tag{A7}$$

We want to expand $p_y(a)$ in terms of the normalized Gaussian probability density

$$p_x(a) = \frac{1}{\sqrt{2\pi}} e^{-a^2/2}, \tag{A8}$$

which has lower order moments

$$m_1 = 0 \qquad m_2 = 1 \qquad m_3 = 0 \qquad m_4 = 3$$

$$m_5 = 0 \qquad m_6 = 15 \qquad m_7 = 0 \qquad m_8 = 105. \tag{A9}$$

Using Eq. A2, we find that $r_3(a) = 0$, so that the lowest order correction term

in the expansion is

$$r_4(a) = \frac{e^{4\sigma_\chi^2} - 2}{16n} (a^4 - 6a^2 + 3), \tag{A10}$$

which is independent of A, B, and m_χ. If we pursue this approach further and evaluate higher order correction terms, we shall find that they are all dominated by $r_4(a)$ for large n. Since Eq. A10 holds for arbitrary linear combinations of a_n and b_n, we can conclude that a_n and b_n converge to jointly Gaussian random variables as n gets large, and Eq. A10 provides an indication of the rate of convergence:

$$p_y(a) \approx p_x(a); \qquad \forall\, a, n \ni |r_4(a)| \ll 1. \tag{A11}$$

We can also show that

$$\overline{a}_n = \overline{b}_n = 0,$$

$$\overline{a_n b_n} = 0,$$

$$\overline{a_n^2} = \overline{b_n^2} = \frac{Z^2 e^{2\left(m_\chi + \sigma_\chi^2\right)}}{2n};$$

therefore, provided the approximation of Eq. A5 is valid, $ue^{j\psi}$ appears to be a zero-mean, complex Gaussian random variable whose real and imaginary parts are identically distributed and independent for large A_t. The conclusions above are borne out by Halme's computer-simulation analysis.[65]

APPENDIX B

Optical Heterodyne Detection

The notation will be generalized to apply to both the optical ground-to-space link and the ground-to-ground link. We have seen in Eqs. 6, 7, and 23 that the complex field amplitude arriving at receiver aperture R consists in a signal $E_o(\vec{r},t)$ and incoherent Gaussian noise radiation $E_b(\vec{r},t)$:

$$E_r(\vec{r},t) = E_o(\vec{r},t) + E_b(\vec{r},t); \qquad \vec{r} \in R,\ t \in \mathcal{T},$$

where

$$\begin{aligned} E_o(\vec{r},t) &= \sqrt{\xi}\ \underrightarrow{U}(\vec{r})\ s(t) \\ \overline{E_b(\vec{r},t)} &= 0 \\ \overline{E_b(\vec{r},t)\,E_b^*(\vec{r}',t')} &\cong 2N_b\lambda^2 u_o(\vec{r}-\vec{r}')\,u_o(t-t'). \end{aligned} \tag{B1}$$

Helstrom has shown that in this situation an optical heterodyne receiver with a strong local-oscillator field reduces the detection problem to the familiar form of an IF signal and additive Gaussian noise.[22] We shall now use a similar approach to demonstrate this by way of review.

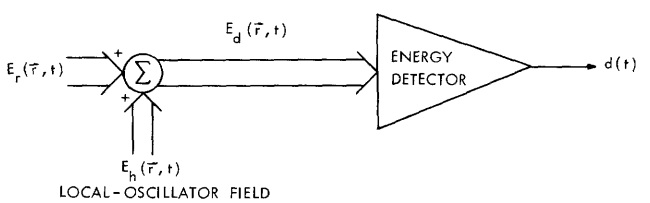

Fig. B-1. Optical heterodyne receiver.

As indicated in Fig. B-1, in the heterodyning process a strong local-oscillator field is added to the field received over aperture R, and their sum is fed to an energy detector. The local-oscillator field is a plane wave over aperture R, with a tilted phase front characterized in general by the direction cosine vector $\vec{\phi}$, and a frequency offset f_h from the signal carrier frequency f_c; its complex envelope is therefore

$$E_h(\vec{r},t) = E_h \exp(jk\vec{\phi}\cdot\vec{r}) \exp(-j2\pi f_h t); \qquad \vec{r} \in R. \tag{B2}$$

The complex envelope of the detector input field is then

$$E_d(\vec{r},t) = E_s(\vec{r},t) + E_b(\vec{r},t); \qquad \vec{r} \in R,\ t \in \mathcal{T}, \tag{B3}$$

where

$$E_s(\vec{r},t) \equiv E_o(\vec{r},t) + E_h(\vec{r},t); \qquad \vec{r} \in R,\ t \in \mathcal{T}. \tag{B4}$$

Under the assumption that the energy detector is an ideal photon detector, the output d(t), conditioned on the atmospheric fading and background noise, is a filtered Poisson process with rate parameter

$$\mu(t) = \frac{\eta}{h\nu} \int_R d\vec{r}\, |E_d(\vec{r},t)|^2, \tag{B5}$$

where η is the quantum efficiency of the detector, h is Planck's constant, and ν is the central frequency of the photon radiation. For simplicity, we have assumed that our fields are normalized so that the characteristic impedance of free space is unity.

Before considering the statistical behavior of the detector output, we should evaluate the mean and covariance of $\mu(t)$ for a given atmospheric channel state. All expectations below are over the noise field $E_b(\vec{r},t)$, conditioned on the fading process $\underset{\rightarrow}{U}(\vec{r})$.

$$\begin{aligned}\overline{\mu(t)} &= \frac{\eta}{h\nu} \int_R d\vec{r} \left[|E_s(\vec{r},t)|^2 + \overline{|E_b(\vec{r},t)|^2} \right] \\ &\cong \frac{\eta}{h\nu} \Big\{ \xi |s(t)|^2 \int_R d\vec{r}\, |\underset{\rightarrow}{U}(\vec{r})|^2 + A_r |E_h|^2 \\ &\quad + 2\sqrt{\xi}\, \mathrm{Re}\left[\underset{\rightarrow}{U}_r(\vec{\phi})\, E_h s(t) \exp(j2\pi f_h t) \right] + A_r I_b \Big\},\end{aligned} \tag{B6}$$

where we have defined the noise current

$$I_b \equiv \frac{1}{A_r} \int_R d\vec{r}\, \overline{|E_b(\vec{r},t)|^2} \tag{B7}$$

and

$$\underset{\rightarrow}{U}_r(\phi) \equiv \int_R d\vec{r}\, \underset{\rightarrow}{U}(\vec{r})\, e^{-jk\vec{\phi} \cdot \vec{r}} \tag{B8}$$

is the angular plane-wave component of $\underset{\rightarrow}{U}(\vec{r})$ with direction cosine vector $\vec{\phi}$.

$$\mathrm{Cov}\left[\mu(\tau)\mu(\sigma)\right] = \left(\frac{\eta}{h\nu}\right)^2 \int_R d\vec{r} \int_R d\vec{r}' \left[\overline{|E_d(\vec{r},\tau)|^2 |E_d(\vec{r}',\sigma)|^2} - \overline{|E_d(\vec{r},\tau)|^2}\ \overline{|E_d(\vec{r}',\sigma)|^2} \right].$$

After much algebraic manipulation, including the use of the moment factoring theorem, we find that the covariance of $\mu(t)$ reduces to

$$\text{Cov}\,[\mu(\tau)\mu(\sigma)] = \left(\frac{\eta}{h\nu}\right)^2 \int_R d\vec{r} \int_R d\vec{r}' \left\{ \left| \overline{E_b(\vec{r},\tau) E_b^*(\vec{r}',\sigma)} \right|^2 + 2\,\text{Re}\left[E_s^*(\vec{r},\tau) E_s(\vec{r}',\sigma) \overline{E_b(\vec{r},\tau) E_b^*(\vec{r}',\sigma)} \right] \right\}.$$

We have noted that the background noise field is approximately white in time and space as represented by the form of the covariance function in Eq. B1. Similarly, we can make the approximation

$$\left| \overline{E_b(\vec{r},\tau) E_b^*(\vec{r}',\sigma)} \right|^2 \cong N_h u_o(\vec{r}-\vec{r}')\, u_o(\tau-\sigma), \tag{B9}$$

where N_h is some appropriate constant. Then the covariance of $\mu(t)$ simplifies to

$$\text{Cov}\,[\mu(\tau)\mu(\sigma)] \cong 4N_b\lambda^2 \left(\frac{\eta}{h\nu}\right)^2 u_o(\tau-\sigma) \left\{ \frac{A_r N_h}{4N_b\lambda^2} + \xi\,|s(\tau)|^2 \int_R d\vec{r}\; |\underset{\rightarrow}{U}(\vec{r})|^2 + A_r |E_h|^2 + 2\sqrt{\xi}\,\text{Re}\left[\underset{\rightarrow}{U}_r(\vec{\phi}) E_h s(\tau) \exp(j2\pi f_h \tau)\right] \right\}. \tag{B10}$$

We now turn our attention to the mean and covariance of the detector output d(t). Note that here d(t) is not a complex envelope – it is a real function of time. We assume for simplicity that the detector produces a deterministic, causal current pulse $h_d(t-\tau)$ in response to an electron emitted at time τ from its photosensitive surface. Then we have

$$\overline{d(t)} = \int_{-\infty}^{\infty} d\tau\; \overline{\mu(\tau)}\, h_d(t-\tau).$$

Let us assume, furthermore, that $\overline{\mu(t)}$ is slowly varying relative to the current pulse width; that is, the detector is wideband relative to $\overline{\mu(t)}$. Then the mean of the detector output is approximately

$$\overline{d(t)} \cong \overline{\mu(t)}\, H_d(0),$$

where $H_d(f)$ is the Fourier transform of $h_d(t)$. Under the assumption that the local-oscillator field is sufficiently strong, we need only retain terms in $\mu(t)$ containing E_h.

$$\overline{d(t)} \cong \left(\frac{\eta}{h\nu}\right) A_r |E_h|^2 H_d(0) + 2\left(\frac{\eta}{h\nu}\right) \sqrt{\xi}\, H_d(0)\,\text{Re}\left[\underset{\rightarrow}{U}_r(\vec{\phi}) E_h s(t) \exp(j2\pi f_h t)\right]. \tag{B11}$$

Using a similar approach for the covariance of d(t), this time only retaining terms containing $|E_h|^2$, we find that

$$\text{Cov}\,[d(t)d(t')] = \int_{-\infty}^{\infty} d\tau\, \overline{\mu(\tau)}\, h_d(t-\tau)\, h_d(t'-\tau) + \int_{-\infty}^{\infty} d\tau \int_{-\infty}^{\infty} d\sigma\, \text{Cov}\,[\mu(\tau)\mu(\sigma)]\, h_d(t-\tau)\, h_d(t'-\sigma)$$

$$\cong \left(\frac{\eta}{h\nu}\right) A_r |E_h|^2 \left[1 + 4N_b\lambda^2\left(\frac{\eta}{h\nu}\right)\right] \int_{-\infty}^{\infty} d\tau\; h_d(t-\tau)\, h_d(t'-\tau).$$

Typically, we have

$$4N_b\lambda^2\left(\frac{\eta}{h\nu}\right) \ll 1$$

so that the covariance of d(t) reduces to

$$\text{Cov}\,[d(t)d(t')] \cong \left(\frac{\eta}{h\nu}\right) A_r |E_h|^2 \int_{-\infty}^{\infty} d\tau\; h_d(\tau)\, h_d(t-t'+\tau). \tag{B12}$$

Finally, let us process the detector output d(t) to get our results in the desired form. Use a bandpass filter centered at frequency f_h to eliminate the DC term in $\overline{d(t)}$, and use

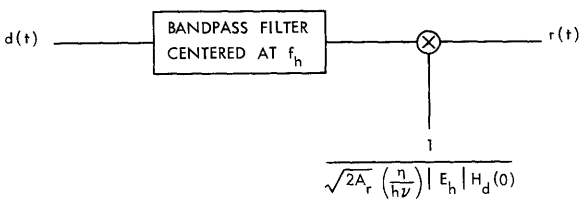

Fig. B-2. Detector output processor.

a multiplier to normalize the output. Then the mean of the receiver signal r(t) is given by

$$\overline{r(t)} \cong \sqrt{\frac{2\xi}{A_r}}\, \text{Re}\left[\underset{\rightarrow}{U}_r(\vec{\phi})\, \frac{E_h}{|E_h|}\, s(t)\, \exp(j2\pi f_h t)\right]. \tag{B13}$$

We can now approximate r(t) by the sum of its mean and a noise term n(t):

$$r(t) \cong \sqrt{\frac{2\xi}{A_r}}\, \text{Re}\left[\underset{\rightarrow}{U}_r(\vec{\phi})\, \frac{E_h}{|E_h|}\, s(t)\, \exp(j2\pi f_h t)\right] + n(t); \qquad t \in \mathcal{T}, \tag{B14}$$

where the correlation function of n(t) is

$$R_n(t-t') \cong \text{Cov}\,[r(t)r(t')] \cong \frac{\int_{-\infty}^{\infty} d\tau\, h_d(\tau)\, h_d(t-t'+\tau)}{2(\eta/h\nu)\, H_d^2(0)}. \tag{B15}$$

This implies that n(t) has a power density function

$$S_n(f) \cong \frac{|H_d(f)|^2}{2(\eta/h\nu)\, H_d^2(0)}. \tag{B16}$$

Since the current pulse $h_d(t)$ is typically very narrow, we can generally make the approximation

$$H_d(f) \approx H_d(0); \qquad |f| < W, \tag{B17}$$

where W is large enough to include the frequency range of r(t). Therefore, over the bandwidth of the signal portion of r(t), n(t) is essentially a white random process with power density function

$$S_n(f) \cong \frac{1}{2(\eta/h\nu)} \equiv \frac{N_o}{2}. \tag{B18}$$

Helstrom[22] examines cumulants of arbitrary order for r(t) and concludes that, if the local-oscillator field is sufficiently intense, the moment-generating function for r(t) approaches that of a Gaussian random process. There is little advantage to be gained by repeating his arguments here, so we simply accept his conclusion that r(t) is a Gaussian random process. This completes the proof of our initial hypothesis.

APPENDIX C

Approximation for the Marcum Q Function

We shall now derive a useful approximation for the Marcum Q function defined by[41]

$$Q_m(a, b) \equiv \int_b^\infty dx\, x\, e^{-\frac{1}{2}(x^2+a^2)} I_o(ax), \tag{C1}$$

where $I_o(\cdot)$ is the zero-order modified Bessel function of the first kind. The large-argument asymptotic approximation for the Bessel function is given by

$$I_o(z) \cong \frac{e^z}{\sqrt{2\pi z}}; \qquad z \gg 1. \tag{C2}$$

Using Eq. C2 in Eq. C1, we have

$$Q_m(a, b) \cong \frac{1}{\sqrt{2\pi a}} \int_b^\infty dx\, \sqrt{x}\, e^{-\frac{1}{2}(x-a)^2}; \qquad ab \gg 1. \tag{C3}$$

If $b \geq a$, we can try to approximate the integral in Eq. C3 by replacing $\sqrt{x}$ with the first two terms of its Taylor series expansion about $x = b$:

$$Q_m(a, b) \cong \underbrace{\sqrt{\frac{b}{2\pi a}} \int_b^\infty dx\, e^{-\frac{1}{2}(x-a)^2}}_{\text{I}}$$

$$+ \underbrace{\frac{1}{2\sqrt{2\pi ab}} \int_b^\infty dx\, (x-b)\, e^{-\frac{1}{2}(x-a)^2}}_{\text{II}}; \qquad b \geq a,\ ab \gg 1. \tag{C4}$$

We can easily determine that

$$\text{I} = \sqrt{\frac{b}{a}}\, Q(b-a) \tag{C5}$$

and

$$\text{II} = \frac{e^{-\frac{1}{2}(b-a)^2}}{2\sqrt{2\pi ab}} - \frac{(b-a)}{2\sqrt{ab}}\, Q(b-a), \tag{C6}$$

where $Q(\cdot)$ is the Gaussian Q function defined by[66]

$$Q(a) \equiv \frac{1}{\sqrt{2\pi}} \int_a^{\infty} dx\, e^{-x^2/2}. \tag{C7}$$

In order for the approximation of Eq. C4 to be accurate, we must satisfy the condition I $\gg$ II. This restriction will be met if and only if we have

$$b \gg \frac{1}{2} f(b-a), \tag{C8}$$

where

$$f(x) \equiv \frac{e^{-x^2/2}}{\sqrt{2\pi}\, Q(x)} - x. \tag{C9}$$

It can be readily verified that f(x) decreases monotonically with increasing x for $x \geq 0$, and that $f(0) \approx 0.4$. Therefore a sufficient condition for satisfying the restriction of Eq. C8 when $b \geq a$ is that $b \gg 0.4$. Then $Q_m(a, b)$ is approximately equal to I:

$$Q_m(a, b) \cong \sqrt{\frac{b}{a}}\, Q(b-a); \qquad ab \gg 1,\ b \gg 0.4,\ b \geq a. \tag{C10}$$

APPENDIX D

Buffering Problem for Optical Burst Communication Links over an Atmospheric Channel

As developed in Section IV, a burst communication system operates according to the following prescription. When the data transmitter senses that the channel is suitable for communication, it transmits information at a rate R bits per second; this event occurs with probability p. With probability 1-p the data transmitter decides that the channel fading is too severe for reliable communication and transmits no information, as long as the channel remains in that condition. Under the assumption that the channel-fading process is ergodic, these probabilities also represent the fractions of time that the channel is suitable or unsuitable for communication.

The data transmitter therefore sends information at an average rate

$$R_{avg} = Rp \text{ bits/second.} \tag{D1}$$

The data source typically emits information at a fixed rate. Under this assumption, the source rate must be R_{avg} bits per second. To accommodate the differences between the fixed data-source rate and the variable data-transmission rate, a buffer must be inserted between the data source and the data transmitter.

In order for the burst communication system to operate continually without interruption, the buffer storage capacity must be large enough to satisfy the following requirements:

(i) The buffer must always contain enough bits of information so that it can emit data at a net rate of $R - R_{avg}$ without emptying whenever the channel is suitable for communication.

(ii) The buffer must be able to store data at rate R_{avg} without saturating, as long as the channel is unsuitable for communication.

If the burst communication system must be operated indefinitely, the buffer storage capacity must be infinite to fulfill these requirements. In any practical situation, however, we only demand that the system be able to sustain continuous operation over a finite interval of time. For this case, the following analysis provides some insight into the problem of deciding what the buffer storage capacity should be.

In lieu of a complete statistical representation of the temporal variations of the channel-fading process, we shall use the following model. We partition our time scale into consecutive, nonoverlapping intervals of length T_c seconds, where T_c is the atmospheric coherence time. We assume that over each of these intervals the channel fading remains constant, but that different intervals have independent fades.

As a starting point, suppose the buffer contains z information bits when the communication system is initially turned on. During the i^{th} succeeding interval of duration T_c

the buffer incurs a net gain of g_i bits. Using Eq. D1, we can say that with probability 1-p, the random variable g_i given by

$$g_i = R_{avg}T_c = RpT_c \equiv a; \tag{D2}$$

with probability p, we have

$$g_i = -(R-R_{avg})T_c = -R(1-p)\ T_c \equiv -b. \tag{D3}$$

By our assumption of independent channel fades, the g_i's for different intervals are statistically independent random variables.

Suppose the buffer has a storage capacity of N bits. As we have noted, the burst communication system can operate without interruption until the buffer overflows or is completely emptied. Let us denote the expected duration of this continuous operation period, conditioned on the initial storage of z bits in the buffer, by D_z seconds. We shall determine D_z in the analysis, as well as the value of z which maximizes D_z.

We have essentially a classical random-walk problem of the sort investigated by Feller,[67] and the analysis that follows is adapted from his work. After the first interval of length T_c, the buffer contains either z+a or z-b bits, and therefore we must have

$$D_z = pD_{z-b} + (1-p)D_{z+a} + T_c; \qquad 0 < z < N \tag{D4}$$

with the boundary conditions

$$D_z = 0; \qquad z \leqslant 0 \quad \text{or} \quad z \geqslant N. \tag{D5}$$

Since Eqs. D2 and D3 imply that pb = (1-p)a, a particular solution of the nonhomogeneous difference equation in Eq. D4 is given by

$$D_z = -\frac{z^2T_c}{pb^2 + (1-p)a^2}. \tag{D6}$$

It is evident that the difference Δ_z of any two solutions of Eq. D4 satisfies the homogeneous difference equation

$$\Delta_z = p\Delta_{z-b} + (1-p)\Delta_{z+a}; \qquad 0 < z < N. \tag{D7}$$

Equation D7 has two complementary solutions:

$$\Delta_z = 1, z. \tag{D8}$$

It follows that all solutions of Eq. D4 are of the form

$$D_z = -\frac{z^2T_c}{pb^2 + (1-p)a^2} + Az + B, \tag{D9}$$

where A and B are arbitrary constants. To satisfy the boundary conditions of Eq. D5, we must have

$$A = \frac{NT_c}{pb^2 + (1-p)a^2}; \qquad B = 0. \tag{D10}$$

Therefore, the required solution D_z which satisfies the boundary conditions is given by

$$D_z = \frac{z(N-z)T_c}{pb^2 + (1-p)a^2}; \qquad 0 < z < N. \tag{D11}$$

We can clearly maximize D_z by setting z equal to N/2. Then the expected duration of the continuous operation period is simply

$$D_{N/2} = \frac{\frac{1}{4}N^2T_c}{pb^2 + (1-p)a^2}, \tag{D12}$$

where a and b are defined in Eqs. D2 and D3. Replacing a and b with the burst communication system parameters R_{avg} and p, we can write Eq. D12 in the form

$$D_{N/2} = \frac{pN^2}{4(1-p)\,R_{avg}^2 T_c}. \tag{D13}$$

To summarize the results above, suppose we have a burst communication system that transmits data at a average information rate R_{avg} bits per second over an atmospheric channel that has a coherence time T_c seconds. The channel is suitable for communication with probability p, and a buffer with a storage capacity of N bits is inserted between the data source and the data transmitter. In order to maximize the expected duration of the period over which the burst communication system operates satisfactorily, we must load the buffer with N/2 source bits before turning on the system. Then the expected duration of the continuous operation period is given in Eq. D13. This provides some indication of the buffer storage capacity required for reliable communication over any given period.

Acknowledgment

I am deeply indebted to Professor Estil V. Hoversten who supervised my doctoral research, as well as the preparation of this report. His capable guidance and scientific insight were of immeasurable value to me.

I also take great pleasure in thanking Professor Peter Elias and Professor Robert S. Kennedy who served as thesis readers. Their criticisms greatly increased the relevance of this final document.

I am grateful to my colleagues, Dr. Seppo J. Halme, Dr. Jeffrey H. Shapiro, and Mr. Richard S. Orr for their friendship and assistance during my research.

Finally, I wish to thank the Research Laboratory of Electronics of the Massachusetts Institute of Technology for supporting me throughout the period of my graduate studies.

References

1. R. S. Orr, "Channel-Measurement Receivers for Slowly Fading Nondispersive Media," Quarterly Progress Report No. 98, Research Laboratory of Electronics, Massachusetts Institute of Technology, July 15, 1970, pp. 81-87.
2. J. H. Shapiro, "Optimal Spatial Modulation for Reciprocal Channels," Technical Report 476, Research Laboratory of Electronics, Massachusetts Institute of Technology, April 30, 1970, p. 13.
3. R. S. Lawrence and J. W. Strohbehn, "A Survey of Clear-Air Propagation Effects Relevant to Optical Communications," Proc. IEEE, Vol. 58, pp. 1523-1545, October 1970.
4. J. H. Shapiro, loc. cit.
5. P. A. Forsyth, E. L. Vogan, D. R. Hansen, and C. O. Himes, "The Principles of JANET-A Meteor-Burst Communication System," Proc. IEEE, Vol. 45, pp. 1642-1647, December 1957.
6. V. I. Tatarski, Wave Propagation in a Turbulent Medium (McGraw-Hill Book Company, New York, 1961).
7. D. L. Fried, G. E. Mevers, and M. P. Keister, Jr., "Measurement of Laser-Beam Scintillation in the Atmosphere," J. Opt. Soc. Am., Vol. 57, pp. 787-797, June 1965.
8. J. E. Ehrenberg, "A Study of the Effects of Atmospheric Turbulence on Intensity Properties at 6328 Å and 1.15 μ," S.M. Thesis, Department of Electrical Engineering, Massachusetts Institute of Technology, February 1968.
9. A. A. A. Saleh, "An Investigation of Laser Wave Depolarization Due to Atmospheric Transmission," IEEE J. Quantum Electronics, Vol. QE-3, pp. 540-543, 1967.
10. S. Karp and R. S. Kennedy (Eds.), "Optical Space Communication," NASA SP-217, 1969, p. 47.
11. E. Brookner, "Atmosphere Propagation and Communication Channel Model for Laser Wavelengths," IEEE Trans., Vol. COM-18, No. 4, pp. 396-416, August 1970.
12. E. V. Hoversten, R. O. Harger, and S. J. Halme, "Communication Theory for the Turbulent Atmosphere," Proc. IEEE, Vol. 58, pp. 1626-1650, October 1970.
13. J. H. Shapiro, loc. cit.
14. E. V. Hoversten, R. O. Harger, and S. J. Halme, op. cit., pp. 1627-1628.
15. R. S. Lawrence and J. W. Strohbehn, loc. cit.
16. R. S. Kennedy and E. V. Hoversten, "On the Atmosphere as an Optical Communication Channel," IEEE Trans. on Information Theory, Vol. IT-14, pp. 717-719, September 1968.
17. S. J. Halme, "Efficient Optical Communication in a Turbulent Atmosphere," Technical Report 474, Research Laboratory of Electronics, Massachusetts Institute of Technology, April 1, 1970, pp. 107-111.
18. B. K. Levitt, "Detector Statistics for Optical Communication through the Turbulent Atmosphere," Quarterly Progress Report No. 99, Research Laboratory of Electronics, Massachusetts Institute of Technology, October 15, 1970, pp. 114-123.
19. S. J. Halme, op. cit., pp. 40-48.
20. Ibid., pp. 39-40.
21. E. V. Hoversten, R. O. Harger, and S. J. Halme, op. cit., p. 1628.
22. C. W. Helstrom, "Detectability of Coherent Optical Signals in a Heterodyne Receiver," J. Opt. Soc. Am., Vol. 57, pp. 353-361, March 1967.

23. S. Karp and R. S. Kennedy (Eds.), op. cit., p. 15.

24. R. S. Kennedy and E. V. Hoversten, op. cit., p. 718.

25. E. V. Hoversten, R. O. Harger, and S. J. Halme, op. cit., p. 1636.

26. J. M. Wozencraft and I. M. Jacobs, Principles of Communication Engineering (John Wiley and Sons, Inc., New York, 1965), p. 518.

27. Ibid., p. 523.

28. Ibid., p. 533.

29. E. V. Hoversten, R. O. Harger, and S. J. Halme, op. cit., p. 1637.

30. S. J. Halme, B. K. Levitt, and R. S. Orr, "Bounds and Approximations for some Integral Expressions Involving Log-Normal Statistics," Quarterly Progress Report No. 93, Research Laboratory of Electronics, Massachusetts Institute of Technology, April 15, 1969, pp. 163-175.

31. S. J. Halme, "On Optimum Reception through a Turbulent Atmosphere," Quarterly Progress Report No. 88, Research Laboratory of Electronics, Massachusetts Institute of Technology, January 15, 1968, pp. 247-254.

32. E. B. Dubro, V. F. Komarovich, and J. G. Lebedinski, "Calculation of Probability Distributions of Signal Amplitude, Narrowband Noise, and Signal-to-Noise Ratios for Rayleigh and Log-Normal Fading," Radiotekhnika i Electronika, Vol. 14, pp. 420-424, 1969.

33. E. V. Hoversten, R. O. Harger, and S. J. Halme, op. cit., p. 1638.

34. Ibid., p. 1634.

35. S. Karp and J. R. Clark, "Photon Counting: A Problem in Classical Noise Theory," IEEE Trans. on Information Theory, Vol. IT-16, pp. 672-680, November 1970; also NASA TR R-334, April 1970.

36. J. R. Clark and E. V. Hoversten, "The Poisson Process as a Statistical Model for Photodetectors Excited by Gaussian Light," Quarterly Progress Report No. 98, Research Laboratory of Electronics, Massachusetts Institute of Technology, July 15, 1970, pp. 95-101.

37. R. L. Mitchell, "Permanence of the Log-Normal Distribution," J. Opt. Soc. Am., Vol. 58, pp. 1267-1272, September 1968.

38. S. J. Halme, "Efficient Optical Communication in a Turbulent Atmosphere," op. cit., pp. 40-48.

39. B. K. Levitt, op. cit., p. 114.

40. W. K. Pratt, Laser Communication Systems (John Wiley and Sons, Inc., New York, 1969), pp. 207-208.

41. J. I. Marcum, "A Statistical Theory of Target Detection by Pulsed Radar," IRE Trans. on Information Theory, Vol. IT-6, pp. 159-160, April 1960.

42. J. I. Marcum, "Table of Q Functions," Rand Corporation RM 339, January 1, 1950.

43. B. K. Levitt, "Direct-Detection Error Probabilities for Optical Communication over a Rayleigh Fading Channel," Quarterly Progress Report No. 99, Research Laboratory of Electronics, Massachusetts Institute of Technology, October 15, 1970, pp. 123-130.

44. J. M. Wozencraft and I. M. Jacobs, op. cit., pp. 82-83.

45. E. V. Hoversten and R. S. Kennedy, "Efficient Optical Communication within the Earth's Atmosphere," in Opto-Electronics Signal-Processing Techniques, AGARD Conference Proceedings, No. 50, February 1970.

46. E. V. Hoversten, R. O. Harger, and S. J. Halme, op. cit., pp. 1642-1643.

47. R. S. Lawrence and J. W. Strohbehn, op. cit., p. 1523.

48. E. V. Hoversten, R. O. Harger, and S. J. Halme, op. cit., p. 1628.

49. D. L. Fried, "Equivalence of Transmitter and Receiver Antenna Gain in a Random Medium," NASA SP-217, 1969, p. 137.

50. J. W. Goodman, Introduction to Fourier Optics (McGraw-Hill Publishing Company, New York, 1968), p. 85.

51. E. V. Hoversten, R. O. Harger, and S. J. Halme, op. cit., pp. 1638, 1643.

52. J. H. Shapiro, op. cit., pp. 106-107.

53. P. A. Button, M. F. Reusch, and B. Sage, "Measurements of the Extent of the Atmospheric Spatial Isoplanatic Region," Paper Tu H 16, Annual Meeting Program, Optical Society of America, September 28 - October 2, 1970, p. 15.

54. B. K. Levitt, "Direct-Detection Error Probabilities for Optical Communication over a Rayleigh Fading Channel," op. cit., p. 126.

55. J. M. Wozencraft and I. M. Jacobs, op. cit., p. 83.

56. J. H. Shapiro, loc. cit.

57. D. L. Fried, "Statistics of a Geometric Representation of Wavefront Distortion," J. Opt. Soc. Am., Vol. 55, pp. 1427-1435, November 1965.

58. D. L. Fried, "Optical Heterodyne Detection of an Atmospherically Distorted Signal Wave Front," Proc. IEEE, Vol. 55, pp. 57-67, January 1967.

59. R. L. Mitchell, loc. cit.

60. S. J. Halme, "Efficient Optical Communication in a Turbulent Atmosphere," op. cit., pp. 40-48.

61. B. K. Levitt, "Detector Statistics for Optical Communication through the Turbulent Atmosphere," loc. cit.

62. D. L. Fried, "Aperture Averaging of Scintillation," J. Opt. Soc. Am., Vol. 57, pp. 169-175, February 1967.

63. J. M. Wozencraft and I. M. Jacobs, op. cit., p. 362.

64. H. Cramér, Mathematical Methods of Statistics (Princeton University Press, Princeton, N. J., 1946), pp. 131-133.

65. S. J. Halme, "Efficient Optical Communication in a Turbulent Atmosphere," op. cit., pp. 40-48.

66. J. M. Wozencraft and I. M. Jacobs, op. cit., pp. 82-83.

67. W. Feller, An Introduction to Probability Theory and Its Applications (John Wiley and Sons, Inc., New York, 1950), pp. 279-288.

JOINT SERVICES ELECTRONICS PROGRAM
REPORTS DISTRIBUTION LIST

Department of Defense

Assistant Director (Research)
Office of Director of Defense, Research & Engineering
The Pentagon, Rm 3C128
Washington, D.C. 20301

Technical Library
DDR&E
Room 3C-122, The Pentagon
Washington, D.C. 20301

Director For Materials Sciences
Advanced Research Projects Agency
1400 Wilson Boulevard
Arlington, Virginia 22209

Chief, R&D Division (340)
Defense Communications Agency
Washington, D.C. 20305

Defense Documentation Center
Attn: DDC-TCA
Cameron Station
Alexandria, Virginia 22314

Dr. Alvin D. Schnitzler
Institute For Defense Analyses
Science and Technology Division
400 Army-Navy Drive
Arlington, Virginia 22202

LTC Norman D. Jorstad
Weapons Systems Evaluation Group
400 Army-Navy Drive
Arlington, Virginia 22202

Central Intelligence Agency
Attn: CRS/ADD/PUBLICATIONS
Washington, D.C. 20505

Department of the Air Force

Hq USAF (AF/RDPE)
Washington, D.C. 20330

Hq USAF/RDPS
Washington, D.C. 20330

Hq USAF (RDSD)
The Pentagon
Washington, D.C. 20330

Colonel E. P. Gaines, Jr.
ESD (MCD)
L. G. Hanscom Field
Bedford, Massachusetts 01730

Dr L. A. Wood, Director
Electronic and Solid State Sciences
Air Force Office of Scientific Research
1400 Wilson Boulevard
Arlington, Virginia 22209

Dr Harvey E. Savely, Director
Life Sciences
Air Force Office of Scientific Research
1400 Wilson Boulevard
Arlington, Virginia 22209

AFSC (CCJ/Mr I. R. Mirman)
Andrews Air Force Base,
Washington, D.C. 20331

Rome Air Development Center
Attn: Documents Library (TDLD)
Griffiss Air Force Base, New York 13440

Mr H. E. Webb, Jr. (ISCP)
Rome Air Development Center
Griffiss Air Force Base, New York 13440

Dr L. M. Hollingsworth
AFCRL (CA)
L. G. Hanscom Field
Bedford, Massachusetts 01730

Hq ESD (TRI)
L. G. Hanscom Field
Bedford, Massachusetts 01730

Professor R. E. Fontana, Head
Dept of Electrical Engineering
Air Force Institute of Technology
Wright-Patterson Air Force Base,
Ohio 45433

Commanding General
USACDC Institute of Land Combat
Attn: Technical Library, Rm 636
2461 Eisenhower Avenue
Alexandria, Virginia 22314

Mr H. T. Darracott (AMXAM-FT)
U.S. Army Advanced Materiel
Concepts Agency
2461 Eisenhower Avenue
Alexandria, Virginia 22314

Dr Berthold Altmann (AMXDO-TI)
Harry Diamond Laboratories
Connecticut Avenue and
Van Ness Street N. W.
Washington, D.C. 20438

Commanding Officer (AMXRD-BAD)
U.S. Army Ballistic Research Laboratory
Aberdeen Proving Ground
Aberdeen, Maryland 21005

U.S. Army Munitions Command
Attn: Science & Technology Information
Branch, Bldg 59
Picatinny Arsenal, SMUPA-RT-S
Dover, New Jersey 07801

Dr Herman Robl
Deputy Chief Scientist
U.S. Army Research Office (Durham)
Box CM, Duke Station
Durham, North Carolina 27706

Richard O. Ulsh (CRDARD-IP)
U.S. Army Research Office (Durham)
Box CM, Duke Station
Durham, North Carolina 27706

Technical Director (SMUFA-A2000-107-1)
Frankford Arsenal
Philadelphia, Pennsylvania 19137

Redstone Scientific Information Center
Attn: Chief, Document Section
U.S. Army Missile Command
Redstone Arsenal, Alabama 35809

Commanding General
U.S. Army Missile Command
Attn: AMSMI-RR
Redstone Arsenal, Alabama 35809

Commanding General
U.S. Army Strategic Communications
Command
Attn: SCC-ATS (Mr Peter B. Pichetto)
Fort Huachuca, Arizona 85613

Dr Homer F. Priest
Chief, Materials Sciences Division,
Bldg 292
Army Materials & Mechanics Research
Center
Watertown, Massachusetts 02172

Commandant
U.S. Army Air Defense School
Attn: Missile Science Division, C&S Dept
P. O. Box 9390
Fort Bliss, Texas 79916

Commandant
U.S. Army Command and General
Staff College
Attn: Acquisitions, Lib Div
Fort Leavenworth, Kansas 66027

Dr Hans K. Ziegler
Army Member TAC/JSEP (AMSEL-XL-D)
U.S. Army Electronics Command
Fort Monmouth, New Jersey 07703

Mr I. A. Balton, AMSEL-XL-D
Executive Secretary, TAC/JSEP
U.S. Army Electronics Command
Fort Monmouth, New Jersey 07703

Director (NV-D)
Night Vision Laboratory, USAECOM
Fort Belvoir, Virginia 22060

Commanding Officer
Atmospheric Sciences Laboratory
U.S. Army Electronics Command
White Sands Missile Range,
New Mexico 88002

Atmospheric Sciences Laboratory
U.S. Army Electronics Command
Attn: AMSEL-BL-DD (Mr Marvin Diamond)
White Sands Missile Range,
New Mexico 88002

Dr H. V. Noble, AFAL/TE
Chief, Electronics Technology Division
Air Force Avionics Laboratory
Wright-Patterson Air Force Base,
Ohio 45433

Director
Air Force Avionics Laboratory
Wright-Patterson Air Force Base,
Ohio 45433

AFAL/TEA (Mr R. D. Larson)
Wright-Patterson Air Force Base,
Ohio 45433

Director of Faculty Research
Department of the Air Force
U.S. Air Force Academy
Colorado 80840

Mr Jules I. Wittebort
Chief, Electronics Branch
Manufacturing Technology Division
AFAL/LTE
Wright-Patterson Air Force Base,
Ohio 45433

Academy Library (DFSLB)
USAF Academy, Colorado 80840

Director of Aerospace Mechanics Sciences
Frank J. Seiler Research
Laboratory (OAR)
USAF Academy, Colorado 80840

Major Richard J. Gowen
Tenure Associate Professor
Dept of Electrical Engineering
USAF Academy, Colorado 80840

Director, USAF PROJECT RAND
Via: Air Force Liaison Office
The RAND Corporation
Attn: Library D
1700 Main Street
Santa Monica, California 90406

AUL3T-9663
Maxwell Air Force Base, Alabama 36112

AFETR Technical Library
(MU-135)
Patrick Air Force Base, Florida 32925

ADTC (SSLT)
Eglin Air Force Base, Florida 32542

Hq AMD (RDR/Lt Col Godden)
Brooks Air Force Base, Texas 78235

USAFSAM (RAT)
Brooks Air Force Base, Texas 78235

Commanding General
Attn: STEWS-AD-L, Technical Library
White Sands Missile Range,
New Mexico 88002

European Office of Aerospace Research
Technical Information Office
Box 14, FPO New York 09510

VELA Seismological Center
312 Montgomery Street
Alexandria, Virginia 22314

Capt C. E. Baum
AFWL (SRE)
Kirtland Air Force Base,
New Mexico 87117

Biomedical Engineering Branch (SCB)
USAF School of Aerospace Medicine (AFSC)
Department of the Air Force
Brooks Air Force Base, Texas 78235

Department of the Army

Director
Physical & Engineering Sciences Division
3045 Columbia Pike
Arlington, Virginia 22204

Commanding General
U.S. Army Security Agency
Attn: IARD-T
Arlington Hall Station
Arlington, Virginia 22212

Commanding General
U.S. Army Materiel Command
Attn: AMCRD-TP (Dr Zarwyn)
Washington, D.C. 20315

Director
U.S. Army Advanced Materiel
Concepts Agency
2461 Eisenhower Avenue
Alexandria, Virginia 22314

Chief
Missile Electronic Warfare Tech
Area (AMSEL-WL-M)
Electronic Warfare Laboratory,
USAECOM
White Sands Missile Range,
New Mexico 88002

Project Manager NAVCON
Attn: AMCPM-NC, Bldg 439
(H. H. Bahr)
Fort Monmouth, New Jersey 07703

Mr A. D. Bedrosian, Rm 26-131
U.S. Army Scientific Liaison Office
Massachusetts Institute of Technology
77 Massachusetts Avenue
Cambridge, Massachusetts 02139

Commanding General
U.S. Army Electronics Command
Fort Monmouth, New Jersey 07703
Attn: AMSEL-RD-O (Dr W. S. McAfee)
GG-DD
XL-D
XL-DT
XL-G (Dr S. Kronenberg)
XL-H (Dr R. G. Buser)
BL-FM-P
CT-D
CT-R
CT-S
CT-L
CT-O
CT-I
CT-A
NL-D (Dr H. Bennett)
NL-A
NL-C
NL-P
NL-P-2
NL-R
NL-S
KL-D
KL-I
KL-E
KL-S
KL-SM
KL-T
VL-D
VL-F
WL-D

Department of the Navy

Director, Electronics Programs
Attn: Code 427
Office of Naval Research
800 North Quincy Street
Arlington, Virginia 22217

Mr Gordon D. Goldstein, Code 437
Information Systems Program
Office of Naval Research
800 North Quincy Street
Arlington, Virginia 22217

Commander
Naval Security Group Command
Naval Security Group Headquarters
Attn: Technical Library (G43)
3801 Nebraska Avenue, N. W.
Washington, D.C. 20390

Director
Naval Research Laboratory
Washington, D.C. 20390
Attn: Code 5200
Mr A. Brodzinsky, Supt,
Electronics Div

Director
Naval Research Laboratory
Attn: Dr H. Rabin, Code 7000
Washington, D.C. 20390

Code 8050
Maury Center Library
Naval Research Laboratory
Washington, D.C. 20390

Dr G. M. R. Winkler
Director, Time Service Division
U.S. Naval Observatory
Washington, D.C. 20390

Naval Air Systems Command
AIR 310 - Research Administrator
Room 424 JP-1
Washington, D.C. 20360

Dr A. L. Slafkosky
Scientific Advisor
Commandant of the Marine Corps (Code AX)
Washington, D.C. 20380

Naval Ship Systems Command
Ship 035
Washington, D.C. 20360

U.S. Naval Weapons Laboratory
Dahlgren, Virginia 22448

Naval Electronic Systems Command
Attn: Code 0311, Rm 7W12, NC #1
Department of the Navy
Washington, D.C. 20360

Commander
U.S. Naval Ordnance Laboratory
Attn: Librarian
White Oak, Maryland 20910

Director
Office of Naval Research
Boston Branch
495 Summer Street
Boston, Massachusetts 02210

Commander (ADL)
Naval Air Development Center
Attn: NADC Library
Johnsville, Warminster,
Pennsylvania,18974

Commanding Officer
Naval Missile Center
Attn: 5632.2, Technical Library
Point Mugu, California 93042

W. A. Eberspacher, Associate Head
Systems Integration Division, Code 5340A
U.S. Naval Missile Center
Point Mugu, California 93041

Commander
Naval Electronics Laboratory Center
Attn: Library
San Diego, California 92152

Deputy Director and Chief Scientist
Office of Naval Research Branch Office
1031 East Green Street
Pasadena, California 91101

Library (Code 2124)
Naval Postgraduate School
Monterey, California93940

Officer in Charge, New London Lab.
Naval Underwater Systems Center
Attn: Technical Library
New London, Connecticut 06320

Commanding Officer
Naval Avionics Facility
Attn: D/035 Technical Library
Indianapolis, Indiana 46241

Director
Naval Research Laboratory
Attn: Library, Code 2629 (ONRL)
Washington, D.C. 20390

Commanding Officer
Naval Training Device Center
Attn: Technical Library
Orlando, Florida 32813

U.S. Naval Oceanographic Office
Attn: M. Rogofsky, Librarian (Code 1640)
Washington, D.C. 20390

Other Government Agencies

Dr H. Harrison
AEC/NASA Space Nuclear Systems Office
AEC Headquarters (F-309)
Washington, D.C. 20545

NASA Lewis Research Center
Attn: Library
21000 Brookpark Road
Cleveland, Ohio 44135

Los Alamos Scientific Laboratory
Attn: Reports Library
P. O. Box 1663
Los Alamos, New Mexico 87544

Mr M. Zane Thornton
Deputy Director
Center for Computer Sciences and Technology
National Bureau of Standards
U.S. Department of Commerce
Washington D.C. 20234

U.S. Postal Service
Library – Room 6012
12th & Pennsylvania Ave., N. W.
Washington, D.C. 20260

Non-Government Agencies

Director
Research Laboratory of Electronics
Massachusetts Institute of Technology
Cambridge, Massachusetts 02139

Mr Jerome Fox, Research Coordinator
Polytechnic Institute of Brooklyn
333 Jay Street
Brooklyn, New York 11201

Director
Columbia Radiation Laboratory
Columbia University
538 West 120th Street
New York, New York 10027

Director
Coordinate Science Laboratory
University of Illinois
Urbana, Illinois 61801

Director
Stanford Electronics Laboratory
Stanford University
Stanford, California 94305

Director
Microwave Laboratory
Stanford University
Stanford, California 94305

Director
Electronics Research Laboratory
University of California
Berkeley, California 94720

Director
Electronics Sciences Laboratory
University of Southern California
Los Angeles, California 90007

Director
Electronics Research Center
The University of Texas at Austin
Engineering-Science Bldg 110
Austin, Texas 78712

Division of Engineering and
Applied Physics
210 Pierce Hall
Harvard University
Cambridge, Massachusetts 02138

Dr G. J. Murphy
The Technological Institute
Northwestern University
Evanston, Illinois 60201

Dr John C. Hancock, Head
School of Electrical Engineering
Purdue University
Lafayette, Indiana 47907

Dept of Electrical Engineering
Texas Technological University
Lubbock, Texas 79409

Aerospace Corporation
P. O. Box 95085
Attn: Library Acquisitions Group
Los Angeles, California 90045

Airborne Instruments Laboratory
Deerpark, New York 11729

The University of Arizona
Department of Electrical Engineering
Tucson, Arizona 85721

Chairman, Electrical Engineering
Arizona State University
Tempe, Arizona 85281

Engineering and Mathematical
Sciences Library
University of California at Los Angeles
405 Hilgred Avenue
Los Angeles, California 90024

Sciences-Engineering Library
University of California
Santa Barbara, California 93106

Professor Nicholas George
California Institute of Technology
Pasadena, California 91109

Aeronautics Library
Graduate Aeronautical Laboratories
California Institute of Technology
1201 E. California Boulevard
Pasadena, California 91109

Hunt Library
Carnegie-Mellon University
Schenley Park
Pittsburgh, Pennsylvania 15213

Dr A. G. Jordan
Head of Dept of Electrical Engineering
Carnegie-Mellon University
Pittsburg, Pennsylvania 15213

Case Western Reserve University
Engineering Division
University Circle
Cleveland, Ohio 44106

Hollander Associates
Attn: Librarian
P. O. Box 2276
Fullerton, California 92633

Walter H. Veazie, Head
Electronic Properties Information Center
Mail Station E-148
Hughes Aircraft Company
Culver City, California 90230

Illinois Institute of Technology
Department of Electrical Engineering
Chicago, Illinois 60616

Government Documents Department
University of Iowa Libraries
Iowa City, Iowa 52240

The Johns Hopkins University
Applied Physics Laboratory
Attn: Document Librarian
8621 Georgia Avenue
Silver Spring, Maryland 20910

Lehigh University
Department of Electrical Engineering
Bethlehem, Pennsylvania 18015

Mr E. K. Peterson
Lenkurt Electric Co. Inc.
1105 Country Road
San Carlos, California 94070

MIT Lincoln Laboratory
Attn: Library A-082
P. O. Box 73
Lexington, Massachusetts 02173

Miss R. Joyce Harman
Project MAC, Room 810
545 Main Street
Cambridge, Massachusetts 02139

Professor R. H. Rediker
Electrical Engineering, Professor
Massachusetts Institute of Technology
Building 13-3050
Cambridge, Massachusetts 02139

Professor Joseph E. Rowe
Chairman, Dept of Electrical Engineering
The University of Michigan
Ann Arbor, Michigan 48104

New York University
Engineering Library
Bronx, New York 10453

Professor James A. Cadzow
Department of Electrical Engineering
State University of New York at Buffalo
Buffalo, New York 14214

Department of Electrical Engineering
Clippinger Laboratory
Ohio University
Athens, Ohio 45701

Raytheon Company
Research Division Library
28 Seyon Street
Waltham, Massachusetts 02154

Rice University
Department of Electrical Engineering
Houston, Texas 77001

Dr Leo Young, Program Manager
Stanford Research Institute
Menlo Park, California 94025

GTE Waltham Research Lab Library
Attn: Documents Librarian
Esther McLaughlin
40 Sylvan Road
Waltham, Massachusetts 02154

Dr W. R. LePage, Chairman
Department of Electrical Engineering
Syracuse University
Syracuse, New York 13210

Dr F. R. Charvat
Union Carbide Corporation
Materials Systems Division
Crystal Products Department
8888 Balboa Avenue
P. O. Box 23017
San Diego, California 92123

Utah State University
Department of Electrical Engineering
Logan, Utah 84321

Research Laboratories for the
Engineering Sciences
School of Engineering and Applied Science
University of Virginia
Charlottesville, Virginia 22903

Yale University
Engineering and Applied Science Library
15 Prospect Street
New Haven, Connecticut 06520

UNCLASSIFIED

Security Classification

DOCUMENT CONTROL DATA - R & D

(Security classification of title, body of abstract and indexing annotation must be entered when the overall report is classified)

1. ORIGINATING ACTIVITY (Corporate author)	2a. REPORT SECURITY CLASSIFICATION
Research Laboratory of Electronics Massachusetts Institute of Technology Cambridge, Massachusetts 02139	Unclassified
	2b. GROUP None

3. REPORT TITLE

Variable-Rate Optical Communication through the Turbulent Atmosphere

4. DESCRIPTIVE NOTES (Type of report and inclusive dates)

Technical Report

5. AUTHOR(S) (First name, middle initial, last name)

Barry K. Levitt

6. REPORT DATE	7a. TOTAL NO. OF PAGES	7b. NO. OF REFS
August 20, 1971	109	67

8a. CONTRACT OR GRANT NO.	9a. ORIGINATOR'S REPORT NUMBER(S)
DA 28-043-AMC-02536(E) b. PROJECT NO. 20061102B31F NASA Grant NGL 22-009-013	Technical Report 483
	9b. OTHER REPORT NO(S) (Any other numbers that may be assigned this report) None

10. DISTRIBUTION STATEMENT

This document has been approved for public release and sale; its distribution is unlimited.

11. SUPPLEMENTARY NOTES	12. SPONSORING MILITARY ACTIVITY
	Joint Services Electronics Program Through U. S. Army Electronics Command

13. ABSTRACT

The performance of optical communication links over atmospheric channels is severely limited because of the effects of turbulence. One method of recovering some of the atmospheric fading losses is to match the instantaneous signalling rate to the channel state. We demonstrate that the data transmitter can extract real-time channel-state information by processing the field received when a pilot tone is sent from the data receiver to the data transmitter. Based on these channel measurements, we derive optimal variable-rate techniques, and show that significant improvements in system performance are obtained, particularly at low bit error rates.

DD FORM 1 NOV 65 1473 (PAGE 1)

S/N 0102-014-6600

UNCLASSIFIED

Security Classification

14. KEY WORDS	LINK A		LINK B		LINK C	
	ROLE	WT	ROLE	WT	ROLE	WT
Log-normal fading						
Optical communication						
Optical direct detection						
Optical heterodyne detection						
Rayleigh fading						
Turbulent atmosphere						
Variable-Rate communication						